PHILIPS

"Miniwatt"

battery receiving tubes

DK 92   DL 92
DF 91   DL 94
DAF 91   DM 70

PHILIPS ELECTRONIC TUBE DIVISION

BATTERY

RECEIVING TUBES

DK 92	DL 92
DF 91	DL 94
DAF 91	DM 70

PREFACE

In addition to the normal mains radio set there are a number of other types of receivers, with which radio reception is possible at places where no mains supply is available. One type is the so-called car radio, which differs from the normal mains receiver only in so far that the power is furnished by a 6 V car battery, the required H.T. being obtained by means of a vibrator system. With the exception of the output tube, for which versions with a comparatively low heater power have been designed, the high power available from a car battery permits the use of normal indirectly heated tubes.

In cases, however, where the use of a heavy storage battery presents exceptional difficulties, an entirely different technique is necessary. As a consequence receivers have been designed in which directly heated tubes with an extraordinarily low power consumption are used, in conjunction with dry batteries for the filament as well as for the H.T. supply. The combined efforts of tube designers, setmakers and battery manufacturers has resulted in tubes of small dimensions and low power consumption, with satisfactory performance on all normal wave ranges, whilst, moreover, the availability of small batteries has permitted of the design of very compact receivers.

All-dry battery receivers are made in different types. There is first of all the portable receiver for use while camping or travelling, in which an H.T. battery of 90 V is normally used. Such a receiver is often built with a supply system allowing of it being operated with either dry batteries or mains supply, the combination then being termed ABC receiver. Particularly the ABC set is gaining more and more in popularity.

When the dimensions have to be reduced to the minimum, as is the case with personal receivers, very small batteries and components must be used. The performance of a personal receiver with an H.T. battery of 67.5 or 45 V is inferior to that of larger sets indicated above, but the dimensions can be made so small that the set fits into a lady's handbag.

Finally, there is the stationary receiver with all-dry battery supply, for use in rural areas without mains. Since this type is intended for stationary use, there is no need to restrict the dimensions and a comparatively large H.T. battery can be employed. The A.F. output can therefore be quite large, particularly when two output tubes are used in a current-saving push-pull arrangement.

The aim of this Bulletin is to describe and discuss the appication of a series of miniature battery receiving tubes, which have been developed to meet the specific requirements for their use in the above-mentioned types of receivers. This range is of universal application and permits the design of small portables, in which economy of power consumption is of primary importance, as well as stationary receivers having a high A.F. output.

CONTENTS

INTRODUCTION

The range of battery tubes dealt with in this Bulletin comprises the following types:

DK 92 — self-oscillating heptode frequency changer;

DF 91 — R.F. pentode;

DAF 91 — diode-A.F. pentode combined in one envelope;

DL 92 — output pentode for low H.T. voltages;

DL 94 — output pentode for higher H.T. voltages;

DM 70 and DM 71 — tuning indicators.

Except for the DM 70 and DM 71 all these types are built in the 7-pin miniature envelope, whilst the filaments are designed for 1,4 V, 50 mA, with the exception of the output tubes DL 92 and DL 94, which have two filament sections to be connected either in parallel (1.4 V, 100 mA) or in series (2.8 V, 50 mA). When a particularly low current consumption of the output stage is required, with the output tubes mentioned above it is also possible to use only one of the two filament sections. The DM 70 and DM 71 are sub-miniature tubes and have a filament for 1.4 V, 25 mA.

Two different types of output pentodes are available. For small sets operating with an H.T. battery of 45 V or 67.5 V the DL 92 is to be preferred, as this tube is specially designed to give satisfactory performance at these low supply voltages. With an H.T. of 90 V either the DL 92 or the DL 94 can be used, but in the case of the DL 92 it is necessary to employ a screen-grid dropper resistor or a tap on the battery to maintain the screen potential at 67.5 V. For this reason the DL 94, the screen grid of which can be operated at 90 V, is the more economical proposition. Also at higher supply volt-

ages, for example 120 V and 150 V, the DL 94 should be used.

The tubes for the first stages of the receiver, DK 92, DF 91 and DAF 91, give optimum performance at supply voltages between 67.5 V and 90 V. Slightly lower but still satisfactory performance is obtained with an H.T. of 45 V, but it should be borne in mind that the gain obtainable is reduced with decreasing H.T., so that an exceptionally low supply voltage should only be used when this is strictly necessary on account of the restricted dimensions of the receiver. This, of course, also applies to the output pentode, the available A.F. output decreasing rapidly with the supply voltage.

In this Bulletin special attention is drawn to the heptode frequency changer DK 92, the oscillator section of which gives very superior performance at wavelengths down to 10 m (30 Mc/s); also with only 45 V H.T. This is a remarkable achievement, which permits the design of personal receivers with a short-wave range.

In reveivers of a more elaborate design a greater A.F. output is normally aimed at, and in this case, as indicated above, the DL 94 output pentode should be used. Two of these tubes in a push-pull Class B arrangement can give an output of 1.2 W when the anode and screen-grid voltages are 120 V and 2.15 W at 150 V.

In ABC receivers the filaments are normally operated in series, and it is then necessary to take account of the fact that the cathode currents of all tubes flow towards one terminal of the filament supply via the filament chain. The means for preventing overloading of individual filaments will be discussed in this Bulletin.

FREQUENCY CHANGER DK 92

DESCRIPTION

The DK 92 tube is a new 50 mA miniature heptode frequency changer for use both in all-dry battery receivers and in ABC receivers. It has a single electrode system, which includes a complete oscillator section. The DK 92 has a variable-mu characteristic making it suitable for applying A.G.C.
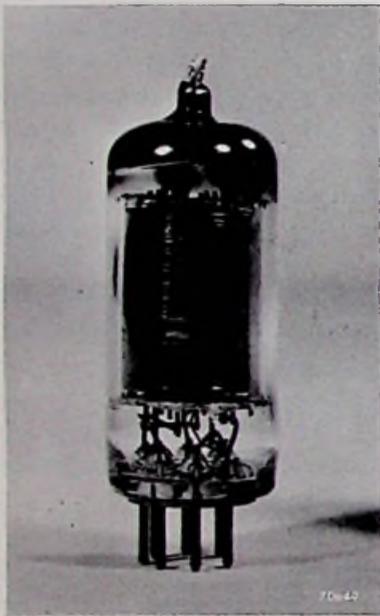

Fig. 1. The frequency changer DK 92.

This heptode may be used at frequencies up to 30 Mc/s (10 m) and will operate and give good reduced voltage performance over the large waveband coverages required at these frequencies, without any change of circuitry or increase of total current consumption. On the range for the highest frequencies capacitance neutralization must be included.

The first and second grids of the DK 92 tube form the oscillator section, the third grid is the signal grid, the fourth the screen grid, followed by a suppressor grid preceding the anode. Contrary to the former DK 91 tube, in the DK 92 the second and fourth grids are not tied to each other internally but connected to seperate base pins. This allows the fourth grid to be earthed capacitively, which reduces the coupling of the signal grid with the oscillator section, thereby reducing radiation and frequency shift. Moreover, with the grids connected to separate base pins, it is possible to choose the potential of the fourth grid independently, giving it such a value that optimum conversion conductance is obtained. In receivers operating with an H.T. of 90 V the conversion conductance of the DK 92 is 325 μA/V and with 67.5 V it is 300 μA/V at $I_{g1} = 130 \mu$A ($R_{g1} = 27$ kΩ).

In the DK 92 tube special measures have been taken to eliminate the main source of microphony. In battery tubes with low heater consumption vibration of the filament usually causes most trouble in this respect. For a given mechanical tension of the filament and a given material, sensitivity to microphony is proportional to the third power of the filament length. Moreover, since in view of the fragility of the filament a given mechanical tension may not be exceeded, with a long filament the resonant frequency necessarily becomes so low that it is no longer possible to improve the situation by artificially reducing the gain of the A.F. part of the receiver for that particular frequency without seriously affecting the quality of reproduction.

The filament of the DK 92 tube is therefore supported in the middle. In this way, in addition to obtaining a very effective damping, the resonant frequency is raised to a range where the A.F. gain of the receiver is already low.

The DK 92 tube requires an unusually low oscillator voltage (4 V$_{rms}$) on the first grid, which is particularly advantageous on the short-wave range. Furthermore, the mutual conductance between the first and second grids, which form the oscillator section, has a high value — viz. 0.9 mA/V at a supply voltage V_b of 90 V, and 0.8 mA/V at a supply voltage V_b of 67.5 V. Normal oscillator coils can, therefore, be used in the short-wave range, whilst the radiation of the local oscillator is particularly low. Owing to the low oscillator voltage requirement the total current drawn from the H.T.

supply is only 2.5 mA, including about 1.6 mA taken by the anode of the local oscillator (second grid) at $V_{g2} = 30$ V.

The comparatively small current of the DK 92 tube drawn from the H.T. supply is mainly due to the low oscillator voltage required on the first grid for obtaining optimum conversion conductance. This has been obtained by giving this grid fine meshes. The fact is that with given circuit constants the direct current to be supplied by the oscillator anode (g_2) is proportional to the required oscillator voltage on the first grid. This may be explained as follows.

Denoting the ratio of the peak value of the fundamental wave to the D.C. component of the anode current of the local oscillator by η, then: [1]

$$\eta = \frac{I_a \infty}{I_a} = \frac{S_{eff} \, V_{g \, osc}}{I_a},$$

where S_{eff} is the effective mutual conductance and $V_{g \, osc}$ is the peak value of the oscillator voltage at the first grid. Now the oscillating circuit satisfies the expression:

$$S_{eff} \, t \, Z = -1,$$

in which t represents the voltage ratio between the feedback coil and the tuned circuit, and Z is the impedance of the tuned circuit. Hence:

$$I_a = \frac{V_{g \, osc}}{\eta \, t \, Z} \, {}^2).$$

At the optimum oscillator voltage of 4 V_{rms} (i.e. 5.6 V peak value) η assumes a value of approximately 1.4, whilst in the short-wave range Z has a minimum value of approximately 3.5 kΩ, to which corresponds a voltage ratio $t = 0.7$. The mean anode current is therefore:

$$I_a = \frac{4 \times 1.4}{1.4 \times 0.7 \times 3.5 \times 10^3} = 1.6 \text{ mA}.$$

If for the optimum conversion conductance an oscillator voltage of 8 V were required the mean anode current of the oscillator would have been twice this value, i.e. approximately 3.2 mA.

When in a battery set the supply voltage has dropped to an extremely low value owing to prolonged use of the batteries, there is a risk of the

tube ceasing to oscillate, so that reception becomes impossible. The DK 92 tube has been so designed that the underrunning performance of the oscillator section is particularly good. In fact, the direct voltage on g_2 may be considerably lower than the supply voltage, so that a dropper resistor of fairly high value can be used, viz. 33 kΩ at $V_b = 90$ V, which largely compensates the effect of decreasing supply voltages on the oscillator performance. In a set designed for supply voltages of $V_b = 90$ V and $V_f = 1.4$ V, the local oscillator will still operate satisfactorily when these voltages have dropped to 65 V and 1.1 V respectively.

In exceptional cases where coils of poor quality are used, giving a low impedance of the tuned circuit, the oscillator performance can be improved at the expense of the current consumption by increasing the anode voltage of the local oscillator to about 45 V. The current consumption of the tube is then increased to almost 4 mA, which is the maximum permissible cathode current, but it should not be necessary to go as far as this.

APPLICATION OF THE DK 92

Since for the application of a frequency changer the oscillator performance is of primary importance, little need be said about the operation of the rest of the tube.

The screen grid g_4 of the DK 92 tube should preferably be operated at about 65 V, for this, in combination with the specified oscillator voltage, gives the optimum conversion conductance. In a receiver operating with an H.T. of 45 V the optimum screen-grid voltage is obviously not available, so that the tube then operates with a somewhat reduced conversion conductance. At an H.T. supply of 90 V the required screen-grid voltage may be obtained either from a tap on the H.T. battery or by connecting the screen grid via a by-passed dropper resistor to the H.T. The latter arrangement is preferable, because it has the advantage that, when the set operates with run-down batteries, there is some compensation of the loss in conversion conductance caused by decreased supply voltages.

In contrast to conventional indirectly heated frequency changers for mains supply, such as the ECH 42, the DK 92 operates with a single electron stream, which is first modulated by the oscillator voltage by means of g_1 and after that by the signal voltage applied to g_3. The first two grids, together with the filament, form the oscillator section, and it will be clear that the electron stream passed on

---

[1] See B. G. D a m m e r s, J. H a a n t j e s, J. O t t e and H. v a n S u c h t e l e n; Application of the Electronic Valve in Radio Receivers and Amplifiers, Volume I.
[2] The right-hand member of this equation would be negative, but since t must also be negative, a positive sign can be maintained when absolute values are substituted.

to the upper half of the tube is influenced by the potentials of both grids.

In an oscillator circuit the alternating voltages on the grid and the anode are in antiphase, so that the influence of the first grid on the electron stream is counteracted by that of the second grid, i.e. the oscillator anode. Since the first grid has a much greater influence on the electron stream than the second grid, the latter has no great demodulating effect, but for the sake of a high conversion conductance the alternating voltage on the second grid should nevertheless be kept low. For this reason the tuned circuit should be connected to the first grid, and the feed-back coil, which has a much smaller number of turns than the tuning coil, to the second grid.

With an oscillator voltage of 4 V_{rms} on the first grid, and a coil combination with a voltage ratio of 0.7 between feedback coil and tuning coil, the demodulating effect of the second grid gives rise to a reduction in conversion conductance of less than 2% compared with the case where the second grid is capacitively earthed.

Since different combinations of the tuning and the feedback coil with differing voltage ratios may be used with the DK 92 tube, in the data the conversion conductance is given for zero alternating voltage on the second grid. As indicated above, the actual conversion conductance obtained with normal oscillator coils does not, however, differ appreciably from the published value.

Another advantage connected with the tuned-grid arrangement is that the variation of the coupling between the oscillator and input circuits is kept small. The coupling between the oscillator section and the signal grid is determined partly by the capacitance between the second grid and the signal grid. In the case of a low oscillator voltage on the second grid the contribution of the above-mentioned capacitance towards the total coupling between the oscillator section and the signal grid is small, so that the variation in the coupling between the oscillator section and the signal grid is also small when the oscillator voltage on the second grid varies with the frequency as a result of variations in the voltage transfer.

The feedback winding can be either series or parallel fed. Series feed is the most satisfactory on short-wave operation, as it gives the best possible oscillator drive and better high-frequency performance than parallel feed. Moreover, with low H.T. supply, say 45 V, the resistor shunted across the feedback winding with parallel feed must have a low value, and this reduces the effective quality factor of the oscillator circuit. Parallel feed can very well be used on the medium and long-wave ranges. It offers the advantage that it gives rise to less variation of the grid current over the wave ranges than series feed. Since, however, in a receiver with three wave ranges the switching over from series feed to parallel feed makes it necessary to use a comparatively large number of swich contacts, series feed will usually be perferred for all wave ranges.

For optimum oscillator performance the grid leak should be connected to the positive end of the filament.

Although the oscillator performance of the DK 92 tube is better than that of similar 1.4 V battery frequency changers, it is advisable to neutralize the induction effect in the short-wave range so as to reduce not only the influence of variations of the input circuit impedance on the oscillator frequency (pulling effect) but also the influence of the A.G.C. on the oscillator frequency (frequency shift). If neutralizing is applied, which is done by connecting a capacitor of 1.5 pF to 2 pF between the first and third grids, the DK 92 tube can be used on frequencies up to 30 Mc/s (10 m). In the normal short-wave range from 20 Mc/s to 6 Mc/s (15 m to 50 m) A.G.C. can then be applied.

The phenomena inherent in the coupling between the oscillator section and the input circuit, which may be observed with all frequency changer tubes, is of sufficient importance to be dealt with at some greater length.

The coupling between the oscillator and the input circuits is caused by various tube and wiring capacitances and also by the induction effect, which may be represented as a negative one-sided capacitance between the first and third grids.

Fig. 2 is the schematical representation of this coupling. In this diagram $C_{1,3}$ and $C_{2,3}$ are the normal coupling capacitances, which may consist partly of wiring capacitances. The capacitance C_{ind} represents the induction effect. This is caused by a sheath of electrons between the second and third grids, the density of which is modulated by the oscillator voltage on the first grid. The variations in density induce currents in the input circuit; the phase and amplitude of these currents correspond to the presence of a negative capacitance between the first and third grids. This capacitance is one-sided because the voltage on the third grid has

practically no influence on the space charge surrounding the cathode, whilst its modulation of the space charge between the second and third grids has little effect on the first grid. The total coupling between the oscillator circuit and the input circuit can now be replaced by an equivalent capacitance:

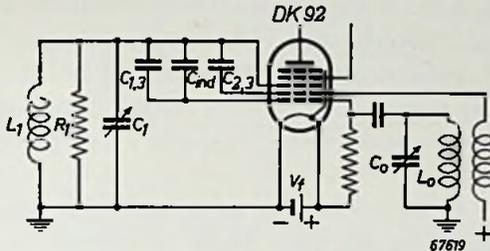$$C_{eq} = C_{1,3} + C_{2,3} \cdot t + C_{1nd}.$$

Fig. 2. Simplified diagram showing the coupling between the oscillator and the input circuit.

In this expression t is the ratio of the alternating voltages on the second and first grids. The first term of the right-hand member is positive, but since the feedback t must be negative the following two terms are both negative. In practice the negative terms preponderate and the total coupling between the first and third grids assumes the form of a negative capacitance.

The presence of this capacitance affects the overall performance, in particular at high frequencies. In the first place a proportion of the oscillator voltage appears at the signal grid and gives rise to radiation, whilst, moreover, trimming of the receiver becomes complicated because of the pulling effect. The oscillator voltage induced in the input circuit is proportional to C_{eq} and to the impedance of the input circuit. It can be shown that the induced voltage is roughly proportional to the third power of the signal frequency. Moreover, the induced voltage increases as the resonant frequency of the input circuit approaches the oscillator frequency. Assuming the input circuit to be correctly tuned, the oscillator voltage on the signal grid is inversely proportional to the intermediate frequency.

On medium and long waves the coupling discussed above does not give rise to difficulties, but on the short-wave range radiation, frequency shift and a reduction of the effective quality factor of the oscillator circuit may be experienced. The latter two effects are caused by the reactive and resistive parts respectively of the impedance formed by the series connection C_{eq} and the input circuit. In extreme cases, when the resonant frequency of the coupling capacitor together with the input circuit approaches the oscillator frequency, the frequency shift of the oscillator may become excessive, and the local oscillator may even cease to function.

These effects can be reduced by means of the following measures:

a) The intermediate frequency should be high to ensure large spacing of the resonant frequencies of the oscillator and input circuits. In this connection a high intermediate frequency of, say, 450 kc/s is recommended.

b) Care should be taken in choosing the padding. Large deviations in the padding curve may nullify the favourable influence of a high intermediate frequency.

c) When the coupling capacitance and the input circuit are in series resonance at the oscillator frequency, the parallel resistance reflected into the oscillator circuit is inversely proportional to the quality factor of the input circuit. It is therefore advisable to keep this quality factor as low as permissible in view of the requirements of preselection and gain.

d) The effective negative capacitance between the first and third grids can be compensated by connecting a normal positive capacitance between these electrodes.

Although it is impracticable to obtain perfect compensation over the entire short-wave range, the reduction of the pulling effect and radiation achieved by capacitance compensation is quite satisfactory in practical circuits.

The fact that ideal compensation cannot be obtained in practice can be explained as follows. The location of the negative space charge between the second and third grids depends on the potentials of g_2 and g_4 and, therefore, also on the oscillator voltage, because in the normal circuit with a dropper resistor in series with the second grid, the automatic bias of the oscillator section influences the average potential of the latter electrode. Compensation is therefore possible only for a fixed set of operating conditions. Moreover, due to transit time effects and the fact that the voltages at g_1 and g_2 are not exactly in antiphase, the coupling cannot be represented by an equivalent negative capacitance at frequencies exceeding 20 Mc/s. At high frequencies the coupling assumes the form of a

combination of capacitance and resistance and ideal compensation can be obtained only by a similar combination of capacitance and resistance, the resistance value being correct at one fixed frequency only. It has been found that a purely capacitive compensation is still satisfactory at frequencies up to 30 Mc/s (10 m).

The quantitative results of measurements of radiation and pulling carried out with the DK 92 tube on short waves are given below. It is seen that this tube gives excellent performance on these waves, and this ensures that on longer waves performance is even better.

PRACTICAL CIRCUIT

A circuit for the two short-wave ranges, viz. 30 Mc/s to 9 Mc/s (10 m — 33 m) and 10 Mc/s to 3.3 Mc/s (30 m — 90 m) is given in fig. 3. The addition

prevents the oscillator voltage from increasing at the upper end of the frequency range. Moreover, a booster coil L_{10} is used to increase the feedback at lower frequencies, the frequency at which L_9 and L_{10} together with the capacitor of 82 pF resonate being approximately 8 Mc/s (38 m).

Fig. 4 shows the current flowing through the oscillator grid leak of 27 kΩ in the range of 30 Mc/s to 9 Mc/s, both at the nominal supply voltage and at reduced filament and H.T. supply voltages. It is seen that the current through the grid leak is fairly constant over the entire wave range. Similar curves have been plotted in fig. 5 for the range of 10 Mc/s to 3.3 Mc/s.

The radiation of the local oscillator and the pulling effect are most likely to become troublesome in the range from 30 Mc/s to 9 Mc/s. The compensating capacitance is therefore adjusted for
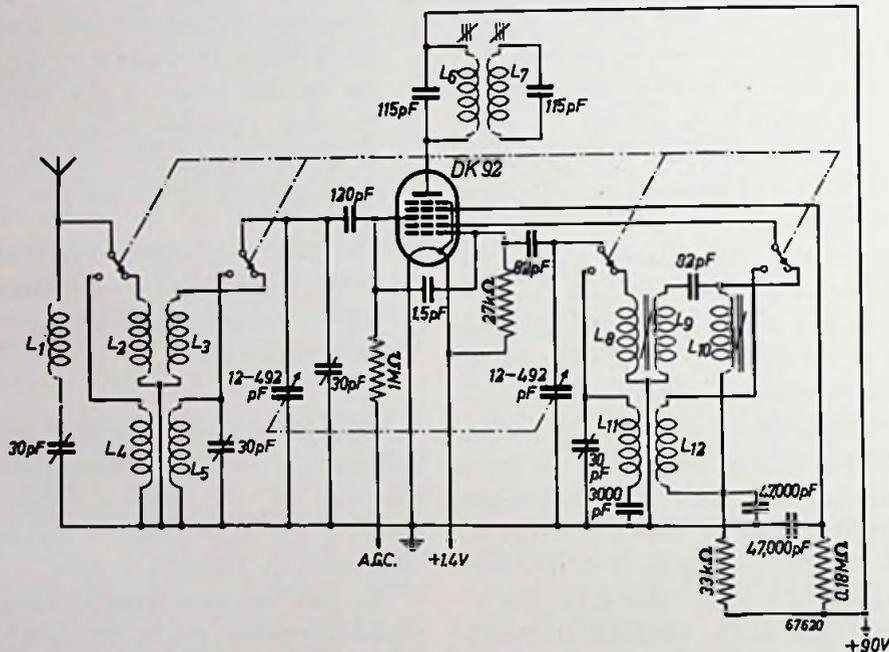

Fig. 3. Frequency changer circuit for the ranges 30 Mc/s to 9 Mc/s (10 m to 33 m) and 10 Mc/s to 3.3 Mc/s (30 m to 90 m). In the range 30 Mc/s to 9 Mc/s the A.G.C. should be switched off.

of a medium- and a long-wave range does not involve any difficulty. The coupling between the oscillator and input circuits is compensated by a small ceramic capacitor of 1.5 pF between the first and third grids.

In the range from 30 Mc/s to 9 Mc/s various steps are taken to ensure a constant oscillator voltage over the entire range. The oscillator coils are provided with an iron dust core, so that the quality factor decreases with increasing frequency. This

minimum radiation at the upper end of this frequency range; the pulling effect is then also reduced to its minimum.

Fig. 6 shows the radiation voltage measured at the aerial terminals as a function of the frequency. During this measurement the aerial terminals were shunted by a resistor of 400 Ω.

In fig. 7 the pulling effect of the oscillator frequency has been plotted as a function of the capacitance variation of the input circuit at an oscil-

lator frequency of 30 Mc/s. This curve also refers to the case where compensation is applied.

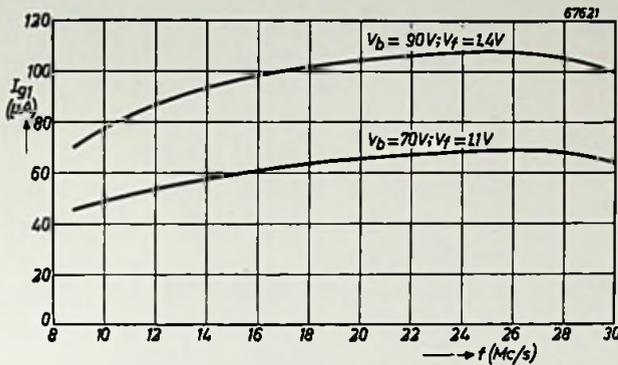At the nominal supply voltages the conversion gain of the DK 92 tube at 30 Mc/s, measured be-

Fig. 4. Current I_{g1} flowing through the grid leak as a function of the frequency f in the range 30 Mc/s to 9 Mc/s for the nominal and reduced supply voltages.

tween the signal grid and the I.F. transformer secondary, is 45. The aerial gain is 1.2, so that the gain measured between the aerial and the I.F. transformer secondary is 54. This gain is practically constant over the entire range of 30 Mc/s to 9 Mc/s.
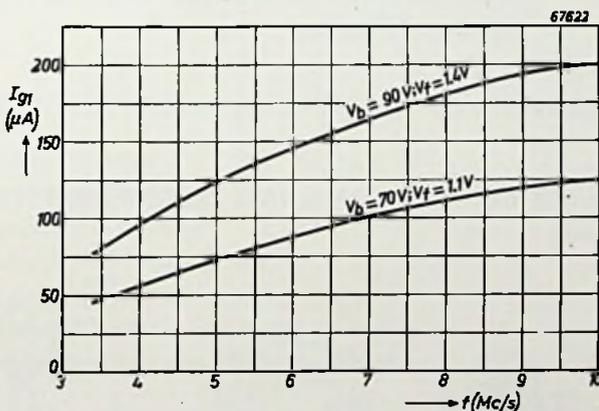

Fig. 5. As fig. 4, but for the range of 10 Mc/s to 3.3 Mc/s.

At 7 Mc/s, in the range of 10 Mc/s to 3.3 Mc/s, the total gain is 60.

As a final note is should be pointed out that it is advisable to short the coils which are not used in a particular range. In the range of 30 Mc/s to 9 Mc/s, for example, the coils L_4L_5 and $L_{11}L_{12}$ should be shorted by the switch. This is necessary to avoid that capacitive couplings via the switch contacts give rise to a considerable reduction of the oscillator voltage at a frequency at which the switch capacitance happens to resonate with the coils of the other range.
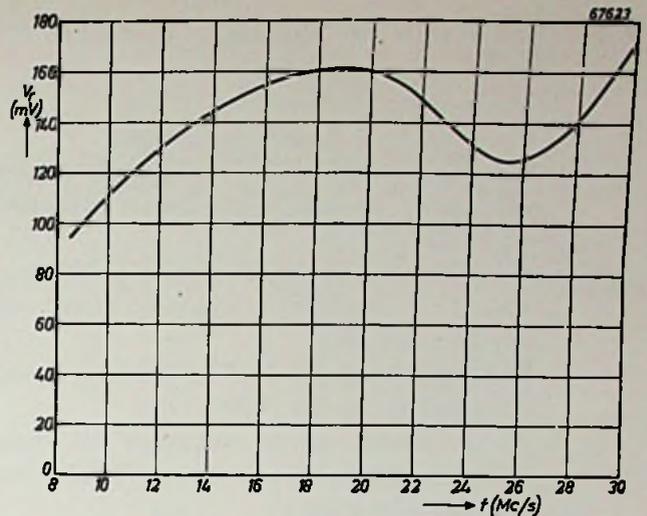

Fig. 6. Radiation voltage at the aerial terminals as a function of frequency.
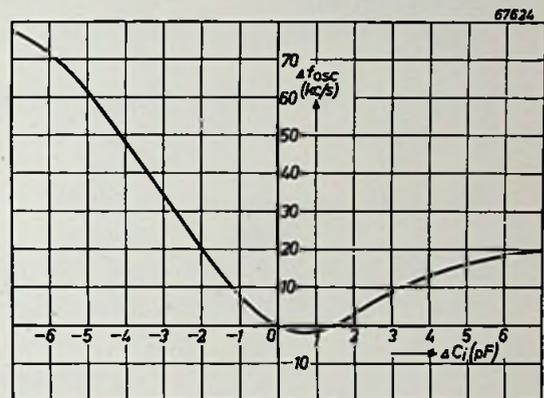

Fig. 7. Pulling effect of the oscillator frequency as a function of the capacitance variation of the input circuit at an oscillator frequency of 30 Mc/s.

The coils used in the circuit of fig. 3 have the following values:

L_1 I.F. wave trap for 452 kc/s.
Inductance 5 mH.
Quality factor $Q = 125$.
Self-capacitance 2.5 pF.

L_2L_3 Aerial coils for the range 30 Mc/s to 9 Mc/s.
Coil former: diameter   9 mm,
                length   50 mm.
Screening can: diameter   27 mm,
                length   55 mm.
L_2: 19¼ turns of 0.1 mm enamelled copper wire; wave wound, width 3 mm; inductance 4 µH.
L_3: 10 turns of 0.5 mm enamelled copper wire; wound in one layer, pitch 0.65 mm; inductance 0.67 µH.
Distance between ends of L_2 and L_3 is 1 mm.
Coupling factor $k = 0.185$.

11

L_4L_3 Aerial coils for the range 10 Mc/s to 3.3 Mc/s.

Coil former: diameter 8 mm, length 30 mm.

L_4: 82½ turns of 0.1 enamelled copper wire; wave wound, width 2 mm; inductance 75 μH.

L_3: 31½ turns of litz wire of 12 × 0.04 mm; wound in one layer, pitch 0.27 mm; inductance 4.7 μH.

Distance between ends of L_4 and L_5 is 1 mm.

Coupling factor k = 0.185.

No screening can is employed for these coils; the former is provided with soldering lugs for wiring in.

L_6L_7 I.F. transformer for 452 kc/s.

Quality factor Q at 452 kc/s is 145 (without extra damping).

Coupling $KQ = 1.05$ (without extra damping).

L_8L_9 Oscillator coils for range 30 Mc/s to 9 Mc/s.

Coil former: diameter 7 mm [3]), length 22 mm.

Iron dust core: diameter 6 mm [4]), length 6 mm.

L_8: 10½ turns of 0.3 mm enamelled copper wire; wound in one layer, pitch 0.75 mm;

inductance 0.64 μH (with iron dust core).

L_9: 9½ turns of 0.3 mm enamelled copper wire; wound in one layer between turns of L_8.

Coupling factor $k = 0.8$.

L_{10} Booster coil for range 30 Mc/s to 9 Mc/s.

Coil former: diameter 7 mm [3]), length 22 mm.

Iron dust core: diameter 6 mm [4]), length 6 mm.

30½ turns of 0.3 mm enamelled copper wire; wound in onze layer, pitch 0.65 mm; inductance 4.5 μH.

$L_{11}L_{22}$ Oscillator coils for range 10 Mc/s to 3.3 Mc/s.

Coil former: diameter 8 mm, length 30 mm.

L_{11}: 28 turns of 0.2 mm enamelled copper wire wound in one layer, pitch 0.66 mm; inductance 4.2 μH.

L_{12}: 12 turns of 0.1 mm enamelled copper wire; wound in one layer without spacing between turns over bottom end of L_{11} with 0.1 mm insulating paper interleaved.

Voltage ratio $L_{12}/L_{11} = 1/2.25$.

No screening can is employed for these coils; the former is provided with soldering lugs for wiring in.

TECHNICAL DATA

FILAMENT DATA

Heating

Direct by battery current, rectified A.C. or D.C.; series or parallel supply.

Parallel supply

Filament voltage	V_f	= 1.4 V
Filament current	I_f	= 0.05 A

Series supply

Filament voltage	V_f	= 1.3 V

Mounting position: any

---

[3]) Threaded on the inside to receive threaded iron dust core.

[4]) Threaded.

BASE CONNECTIONS AND DIMENSIONS (in mm)
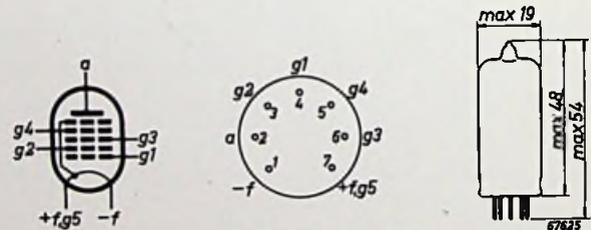
Fig. 8.

CAPACITANCES

C_a	=	8.4 pF
C_{g3}	=	7.5 pF
C_{g2}	=	4.8 pF
C_{g1}	=	3.9 pF
C_{ag3}	<	0.36 pF
C_{ag2}	<	0.3 pF
C_{ag1}	<	0.11 pF
C_{g1g3}	<	0.2 pF
C_{g1g2}	=	3.0 pF
C_{g2g3}	=	1.6 pF

OPERATING CHARACTERISTICS *(with separate excitation)*

Supply voltage	V_b[5])	41	63.5	85	V
Anode voltage	V_a	41	63.5	85	V
Screen-grid voltage	V_{g4}	41	63.5	60	V
Signal-grid voltage	V_{g3}	0	0	0	V
D.C. voltage on second grid	V_{g2}	29	30	30	V
Oscillator voltage on first grid	V_{osc}	2.5	4	4	V_{rms}
Screen-grid resistor	R_{g4}	0	0	180	kΩ
Series resistor for osc. anode (g_2)	R_{g2}	6.8	22	33	kΩ
Leak resistor of first grid	R_{g1}	27	27	27	kΩ [6])
Anode current	I_a	0.25	0.70	0.65	mA
Screen-grid current	I_{g4}	0.09	0.15	0.14	mA
Current of second grid	I_{g2}	1.75	1.55	1.65	mA
Oscillator current	I_{g1}	80	130	130	μA
Conversion conductance	S_c	180	300	325	μA/V [7])
Bias at g_3 for $S_c' = \frac{1}{100} S_c$	V_{g3}	—2.9	—4	—6	V
Internal resistance ($V_{g3} = 0$ V)	R_i	0.75	0.9	1.0	MΩ
Equivalent noise resistance	R_{eq}	115	120	100	kΩ

[5]) Based on a battery voltage of 45, 67.5 or 90 V reduced by the bias for the output tube.
[6]) Connected to $+$ f.
[7]) The DK 92 will normally be used with self-excitation. With grid tuning and on the normal wave ranges the conversion conductance will then be a few per cent smaller than that obtained with separate excitation.

TYPICAL CHARACTERISTICS OF THE OSCILLATOR SECTION

Anode voltage	V_a	41	63.5	85	V
Screen-grid voltage	V_{g4}	41	63.5	60	V
Signal-grid voltage	V_{g3}	0	0	0	V
Voltage at second grid	V_{g2}	29	30	30	V
Current of second grid	I_{g2}	3	2.2	2.5	mA
Transconductance between g_2 and g_1	S_{g2g1}	1.1	0.8	0.9	mA/V
Amplification factor between g_2 and g_1	μ_{g2g1}	9	7.5	7.5	

LIMITING VALUES

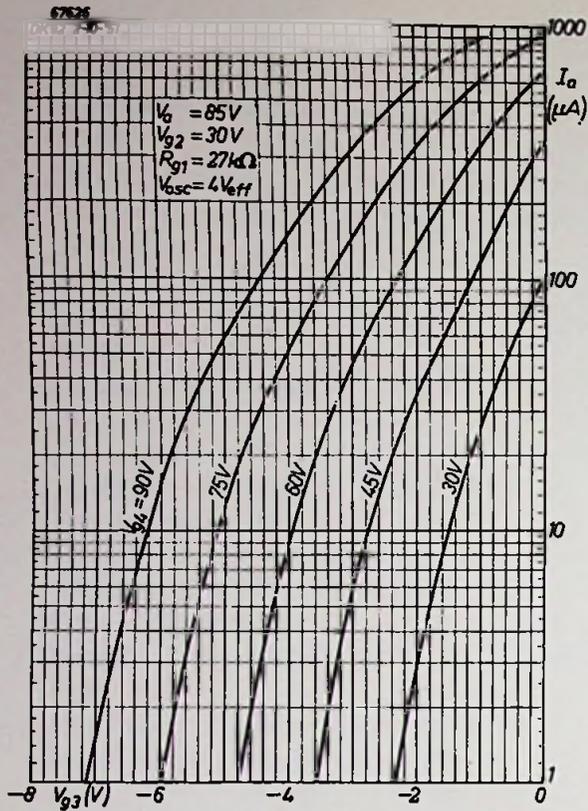|				
Supply voltage	V_b	max.	120	V [8])
Anode voltage	V_a	max.	90	V
Anode dissipation	W_a	max.	0.2	W
Screen-grid voltage	V_{g4}	max.	90	V
Screen-grid dissipation	W_{g4}	max.	0.1	W
Voltage on second grid	V_{g2}	max.	60	V
Dissipation of second grid	W_{g2}	max.	0.2	W
Cathode current	I_k	max.	4	mA
External resistance between g_3 and −f	R_{g3}	max.	3	MΩ
First grid voltage for $I_{g1} = +0.3$ μA	V_{g1}	max.	—0.2	V

[8]) Absolute value 140 V.

Fig. 9. Anode current as a function of the third-grid voltage with the screen-grid voltage as parameter, for $V_a =$ 85 V.
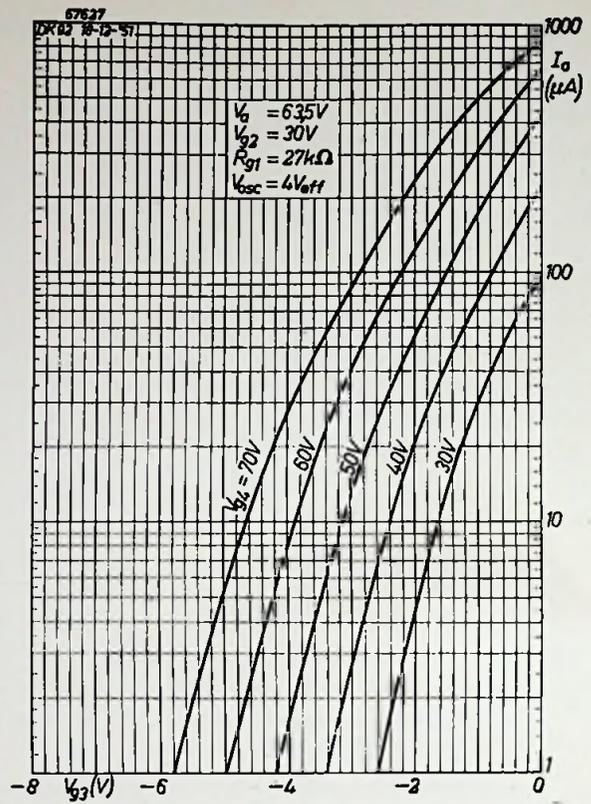

Fig. 10. Anode current as a function of the third-grid voltage with the screen-grid voltage as parameter, for $V_a =$ 63.5 V.
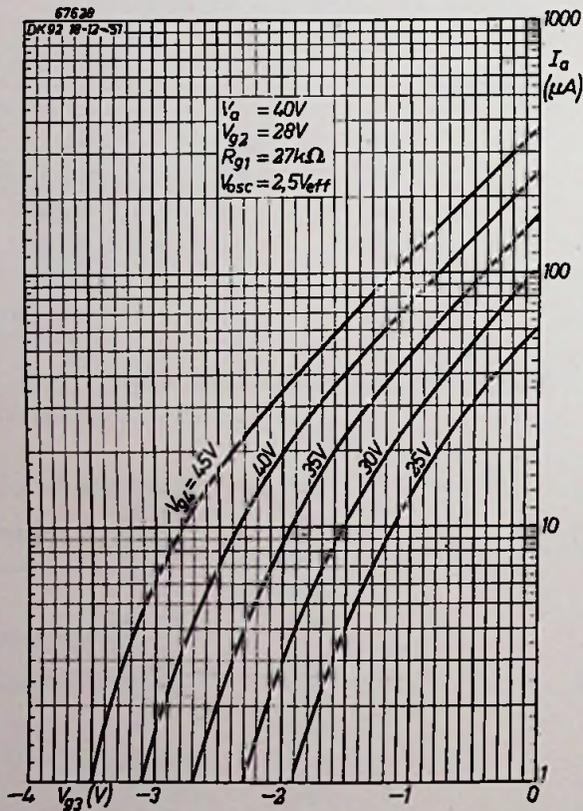

Fig. 11. Anode current as a function of the third-grid voltage with the screen-grid voltage as parameter, for $V_a =$ 40 V.
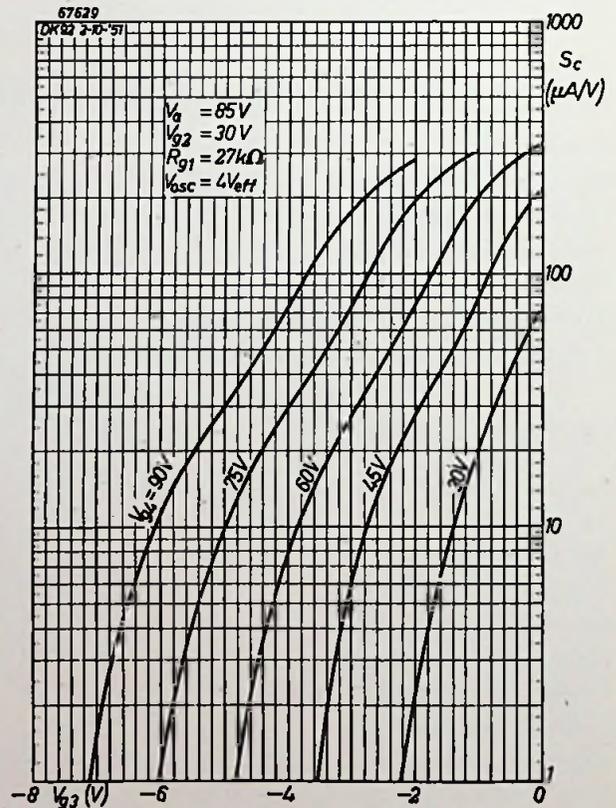

Fig. 12. Conversion conductance as a function of the third-grid voltage with the screen-grid voltage as parameter, for $V_a =$ 85 V.
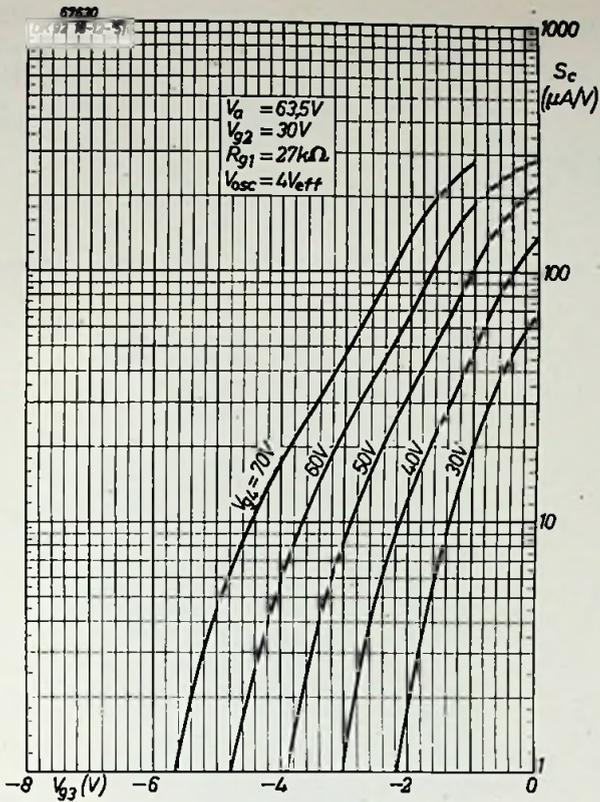
14

Fig. 13. Conversion conductance as a function of the third-grid voltage with the screen-grid voltage as parameter, for $V_a = 63.5$ V.
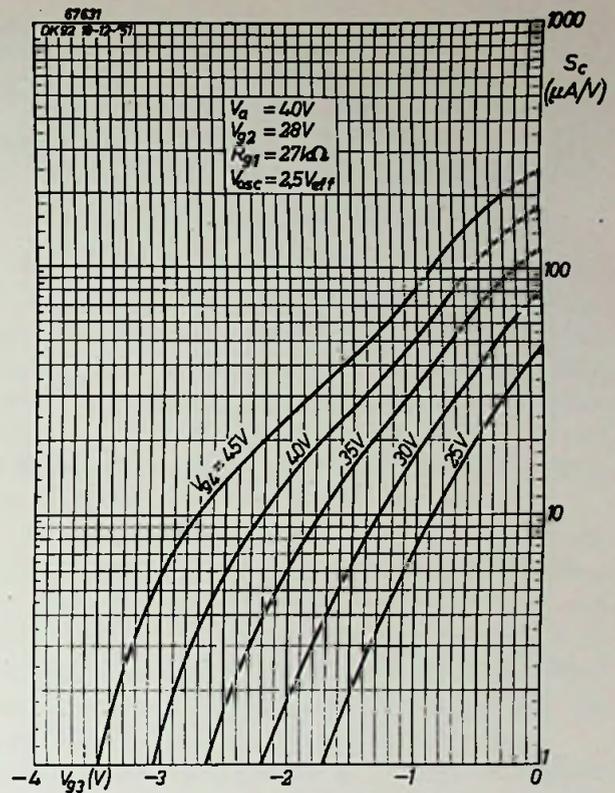

Fig. 14. Conversion conductance as a function of the third-grid voltage with the screen-grid voltage as parameter, for $V_a = 40$ V.
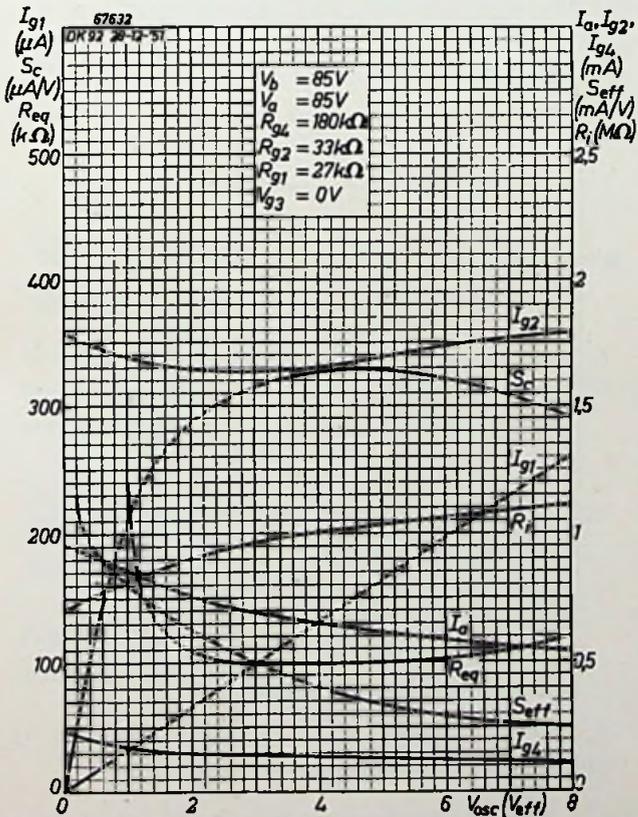

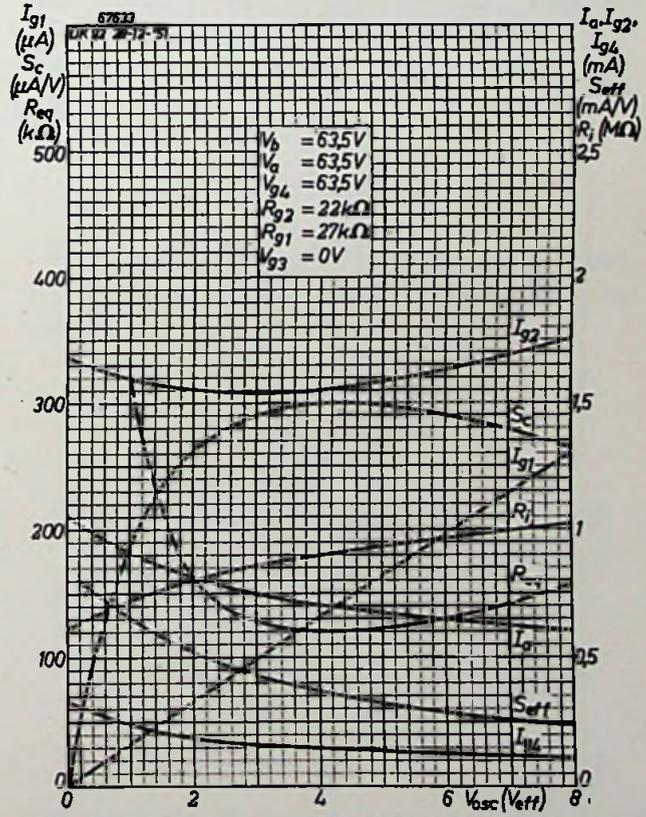*Fig. 15.* Performance of the DK 92 as a function of the oscillator voltage, for $V_a = 85$ V.

Fig. 16. Performance of the DK 92 as a function of the oscillator voltage, for $V_a = 63.5$ V.
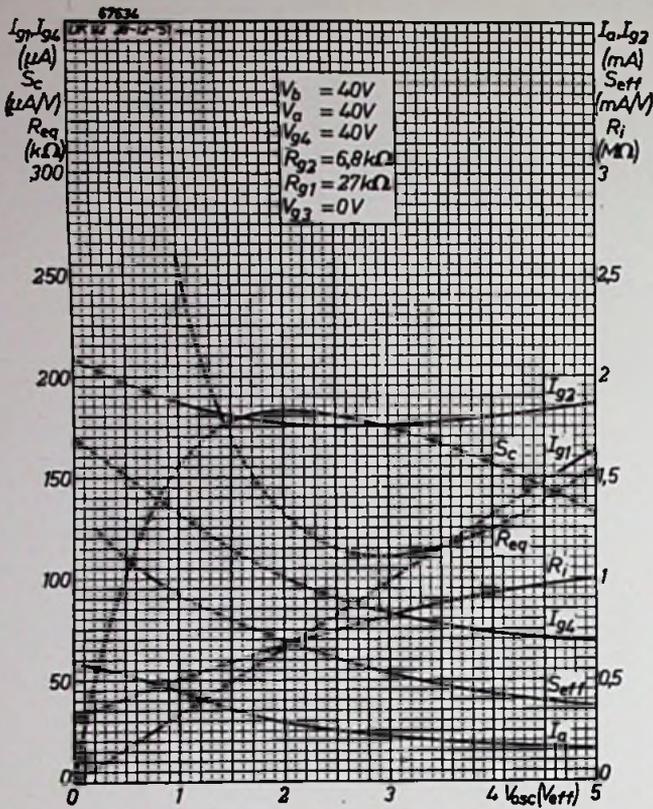
Fig. 17. Performance of the DK 92 as a function of the oscillator voltage, for $V_a = 40$ V.

Fig. 18. Currents, conversion conductance and internal resistance plotted against the third-grid voltage, for optimum oscillator voltage and an anode voltage of 85 V.
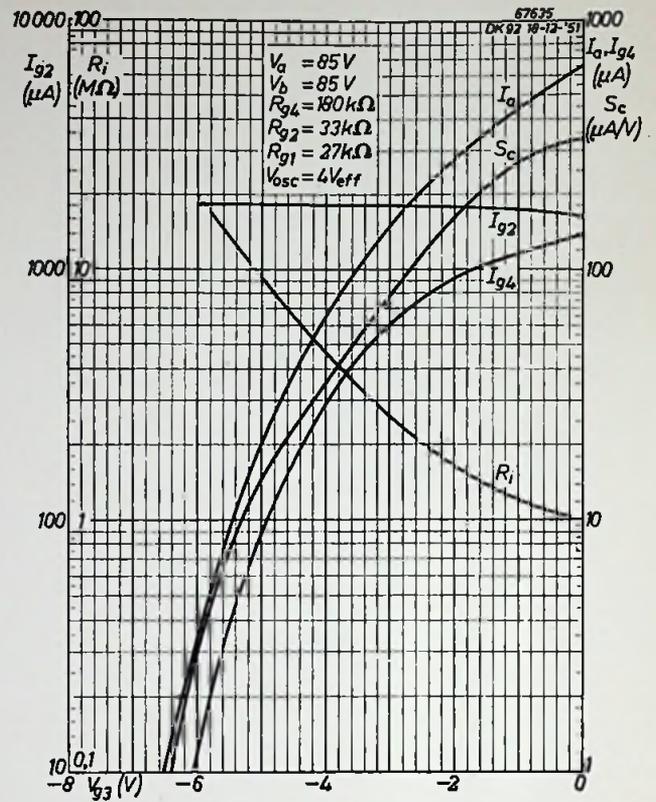

Fig. 19. Currents, conversion conductance and internal resistance plotted against the third-grid voltage, for optimum oscillator voltage and an anode voltage of 63.5 V.

Fig. 20. Currents, conversion conductance and internal resistance plotted against the third-grid voltage, for optimum oscillator voltage and an anode voltage of 40 V.
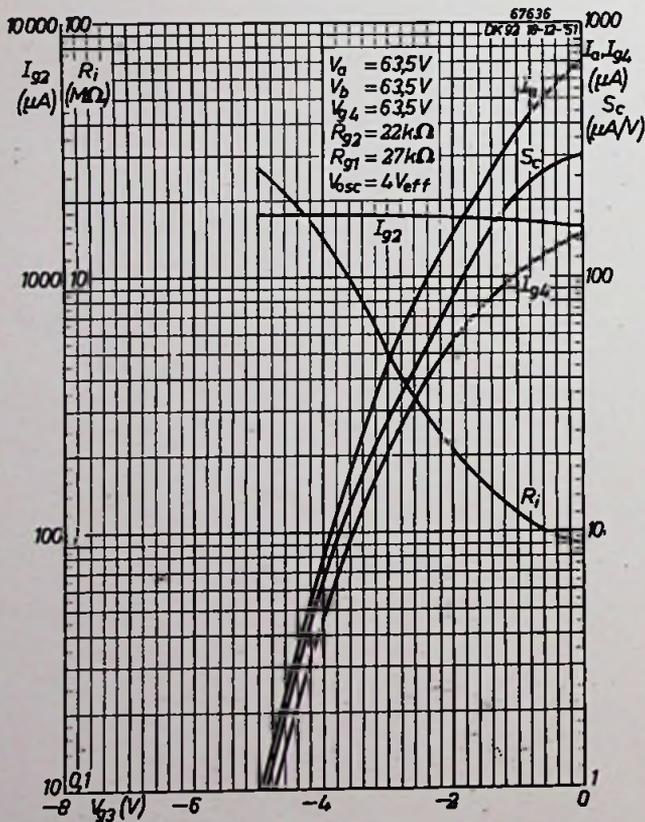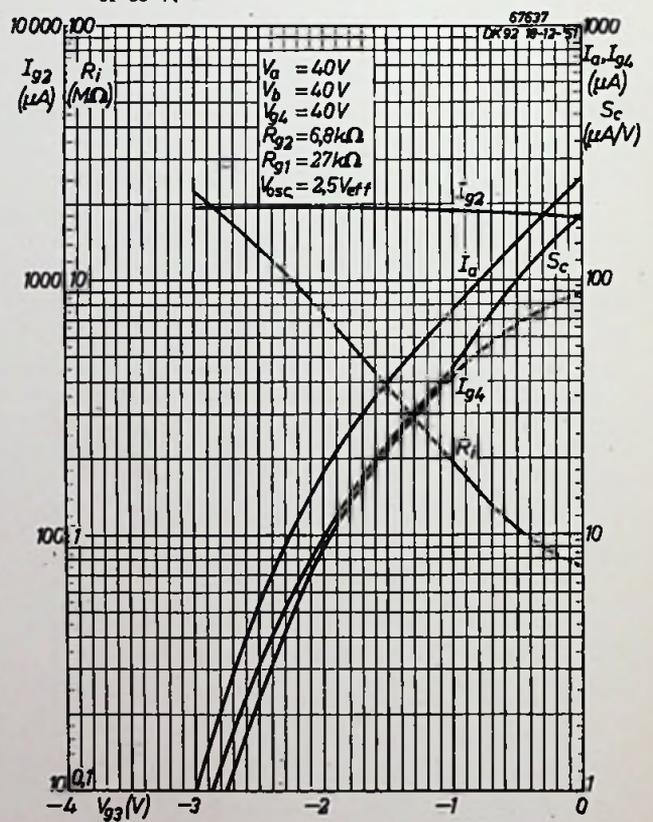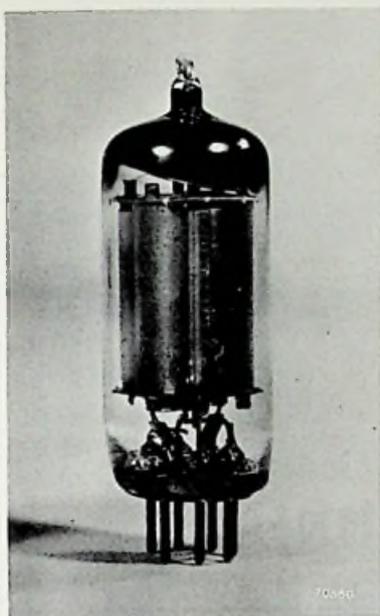
16

R.F. PENTODE DF 91

Fig. 21. The R.F. pentode DF 91.

The DF 91 is a 7-pin miniature pentode for battery, rectified A.C. or D.C. mains supply. The filament current is 50 mA at 1.4 V for parallel supply. With series supply it is recommended to reduce the filament voltage to 1.3 V, in order to prevent filament overloading as a result of mains voltage fluctuations.

The DF 91 has a variable-mu characteristic, the bias required for reducing the mutual conductance to 10 μA/V being 10 V in the case of a screen-grid voltage of 45 V. Since the frequency changer DK 92 is also suitable for A.G.C., in a receiver the control voltage can be applied to two tubes, and this ensures a favourable A.G.C. curve.

The operation of the DF 91, with a screen-grid voltage of 45 V instead of 67.5 V is favourable with regard to cross modulation and gain control. It is true that with $V_{g2} = 67.5$ V a slightly higher mutual conductance can be obtained, but with $V_{g2} = 45$ V the mutual conductance is but little reduced, whilst the current consumption is much lower.

TECHNICAL DATA

FILAMENT DATA

Heating
Direct by battery current, rectified A.C. or D.C., series or parallel supply.

Parallel supply

Filament voltage	V_f	= 1.4 V
Filament current	I_f	= 0.05 A

Series supply

Filament voltage	V_f	= 1.3 V

CAPACITANCES		
	C_a	= 7.5 pF
	C_{g1}	= 3.6 pF
	C_{ag1}	< 0.01 pF [o])

[o]) Measured with external screening.

BASE CONNECTIONS AND DIMENSIONS (in mm)
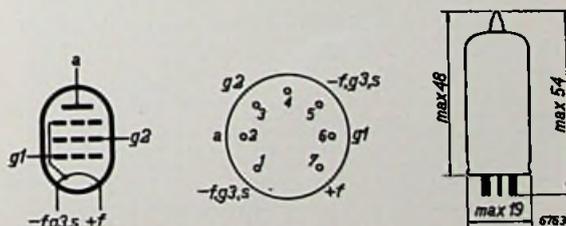
Fig. 22.

Mounting position: any

OPERATING CHARACTERISTICS

		V_a 45		V_a 67.5		V_a 90		
Anode voltage	V_a	45		67.5		90		V
Screen-grid voltage	V_{g2}	45		45		45		V
Control grid voltage	V_{g1}	0	—10	0	—10	0	—10	V
Anode current	I_a	1.7	—	1.75	—	1.8	—	mA
Screen-grid current	I_{g2}	0.7	—	0.68	—	0.65	—	mA
Mutual conductance	S	700	10	725	10	750	10	μA/V
Internal resistance	R_i	0.35	>10	0.6	>10	0.8	>10	MΩ
Amplification factor between screen grid and control grid	μ_{g2g1}	11	—	11	—	11	—	
Equivalent noise resistance	R_{eq}	18	—	17	—	16	—	kΩ

LIMITING VALUES

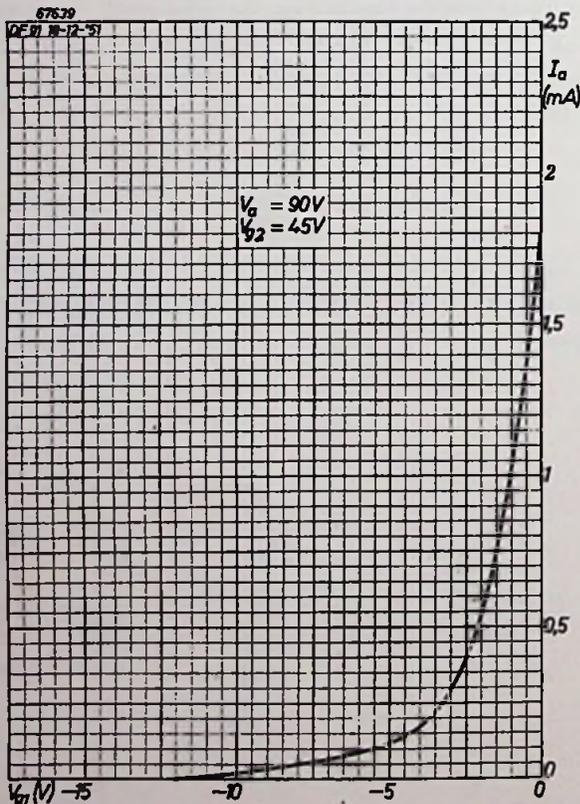|				
Supply voltage	V_b	max.	120	V [10])
Anode voltage	V_a	max.	90	V
Anode dissipation	W_a	max.	0.5	W
Screen-grid voltage	V_{g2}	max.	67.5	V
Screen-grid disipation	W_{g2}	max.	0.2	W
Cathode current	I_k	max.	5.5	mA
External resistance between g_1 and $-f$	R_{g1}	max.	3	MΩ
Control-grid voltage for $I_{g1} = +0.3\ \mu$A	V_{g1}	max.	—0.2	V

[10]) Absolute value 140 V.

Fig. 23. Anode current plotted against control-grid voltage for $V_{g2} = 45$ V and $V_a = 90$ V.

Fig. 24. Anode current, screen-grid current, mutual conductance and internal resistance plotted against the control-grid voltage, for $V_a = V_{g2} = 45$ V.
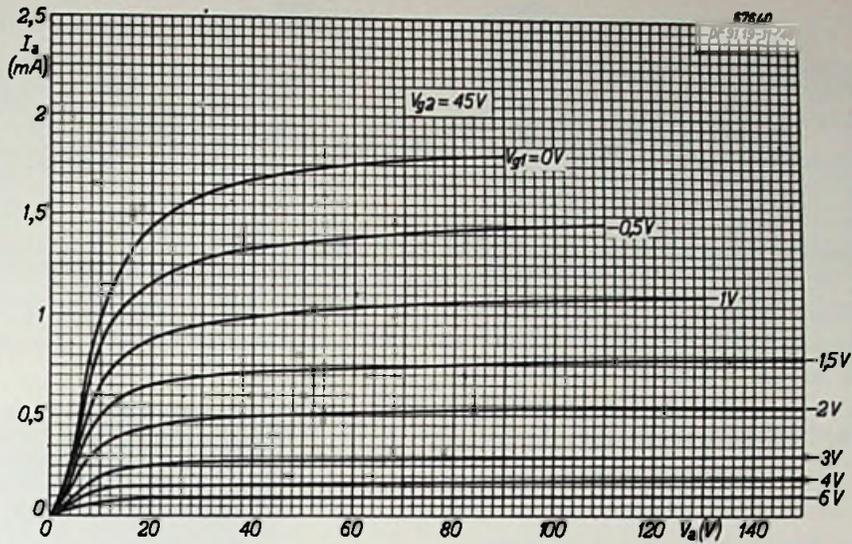
Fig. 25. Anode current plotted against anode voltage with V_{g1} as parameter, for $V_{g2} = 45$ V.
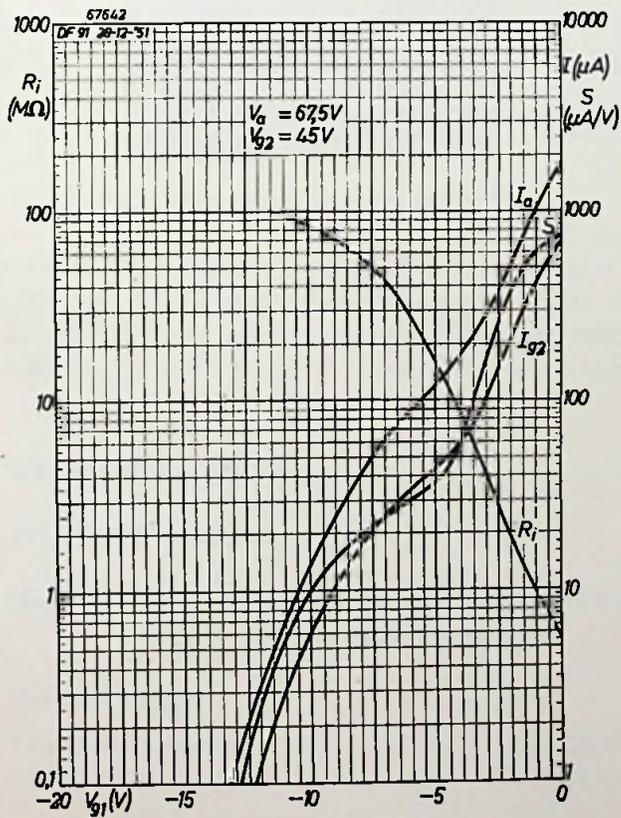
Fig. 26. Anode current, screen-grid current, mutual conductance and internal resistance plotted against the control-grid voltage, for $V_a = 67.5$ V and $V_{g2} = 45$ V.
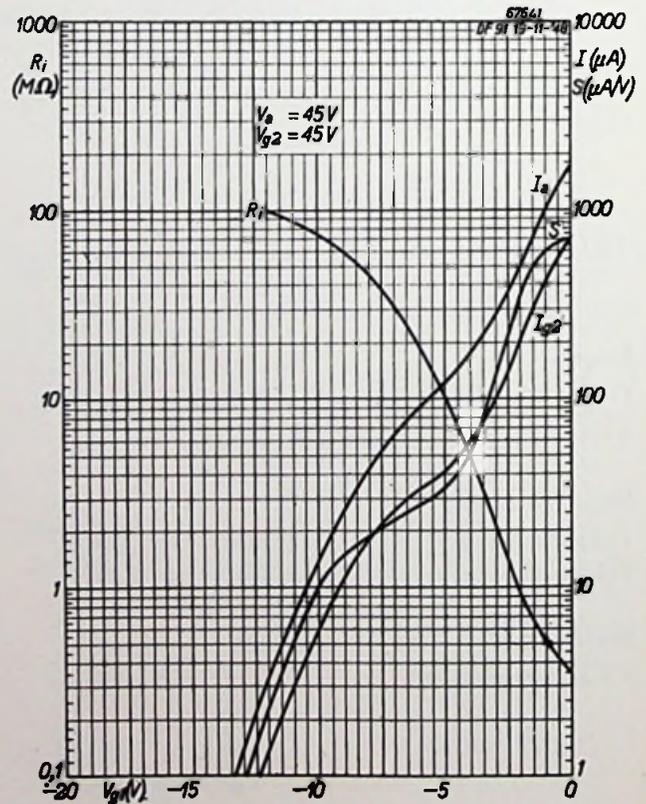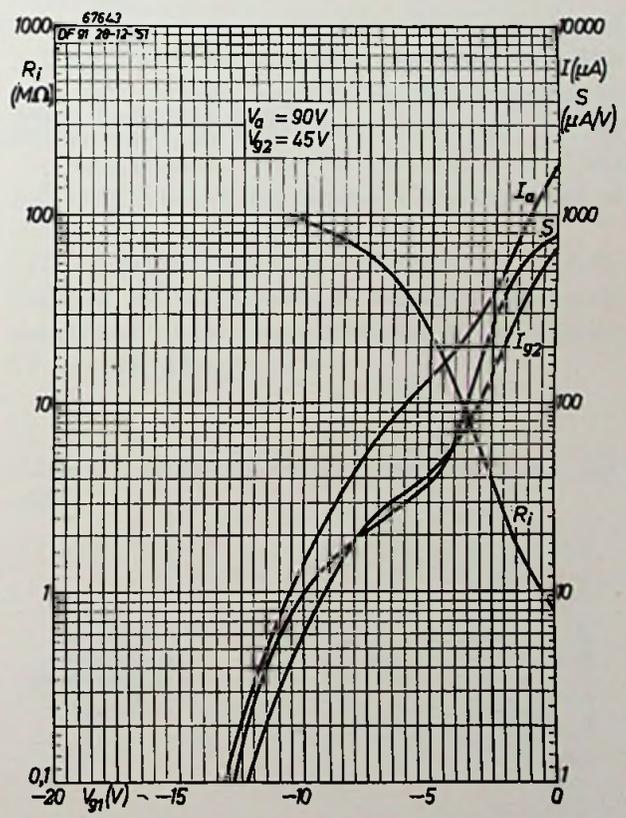

Fig. 27. Anode current, screen-grid current, mutual conductance and internal resistance plotted against the control-grid voltage, for $V_a = 90$ V and $V_{g2} = 45$ V.

19
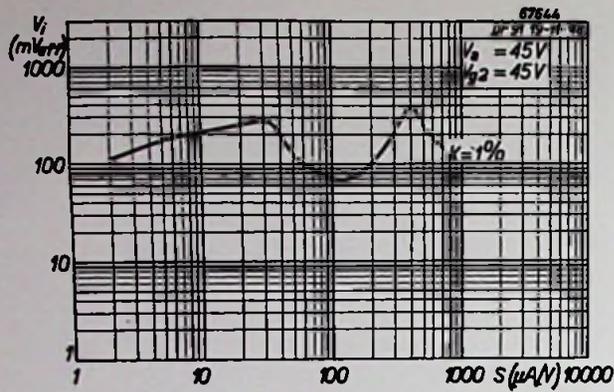
Fig. 28. Input signal plotted against the mutual conductance for a cross modulation of 1%, for $V_a = V_{g2} = 45$ V.
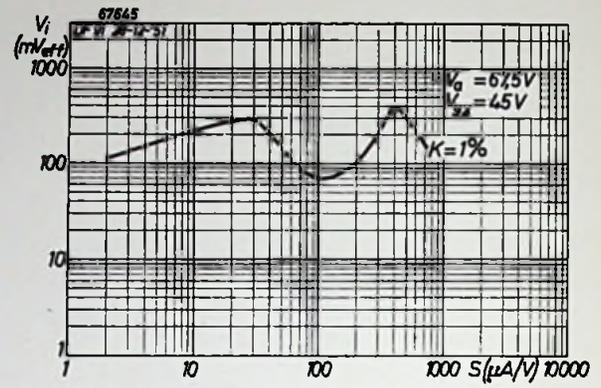
Fig. 29. Input signal plotted against the mutual conductance for a cross modulation of 1%, for $V_a = 67.5$ V and $V_{g2} = 45$ V.
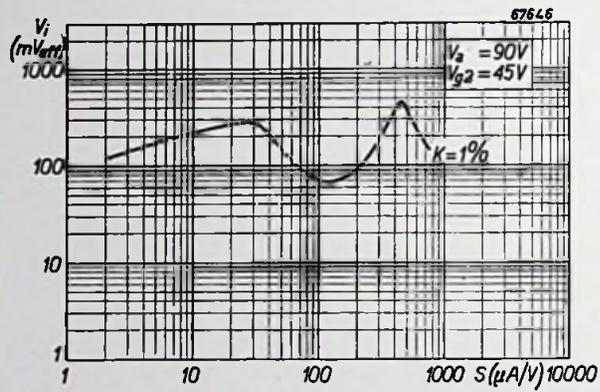
Fig. 30. Input signal plotted against the mutual conductance for a cross modulation of 1%, for $V_a = 90$ V and $V_{g2} = 45$ V.

DIODE A.F. PENTODE DAF 91

The DAF 91 is designed for performing the functions of a combined detector and A.F. amplifier preceding the output tube. In the circuit given on the next page the maximum obtainable A.F.

Fig. 31. The diode A.F. pentode DAF 91.

gain is 70. An output voltage of 5 V_{rms} is obtainable and this is more than sufficient to drive a DL 92 or DL 94 output pentode. The tube may also be used as a triode A.F. amplifier, when the

gain is about 11 and the distortion at 5 V_{rms} output about 1%.

When the tube is used at a very high sensitivity it may be advisable to take precautions against microphony. Whether this is necessary or not depends on the mechanical lay-out of the receiver and on the acoustical efficiency of the loudspeaker. In the average receiver in which a loudspeaker with an acoustical efficiency of 5% is used, no precautions against microphony are required when the input voltage at the control grid of the DAF 91, for 50 mW output of the output stage, is greater than 40 mV. As already indicated, this figure only serves as a general guide. As a general rule when the input voltage at the DAF 91 for 50 mW output of the receiver is smaller than 40 mV it is advisable to use a resilient tube holder, or, in extreme cases, to employ a sound absorbing shield around the tube.

In practical cases it may therefore be preferred not to employ the DAF 91 at optimum gain. The reduction in gain should then be obtained by reducing the dynamic anode load only, i.e. by choosing a lower value for the grid leak of the following tube, as this ensures a low sensitivity of the DAF 91 to vibrations.

The pentode section of the DAF 91 is specially designed for use as an A.F. voltage amplifier. It should not, therefore, be attempted to use it as an I.F. or H.F. tube.

TECHNICAL DATA

FILAMENT DATA

Heating   direct by battery current, rectified A.C. or D.C.; series or parallel supply.

Parallel supply

Filament voltage	V_f	= 1.4 V
Filament current	I_f	= 0.05 A

Series supply

Filament voltage	V_f	= 1.3 V

BASE CONNECTIONS AND DIMENSIONS (in mm)
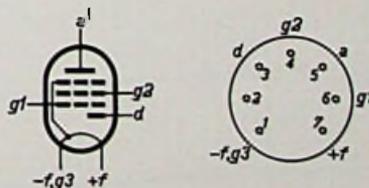
Fig. 32.
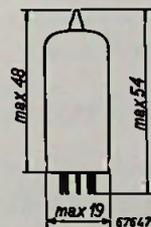
Mounting position: any

OPERATING CHARACTERISTICS AS A.F. AMPLIFIER

Pentode connection

V_b (V)	R_a (MΩ)	R_{g2} (MΩ)	I_b (μA)	$\dfrac{V_o}{V_i}$	d_{tot} (%) $V_o = 5\ \text{V}_{rms}$
45	1	3.9	40	42	5
67.5	1	3.9	60	55	3
90	1	3.9	85	60	2
120	1	3.9	115	66	1.8
45	1	4.7	30	40	8
67.5	1	4.7	55	55	2.5
90	1	4.7	80	64	1.7
120	1	4.7	110	70	1.5
45	0.47	1.8	70	38	4
67.5	0.47	1.8	125	50	1
90	0.47	1.8	170	56	1
120	0.47	1.8	260	60	3
45	0.47	2.2	60	37	5
67.5	0.47	2.2	115	50	1
90	0.47	2.2	160	57	1
120	0.47	2.2	240	66	1

The tube can be used without special precautions against microphony in circuits in which the input voltage $V_i \geqslant 40\ \text{mV}_{rms}$ for an output of 50 mW of the output tube. With this figure an acoustical loudspeaker efficiency of 5% is assumed.

TYPICAL CHARACTERISTICS *(pentode section)*

Anode voltage . . . . V_a

Screen-grid voltage . . . . V_{g2}

Control grid voltage . . . . V_{g1}

Anode current . . . . I_a

Screen-grid current . . . . I_{g2}

Mutual conductance . . . . S

Internal resistance . . . . R_i

Amplification factor between screen grid and control grid . . . . μ_{g2g1}

LIMITING VALUES

Anode voltage . . . . V_a max.

Anode dissipation . . . . W_a max.

Screen-grid voltage . . . . V_{g2} max.

Screen-grid dissipation . . . . . W_{g2} max.

Cathode current . . . . I_k max.

External resistance between g_1 and $-f$ . . . R_{g1} max.

Fig. 33. Circuit diagram for the use of the pentode section as A.F. amplifier.

CAPACITANCES

$$C_a = 2.8\ \text{pF}$$
$$C_{g1} = 2.0\ \text{pF}$$
$$C_{ag1} < 0.4\ \text{pF}$$
$$C_d = 1.5\ \text{pF}$$

OPERATING CHARACTERISTICS AS A.F. AMPLIFIER

Triode connection (screen grid tied to anode; grid leak is 10 MΩ and grid leak of next tube 1 MΩ)

V_b (V)	R_a (MΩ)	I_b (μA)	$\dfrac{V_o}{V_i}$	d_{tot} (%) $V_o = 5\ \text{V}_{rms}$
45	0.47	45	10	3
67.5	0.47	85	11	1
90	0.47	140	11.5	0.7
120	0.47	200	12	0.5
45	0.22	85	9.5	2.5
67.5	0.22	170	10.5	0.9
90	0.22	270	11	0.6
120	0.22	380	11.5	1

V_a	45	67.5	90 V
V_{g2}	45	67.5	90 V
V_{g1}	0	0	0 V
I_a	0.75	1.6	2.7 mA
I_{g2}	0.15	0.4	0.5 mA
S	420	625	720 μA/V
R_i	0.6	0.6	0.5 MΩ
μ_{g2g1}	13.5	13.5	13.5

V_a	max.	90 V
W_a	max.	0.25 W
V_{g2}	max.	90 V
W_{g2}	max.	0.1 W
I_k	max.	4.5 mA
R_{g1}	max.	3 MΩ[11])

Control grid voltage for $I_{g1} = +0.3$ μA . . .	V_{g1}	max.	—0.2 V
Peak inverse voltage on diode	$V_{d\ inv\ p}$	max.	100 V
Average diode current	I_d	max.	0.2 mA
Peak diode current	$I_{d\ p}$	max.	1.2 mA

[11]) With biasing by means of grid current $R_{g1} = $ max. 22 MΩ.
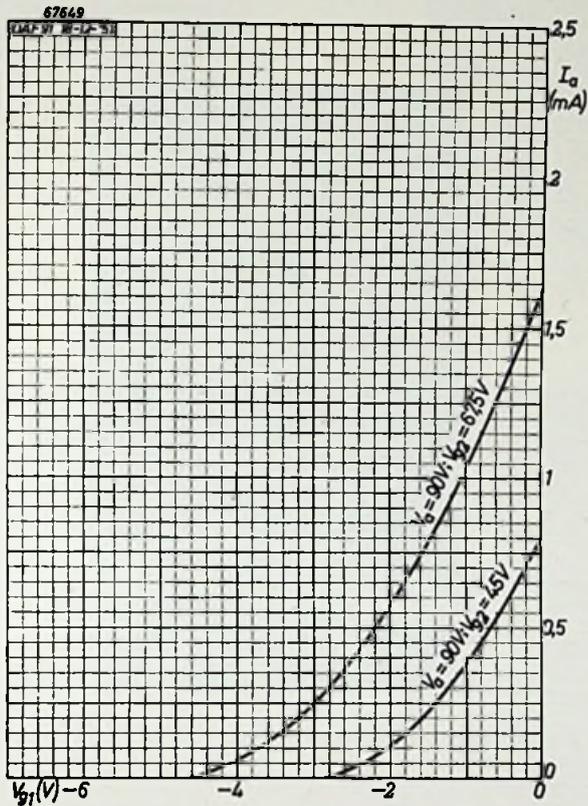
Fig. 34. Anode current plotted against the control-grid voltage with the screen-grid voltage as parameter, for $V_a = 90$ V.
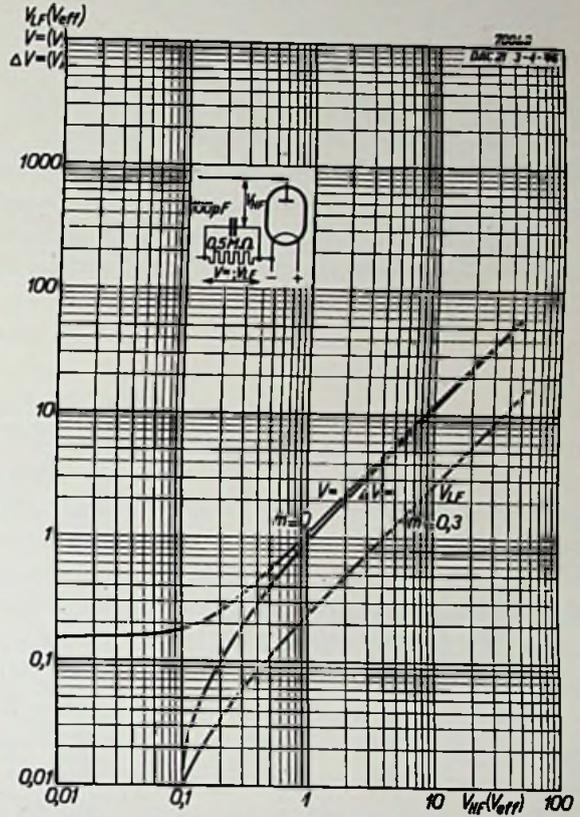
Fig. 36. Direct voltage, variation in direct voltage and A.F. voltage (at $m = 30\%$) developed across a detector load of 0.5 MΩ plotted against the H.F. signal.
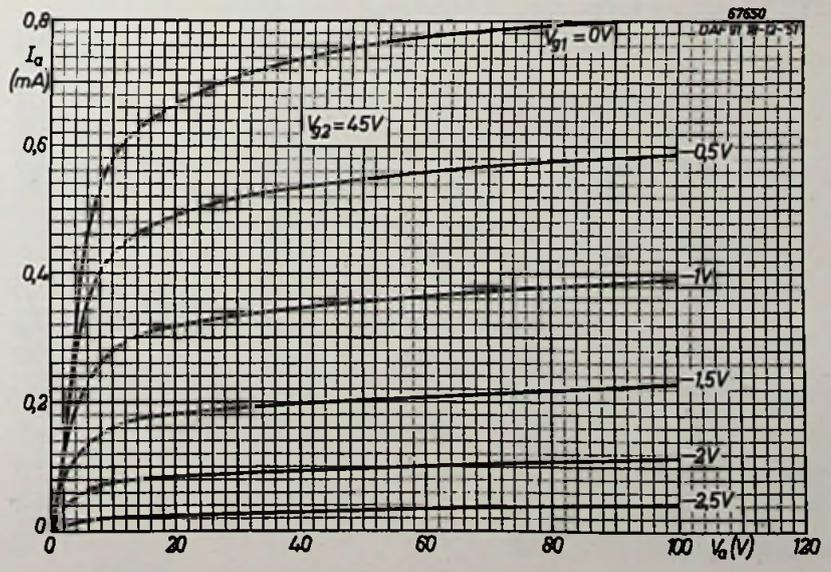
Fig. 35. Anode current plotted against anode voltage with V_{g1} as parameter, for $V_{g2} = 45$ V.
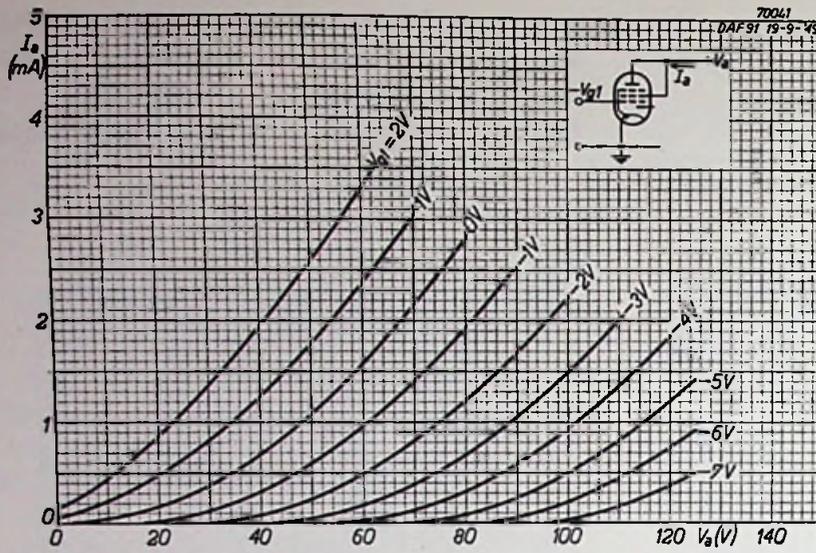
Fig. 37. Anode current plotted against anode voltage with V_{g1} as parameter when the anode and the screen grid are interconnected (triode connection).

Fig. 38. Anode current plotted against anode voltage with V_{g1} parameter, for $V_{g2} = 67.5$ V.
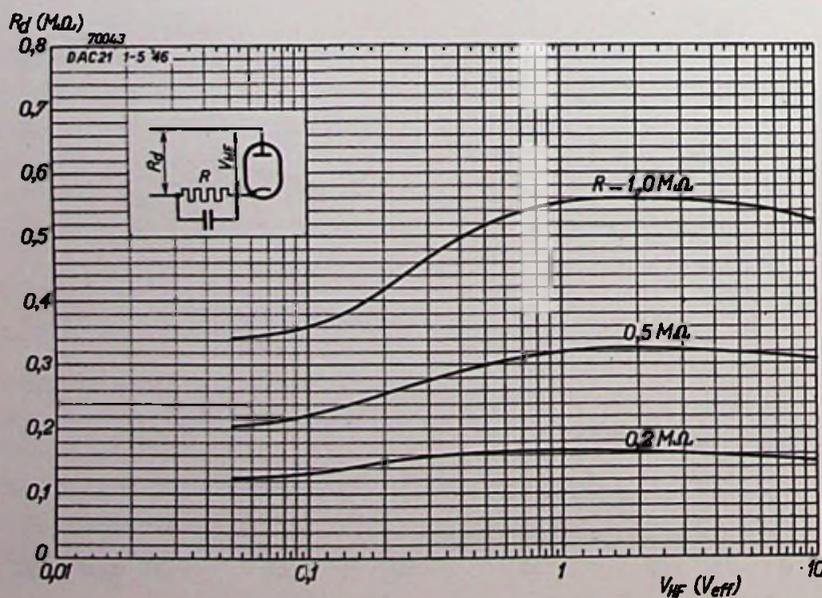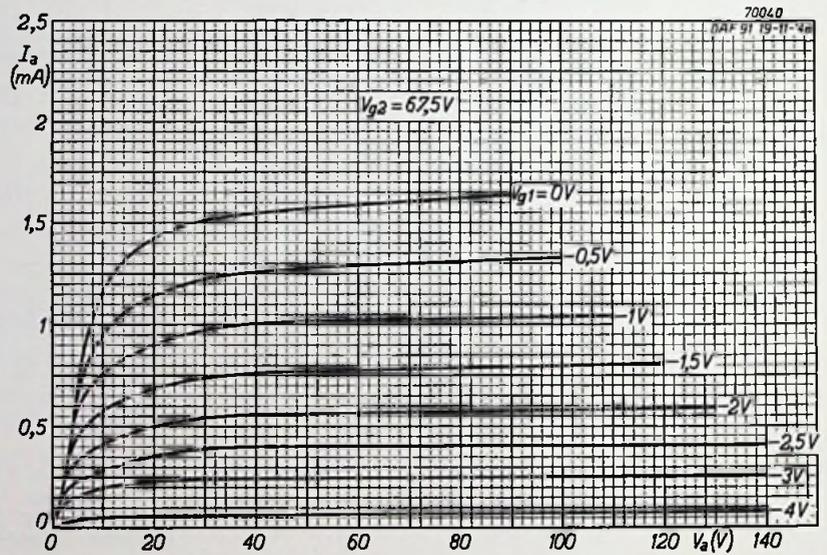
Fig. 39. Damping across the tuned circuit feeding the detector plotted against the H.F. signal with the diode load as parameter.

24

OUTPUT PENTODE DL 92

The 7-pin miniature output pentode type DL 92 is primarily intended for use in very small all-dry battery receivers. Particular attention has been paid to its performance at anode and screen-grid potentials of 67.5 V. Under these conditions an output of 180 mW is obtainable with the two filament sections connected in parallel, or 160 mW with the series filament arrangement. The drive voltage for maximum output in either case is 5.5 V$_{rms}$.

Greater output can be obtained if the anode voltage is increased to 90 V, the screen-grid voltage remaining at 67.5 V. In this case the output with parallel filament connection is 270 mW and with series filament connection 235 mW.

The DL 92, being specially designed for operation with low H.T. battery voltages, may also be used at anode and screen-grid potentials of 45 V. The output is then, of course, considerably reduced, but it will still be sufficient for a number of applications. With the parallel filament arrangement the output obtainable is 65 mW and with the filament sections connected in series 50 mW.

Fig. 40. The output pentode DL 92.

TECHNICAL DATA

FILAMENT DATA

Heating: direct by battery current, rectified A.C. or D.C.; series or parallel supply.

Parallel supply

Filament voltage	V_f =	1.4	2.8 V
Filament current	I_f =	0.1	0.05 A
Base pins		5—(1+7)	1—7

Series supply

Filament voltage	V_f =	1.3	2.6 V
Base pins		5—(1+7)	1—7

BASE CONNECTIONS AND DIMENSIONS
(in mm)

Fig. 41.

Mounting position: any

CAPACITANCES			
	C_a	=	6.0 pF
	C_{g1}	=	4.35 pF
	C_{ag1}	<	0.4 pF

25

OPERATING CHARACTERISTICS

A. With $V_f = 1.4$ V; $I_f = 0.1$ A

Anode voltage	V_a	45	41	67.5	61	90	84	V
Screen-grid voltage	V_{g2}	45	41	67.5	61	67.5	*)	V
Control grid voltage	V_{g1}	—4.5	—3.5	—7	—6	—7	—6.5	V
Anode current	I_a	3.8	4.0	7.2	6.6	7.4	8.0	mA
Screen-grid current	I_{g2}	0.8	0.8	1.5	1.4	1.4	1.7	mA
Mutual conductance	S	1.25	1.3	1.55	1.5	1.57	1.55	mA/V
Amplification factor between screen-grid and control grid	μ_{g2g1}	5	4.5	5	4.5	5	4.5	
Internal resistance	R_i	100	90	100	100	100	100	kΩ
Load resistance	R_a	8	7	5	7	8	7	kΩ
Output	W_o	65	45	180	125	270	190	mW
Input signal	V_i	3.5	2.9	5.5	4.5	5.1	5.1	V_{rms}
Total distortion	d_{tot}	12	13	10	14	12	13	%
Input signal for $W_o = 50$ mW	V_i	2.8	—	2.5	2.0	1.95	1.9	V_{rms}

*) $R_{g2} = 10$ kΩ, decoupled with 0.5 μF ($V_{bg2} = 84$ V).

B. With $V_f = 2.8$; $I_f = 0.05$ A

Anode voltage	V_a	45	41	67.5	61	90	84	V
Screen-grid voltage	V_{g2}	45	41	67.5	61	67.5	*)	V
Control grid voltage	V_{g1}	—4.5	—3.5	—7	—5.5	—7	—6	V
Anode current	I_a	3.0	3.2	6.0	6.5	6.1	7.6	mA
Screen-grid current	I_{g2}	0.7	0.7	1.2	1.4	1.1	1.6	mA
Mutual conductance	S	1.1	1.15	1.4	1.45	1.42	1.5	mA/V
Amplification factor between screen-grid and control grid	μ_{g2g1}	5	4.5	5	4.5	5	4.5	
Internal resistance	R_i	100	110	100	·100	100	105	kΩ
Load resistance	R_a	8	7	5	7	8	7	kΩ
Output	W_o	50	38	160	120	235	180	mW
Input signal	V_i	3.5	2.8	5.5	4.4	4.7	4.7	V_{rms}
Total distortion	d_{tot}	12.5	13	12	14	13	13	%
Input signal for $W_o = 50$ mW	V_i	3.5	—	2.5	2.0	1.95	1.9	V_{rms}

*). $R_{g2} = 10$ kΩ, decoupled with 0.5 μF ($V_{bg2} = 84$ V).

LIMITING VALUES

Anode voltage	V_a	max.	90 V
Anode dissipation	W_a	max.	0.7 W
Screen-grid voltage	V_{g2}	max.	67.5 V
Screen-grid dissipation	W_{g2}	max.	0.2 W
Cathode current	I_k	max.	11 mA
External resistance between g_1 and —f	R_{g1}	max.	2 MΩ
Control-grid voltage for $I_{g1} = +0.3$ μA	V_{g1}	max.	—0.2 V

Fig. 42. Anode current and screen-grid current plotted against the control grid voltage for $V_a = V_{g2} = 45$ V when the two filament sections are connected in parallel ($V_f = 1.4$ V and $I_f = 0.1$ A).

Fig. 43. Anode current and screen-grid current plotted against the control grid voltage for $V_a = V_{g2} = 67.5$ V when the two filament sections are connected in parallel ($V_f = 1.4$ V and $I_f = 0.1$ A).
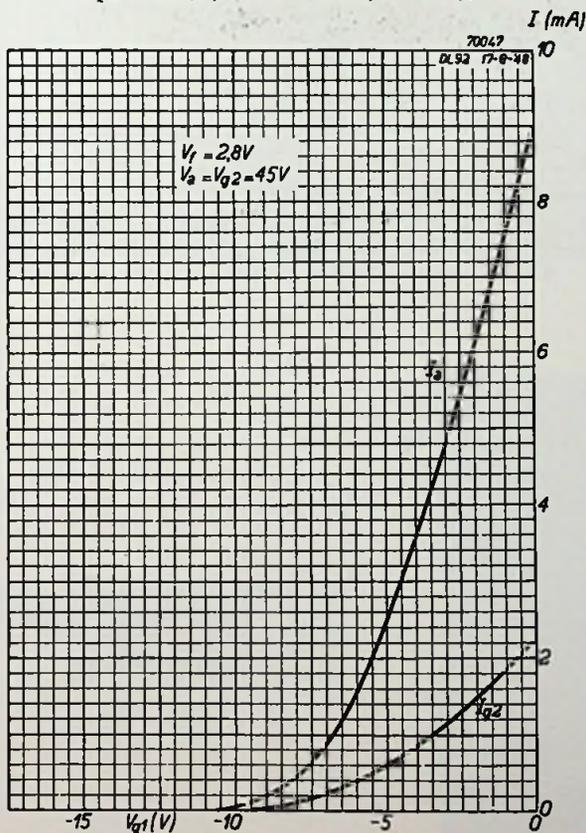
Fig. 44. Anode current and screen-grid current plotted against the control grid voltage for $V_a = V_{g2} = 45$ V when the two filament sections are connected in series ($V_f = 2.8$ V and $I_f = 0.05$ A).
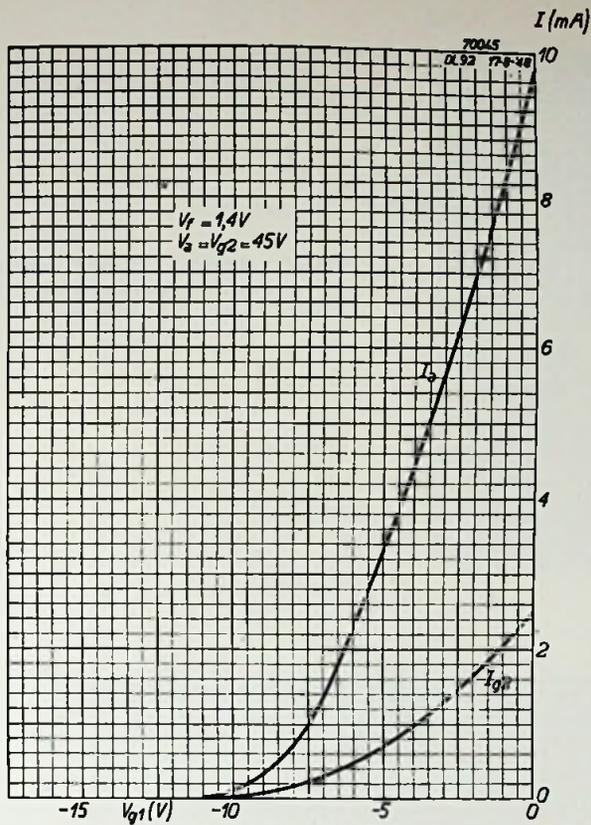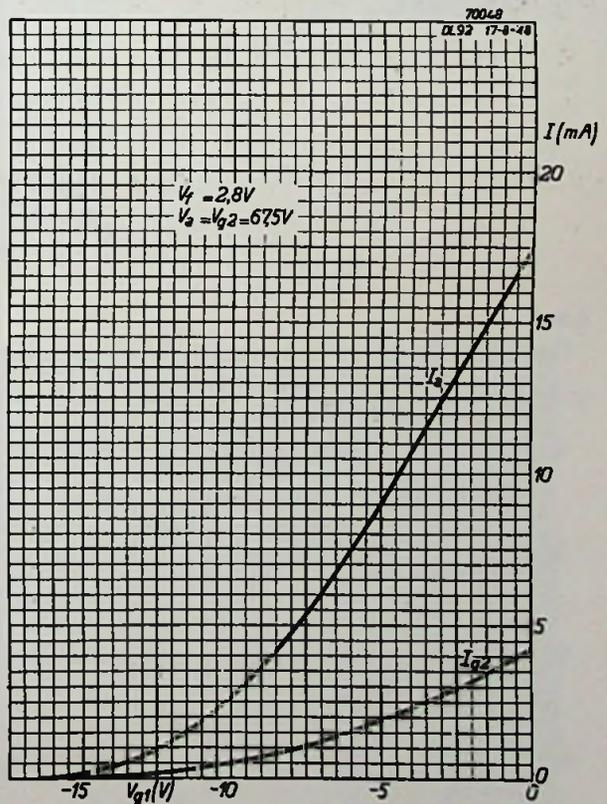

Fig. 45. Anode current and screen-grid current plotted against the control grid voltage for $V_a = V_{g2} = 67.5$ V when the two filament sections are connected in series ($V_f = 2.8$ V and $I_f = 0.05$ A).

I_a (mA)
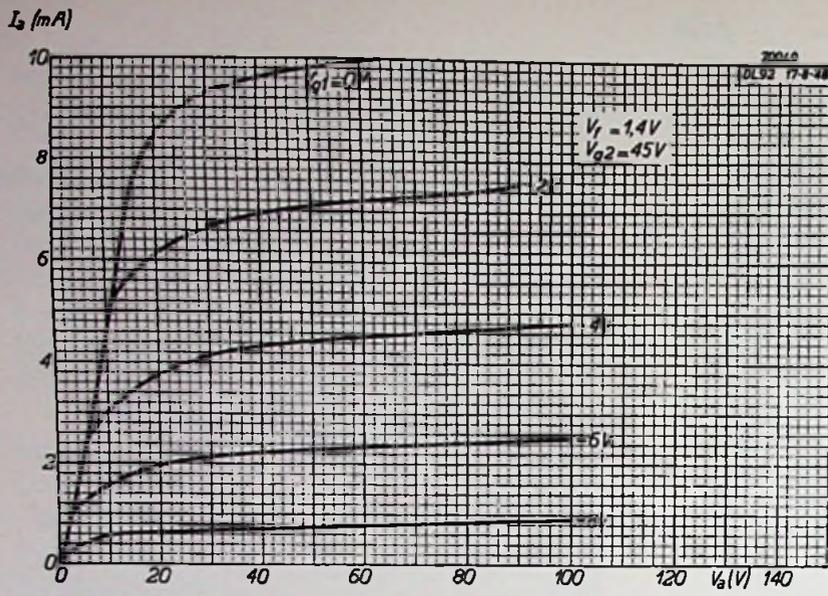
Fig. 46. Anode current plotted against anode voltage for $V_{g2} = 45$ V and $V_f = 1.4$ V. $I_f = 0.1$ A.

I_a (mA)

Fig. 47. Anode current plotted against anode voltage for $V_{g2} = 67.5$ V and $V_f = 1.4$ V. $I_f = 0.1$ A.

I_a (mA)
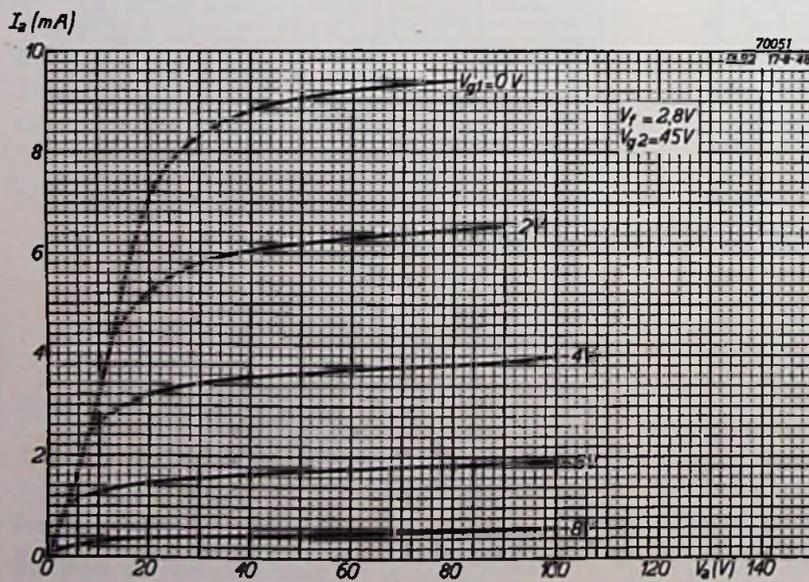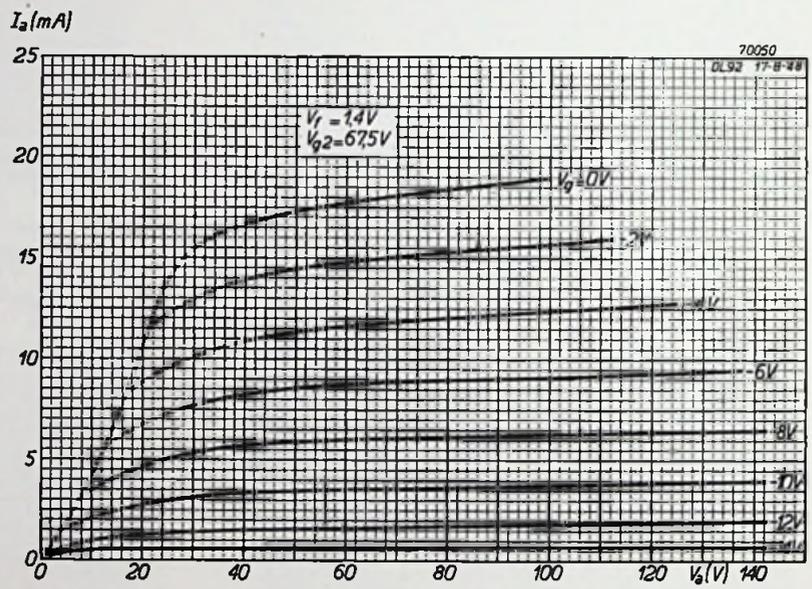
Fig. 48. Anode current plotted against anode voltage for $V_{g2} = 45$ V and $V_f = 2.8$ V. $I_f = 0.05$ A.

28

Fig. 49. Anode current plotted against anode voltage for $V_{g2} = 67.5$ V and $V_f = 2.8$ V. $I_f = 0.05$ A.
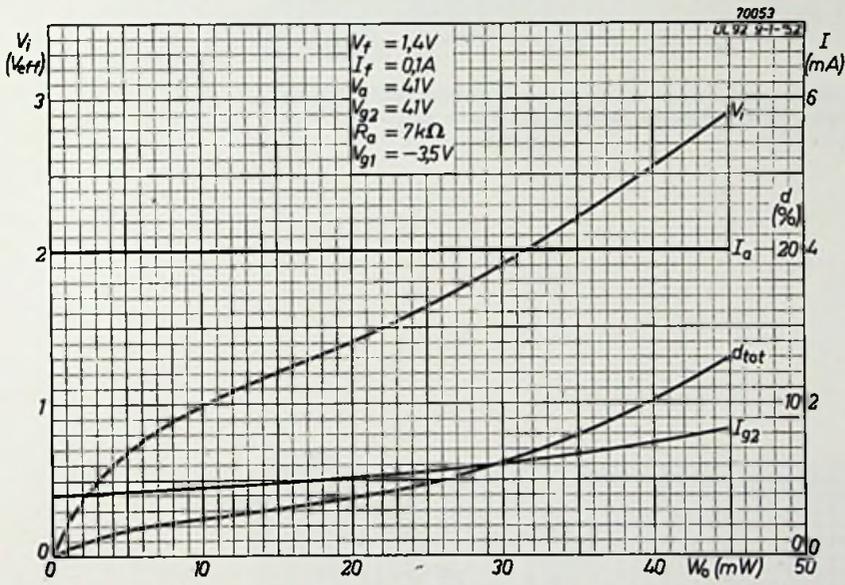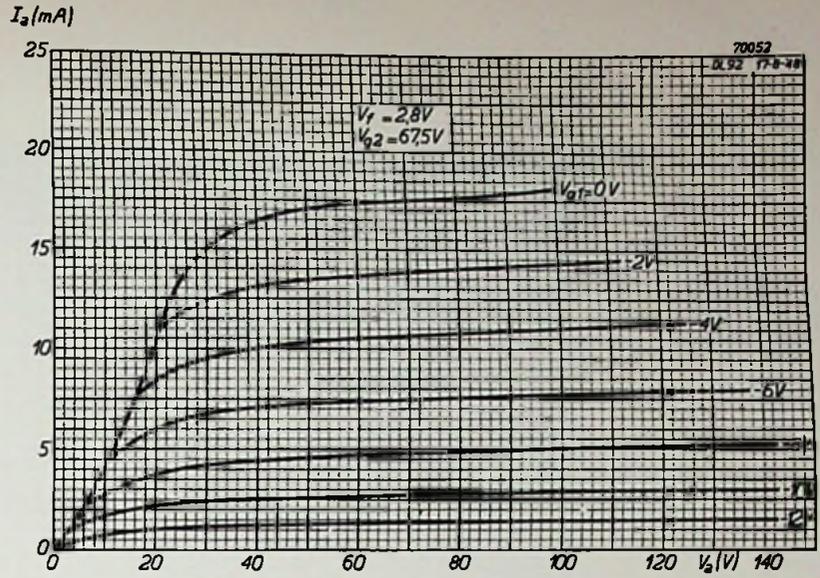
Fig. 50. Anode current, screen-grid current, input voltage and total distortion plotted against the output for $V_b = 45$ V and $V_f = 1.4$ V, $I_f = 0.1$ A.

Fig. 51. Anode current, screen-grid current, input voltage and distortion plotted against the output for $V_b = 67.5$ V and $V_f = 1.4$ V, $I_f = 0.1$ A.

29
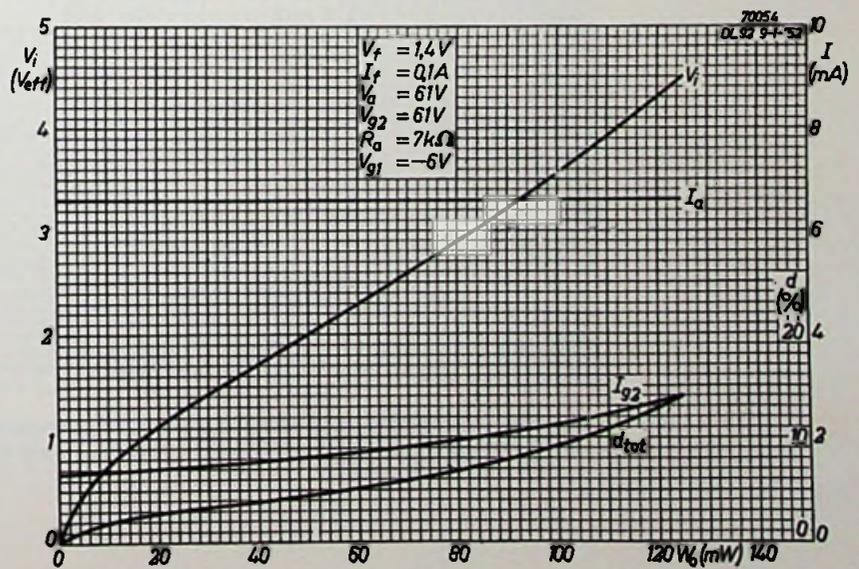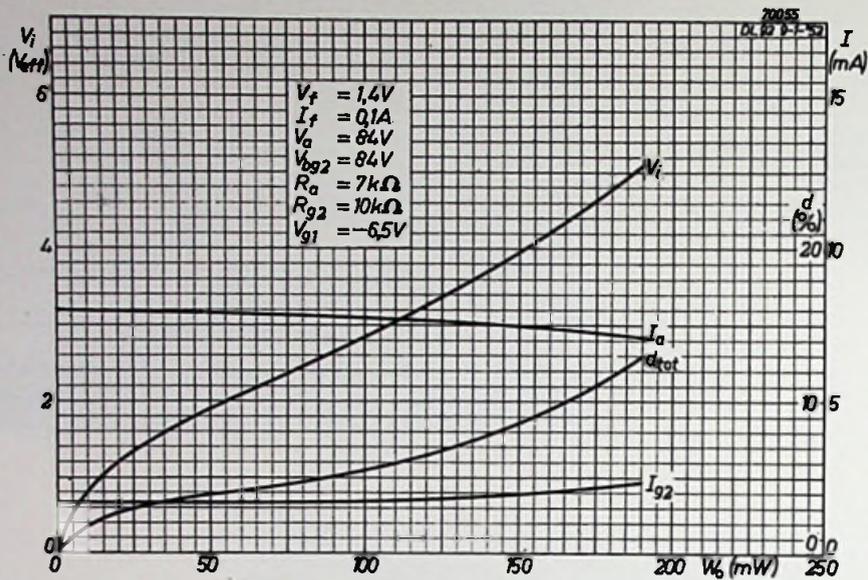
Fig. 52. Anode current, screen-grid current, input voltage and total distortion plotted against the output for $V_b = 90$ V, and $V_f = 1.4$ V, $I_f = 0.1$ A.

Fig. 53. Anode current, screen-grid current, input voltage and total distortion plotted against the output for $V_b = 45$ V, and $V_f = 2.8$ V, $I_f = 0.05$ A.
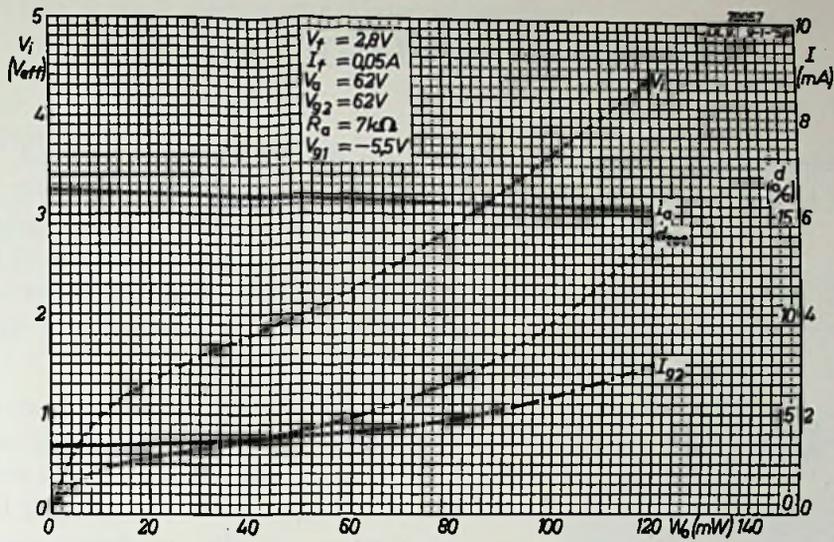
Fig. 54. Anode current, screen-grid current, input voltage and total distortion plotted against the output for $V_b = 67.5$ V, and $V_f = 2.8$ V, $I_f = 0.05$ A.
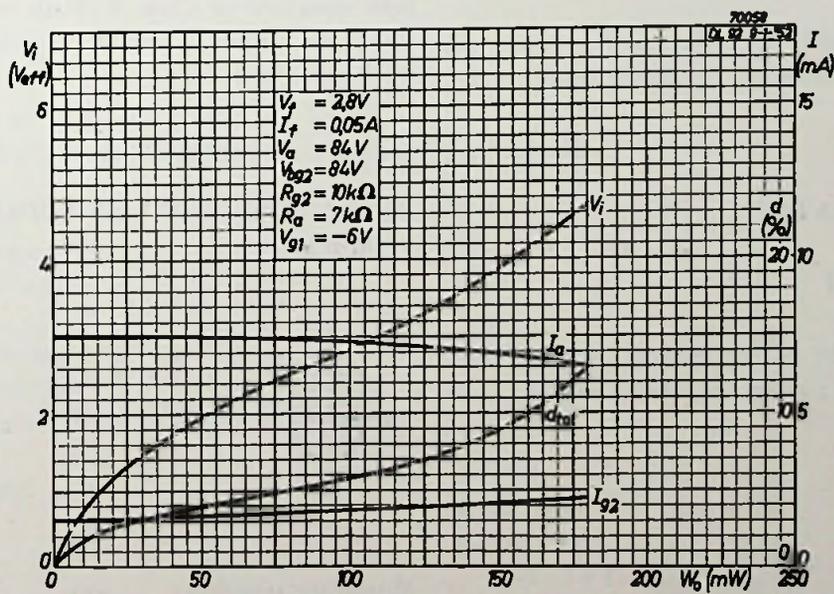
Fig. 55. Anode current, screen-grid current, input voltage and total distortion plotted against the output for $V_b = 90$ V, and $V_f = 2.8$ V, $I_f = 0.05$ A.
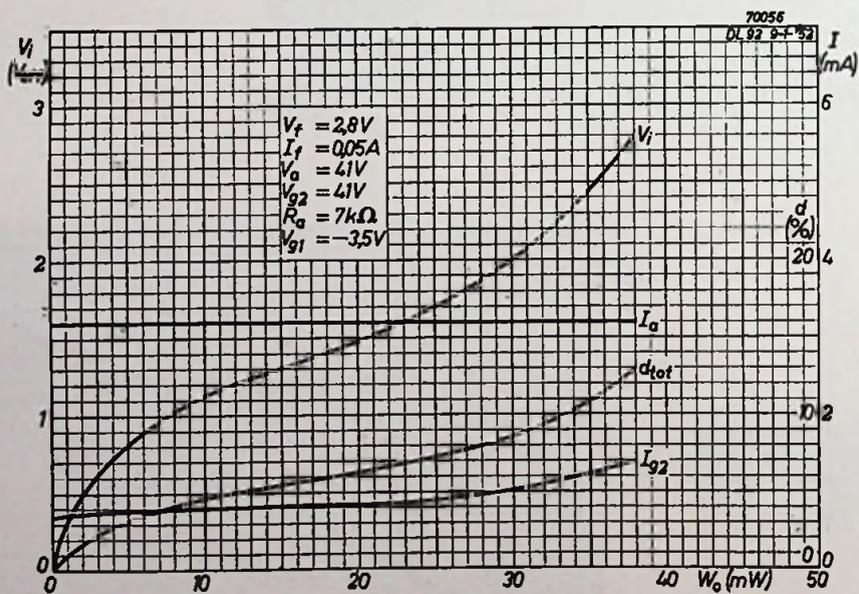
OUTPUT PENTODE DL 94

The 7-pin miniature output pentode DL 94 is specially designed to give optimum performance
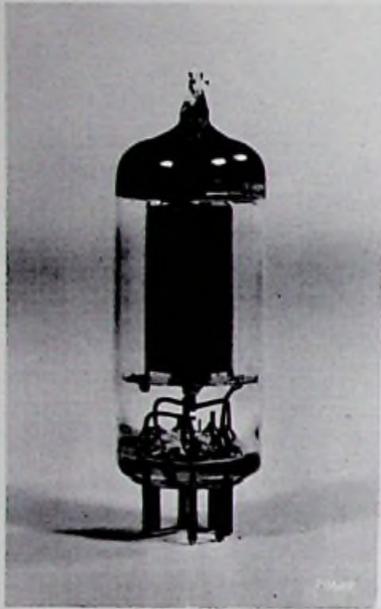
Fig. 56. The output pentode DL 94.

in receivers in which an H.T. supply voltage of 90 V or more is available. For lower supply volt-ages the DL 92 should be used. The output of a single DL 94 tube operated with the two filament sections in parallel is 340 mW when the anode and screen-grid voltages are both 90 V. With the filament sections connected in series the output is 290 mW, also with anode and screen-grid voltages of 90 V.

Reduced H.T. and L.T. battery current drain can be obtained by using only one section of the filament, this, of course, also reducing the available output. This arrangement is particularly attractive in ABC receivers, using both filament sections of the output tube with mains supply and one section when the set is operated on dry batteries.

When a large output is required two DL 94 pentodes can be operated in Class B push-pull with anode voltages of either 120 or 150 V. Although the addition of another output pentode in a receiver increases the total L.T. drain, the average H.T. current drain of the two tubes operated in Class B is usually lower than that of a single tube operated in Class A. With anode voltages of 150 V the output of two DL 94 pentodes in Class B is about 2 W.

TECHNICAL DATA

FILAMENT DATA

Heating: direct by battery current, rectified A.C. or D.C.; series or parallel supply.

Parallel supply

Filament voltage	V_f	=	1.4	2.8 V
Filament current	I_f	=	0.1	0.05 A
Base pins		5—(1+7)	1—7	

Series supply

Filament voltage	V_f	=	1.3	2.6 V
Base pins		5—(1+7)	1—7	

BASE CONNECTIONS AND DIMENSIONS
(in mm)
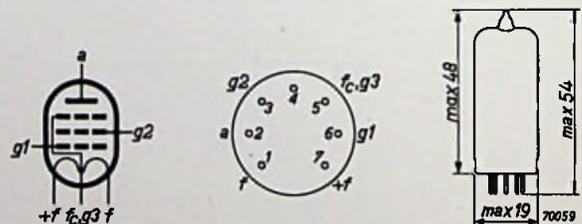
Fig. 57.

Mounting position: any

CAPACITANCES			
C_a	=	3.8	pF
C_{g1}	=	5.0	pF
C_{ag1}	<	0.40	pF

A. $V_f = 1.4$ V; $I_f = 0.05$ A, (using one filament section).

Anode voltage	V_a	90	86	120	113 V
Screen-grid voltage	V_{g2}	90	86	120	113 V
Control grid voltage	V_{g1}	−5.5	−4.5	−8.5	−7.5 V
Anode current	I_a	4.0	4.5	5.0	5.0 mA
Screen-grid current	I_{g2}	0.8	0.9	1.0	1.0 mA
Mutual conductance	S	1.0	1.0	1.0	1.0 mA/V
Amplification factor between screen grid and control grid	μ_{g2g1}	7.2	7.2	7.3	7.3
Internal resistance	R_i	200	180	200	180 kΩ
Load resistance	R_a	20	20	20	20 kΩ
Output	W_o	180	160	350	300 mW
Input signal	V_i	4.7	4.2	7.2	6.3 V_{rms}
Total distortion	d_{tot}	13	12	15	14.5 %
Output at $d_{tot} = 10\%$	W_o	170	150	290	250 mW
Input signal for $d_{tot} = 10\%$	V_i	4.1	3.9	5.1	5.1 V_{rms}
Input signal for $W_o = 50$ mW	V_i	1.8	1.8	1.7	1.7 V_{rms}

B. $V_f = 1.4$ V; $I_f = 0.1$ A, (filament sections in parallel).

Anode voltage	V_a	90	86	120	113 V
Screen-grid voltage	V_{g2}	90	86	120	113 V
Control grid voltage	V_{g1}	−5.1	−4.5	−8.1	−7.1 V
Anode current	I_a	8.0	8.0	10	10 mA
Screen-grid current	I_{g2}	1.8	1.8	2.3	2.3 mA
Mutual conductance	S	2.0	2.0	2.0	2.0 mA/V
Amplification factor between screen grid and control grid	μ_{g2g1}	7.3	7.3	7.3	7.3
Internal resistance	R_i	110	110	110	110 kΩ
Load resistance	R_a	8	8	8	8 kΩ
Output	W_o	340	290	680	570 mW
Input signal	V_i	4.5	4.1	6.6	5.9 V_{rms}
Total distortion	d_{tot}	12	11	15	14 %
Output at $d_{tot} = 10\%$	W_o	310	280	550	500 mW
Input signal for $d_{tot} = 10\%$	V_i	4.1	4.0	5.0	4.9 V_{rms}
Input signal for $W_o = 50$ mW	V_i	1.35	1.35	1.3	1.3 V_{rms}

C. $V_f = 2.8$ V; $I_f = 0.05$ A (filament sections in series).

Anode voltage	V_a	90	86	120	113 V
Screen-grid voltage	V_{g2}	90	86	120	113 V
Control grid voltage	V_{g1}	—4.2	—4.3	—8.1	—7.2 V
Anode current	I_a	8.0	7.0	9.0	9.0 mA
Screen-grid current	I_{g2}	1.7	1.5	1.8	1.8 mA
Mutual conductance	S	2.0	1.9	2.0	2.0 mA/V
Amplification factor between screen grid and control grid	μ_{g2g1}	7.3	7.3	7.3	7.3
Internal resistance	R_i	120	120	120	120 kΩ
Load resistance	R_a	10	10	10	10 kΩ
Output	W_o	290	270	620	525 mW
Input signal	V_i	4.0	4.0	6.6	6.1 V_{rms}
Total distortion	d_{tot}	12	11.5	17	16 %
Output at $d_{tot} = 10\%$	W_o	280	250	500	420 mW
Input signal for $d_{tot} = 10\%$	V_i	3.8	3.7	4.8	4.4 V_{rms}
Input signal for $W_o = 50$ mW	V_i	1.35	1.40	1.35	1.35 V_{rms}

OPERATING CHARACTERISTICS *(two tubes in Class A push-pull)*

A. $V_f = 1.4$ V; $I_f = 2 \times 0.05$ A, (using one filament section of each tube).

Anode voltage	V_a	90	85	120	113 V
Screen-grid voltage	V_{g2}	90	85	120	113 V
Control grid voltage	V_{g1}	—5.5	—5.4	—8.5	—7.5 V
Anode current	I_a	2x4	2x3.25	2x5	2x5 mA
Screen-grid current	I_{g2}	2x0.8	2x0.7	2x1.0	2x1.0 mA
Load resistance between anodes	R_{aa}	28	28	28	28 kΩ
Input signal	V_i	4.8	4.8	7.5	6.6 V_{rms}
Output	W_o	340	320	750	650 mW
Total distortion	d_{tot}	8	8	10	10 %
Input signal for $W_o = 50$ mW	V_i	1.45	1.5	1.35	1.35 V_{rms}

B. $V_f = 1.4$ V; $I_f = 2 \times 0.1$ A, (four filament sections in parallel).

Anode voltage	V_a	90	85	120	113 V
Screen-grid voltage	V_{g2}	90	85	120	113 V
Control grid voltage	V_{g1}	—5.1	—5.2	—8.1	—7.1 V
Anode current	I_a	2x8	2x6.5	2x10	2x10 mA
Screen-grid current	I_{g2}	2x1.8	2x1.4	2x2.3	2x2.3 mA
Load resistance between anodes	R_{aa}	14	14	14	14 kΩ
Input signal	V_i	4.4	4.5	6.8	5.9 V_{rms}
Output	W_o	650	550	1300	1160 mW
Total distortion	d_{tot}	10	10	10	10 %
Input signal for $W_o = 50$ mW	V_i	1.0	1.0	0.95	0.95 V_{rms}

C. $V_f = 2.8$ V; $I_f = 2 \times 0.05$ A, (filament sections of each tube in series, filaments of the two tubes together in parallel).

Anode voltage	V_a	90	85	120	113 V
Screen-grid voltage	V_{g2}	90	85	120	113 V
Control grid voltage	V_{g1}	—5.2	—4.8	—8.2	—7.2 V
Anode current	I_a	2x6	2x5.5	2x8	2x8 mA
Screen-grid current	I_{g2}	2x1.3	2x1.2	2x1.8	2x1.8 mA/V
Load resistance between anodes	R_{aa}	16	16	14	14 kΩ
Input signal	V_i	4.8	4.3	6.9	6.0 V$_{rms}$
Output	W_o	550	500	1200	1000 mW
Total distortion	d_{tot}	10	10	10	10 %
Input signal for $W_o = 50$ mW	V_i	1.1	1.1	1.05	1.05 V$_{rms}$

OPERATING CHARACTERISTICS (two tubes in Class B push-pull)

A. $V_f = 1.4$ V; $I_f = 2 \times 0.05$A, (using one filament section of each tube).

Anode voltage	V_a		90	82	V
Screen-grid voltage	V_{g2}		90	82	V
Control-grid voltage	V_{g1}		—8.5	—7.5	V
Load resistance between anodes	R_{aa}		28	28	kΩ
Input signal for $W_o = 50$ mW	V_i		2.5	2.6	V$_{rms}$
Input signal	V_i	0 7.2	0 6.4		V$_{rms}$
Anode current	I_a	2x1 2x3.2	2x1 2x3		mA
Screen-grid current	I_{g2}	2x0.2 2x1.05	2x0.2 2x1		mA
Output	W_o	0 300	0 265		mW
Total distortion	d_{tot}	— 3,5	— 4		%

B. $V_f = 1.4$ V; $I_f = 2 \times 0.1$A. (four filament sections in parallel).

Anode voltage	V_a	90		82		120		108		150 V
Screen-grid voltage	V_{g2}	90		82		120		108		150 V
Control grid voltage	V_{g1}	—9.8		—8.3		—13.7		—12.2		—17.4 V
Load resistance between anodes	R_{aa}	14		14		14		14		12 kΩ
Input signal for $W_o = 50$ mW	V_i	2		2		2.4		2.5		2.3 V$_{rms}$
Input signal	V_i	0	8	0	6.6	0	11	0	10	0 13.3 V$_{rms}$
Anode current	I_a	2x1.5	2x6.3	2x1.5	2x5.25	2x1.5	2x9	2x1.5	2x8	2x2 2x12.5 mA
Screen-grid current	I_{g2}	2x0.32	2x2.25	2x0.32	2x1.75	2x0.32	2x3.1	2x0.32	2x2.6	2x0.42 2x4.4 mA
Output	W_o	0	580	0	445	0	1200	0	900	0 2150 mW
Total distortion	d_{tot}	—	5	—	4	—	5	—	5	— 4.5 %

C. $V_f = 2.8$ V; $I_f = 2 \times 0.05$ A, (filament sections of each tube in series, filaments of the two tubes together in parallel).

Anode voltage	V_a		90		82		120		108		150	V
Screen-grid voltage	V_{g2}		90		82		120		108		150	V
Control grid voltage	V_{g1}		—8.8		—7.6		—13		—11		—16.8	V
Load resistance between anodes	R_{aa}		14		14		14		14		14	kΩ
Input signal for $W_o = 50$ mW	V_i		2.25		2.3		2.4		2.4		2.4	V_{rms}
Input signal	V_i	0	7.6	0	6.4	0	10	0	9.0	0	13	V_{rms}
Anode current	I_a	2x1.5	2x5.75	2x1.5	2x5.25	2x1.5	2x8.5	2x1.5	2x7.5	2x2	2x11.5	mA
Screen-grid current	I_{g2}	2x0.32	2x1.7	2x0.32	2x1.5	2x032	2x3	2x0.32	2x2.4	2x0.47	2x4.3	mA
Output	W_o	0	530	0	420	0	1100	0	850	0	2000	mW
Total distortion	d_{tot}	—	4	—	3.5	—	6	—	4	—	4.5	%

OPERATING CHARACTERISTICS (two tubes in Class AB push-pull)

A. $V_f = 1.4$ V; $I_f = 2 \times 0.1$ A, (four filament sections in parallel).

Anode supply voltage	V_{ba}		120	V
Screen-grid supply voltage	V_{bg2}		120	V
Cathode resistor	R_k		470	Ω [12])
Load resistance between anodes	R_{aa}		14	kΩ
Input signal for $W_o = 50$ mW	V_i		1.2	V_{rms}
Input signal	V_i	0	9.9	V_{rms}
Anode current	I_a	2x5.7	2x7.65	mA
Screen-grid current	I_{g2}	2x1.25	2x2.9	mA
Output	W_o	0	900	mW
Total distortion	d_{tot}	—	5	%

B. $V_f = 2.8$ V; $I_f = 2 \times 50$ mA, (filament sections of each tube in series, filaments of the two tubes together in parallel).

Anode supply voltage	V_{ba}		120	V
Screen-grid supply voltage	V_{bg2}		120	V
Cathode resistor	R_k		470 ·	Ω [12])
Load resistance between anodes	R_{aa}		14	kΩ
Input signal for $W_o = 50$ mW	V_i		1.3	V_{rms}
Input signal	V_i	0	9.7	V_{rms}
Anode current	I_a	2x5.3	2x7.5	mA
Screen-grid current	I_{g2}	2x1.1	2x2.6	mA
Output	W_o	0	850	mW
Total distortion	d_{tot}	—	5	%

[12]) R_k is taken up in the negative lead of the H.T. supply. It is assumed that an additional current of 5 mA from the tubes preceding the push-pull stage also flows through R_k.

Anode voltage . . . . V_a	max.	150	V [13])
Anode dissipation . . . . W_a	max.	1.2	W
Screen-grid voltage . . . . V_{g2}	max.	150	V [13])
Screen-grid disipation . . . . W_{g2}	max.	0.45	W
Cathode current for one filament section . . . . I_k	max.	6	mA
External resistance between g_1 and —f . . . R_{g1}	max.	1	MΩ
Control grid voltage $I_{g1} = +0.3 \mu A$ . . . . V_{g1}	max.	—0.2	V

[13]) With $V_t = 0$ V the anode and screen-grid potentials may rise to 180 V max.
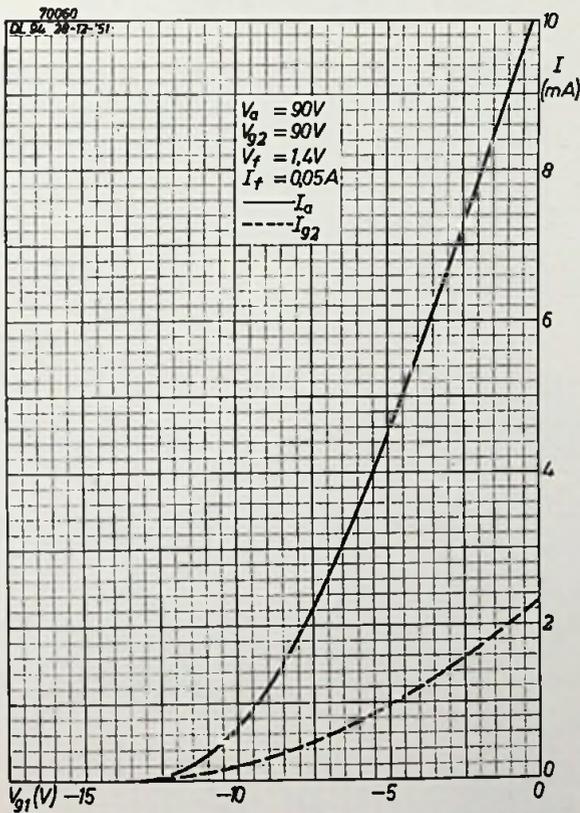

Fig. 58. Anode current and screen-grid current plotted against the control grid voltage for $V_a = V_{g2} = 90$ V and $V_f = 1.4$ V, $I_f = 0.05$ A (using one filament section).
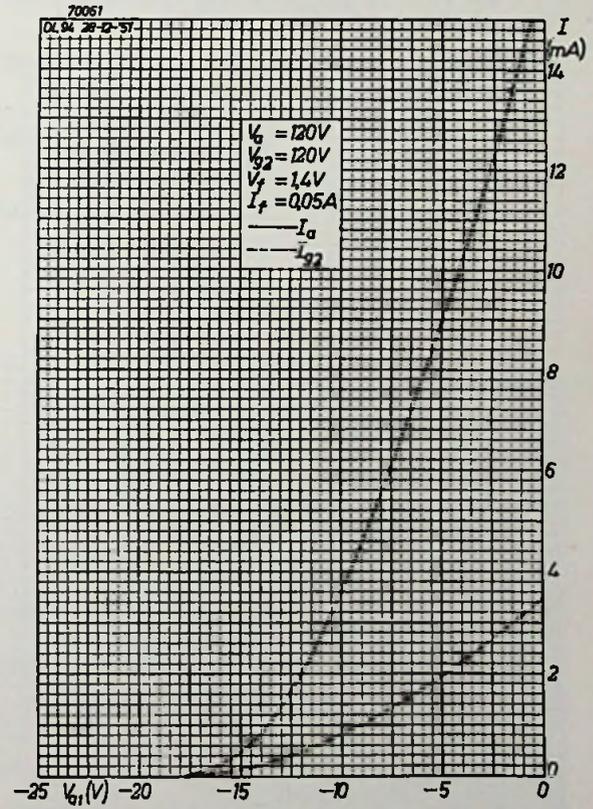

Fig. 59. Anode current and screen-grid current plotted against the control grid voltage for $V_a = V_{g2} = 120$ V and $V_f = 1.4$ V, $I_f = 0.05$ A (using one filament section).
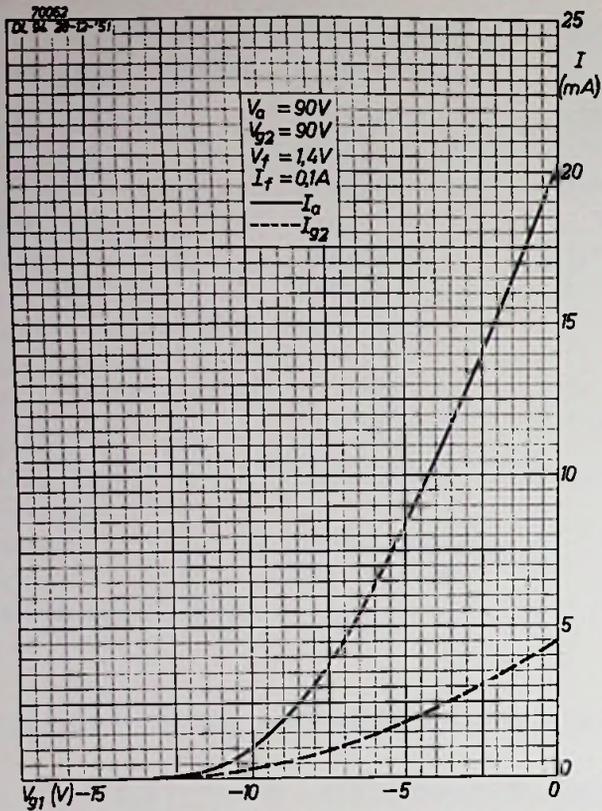
Fig. 60. Anode current and screen-grid current plotted against the control grid voltage for $V_a = V_{g2} = 90$ V and $V_f = 1.4$. $I_f = 0.1$ A (two filament sections in parallel).
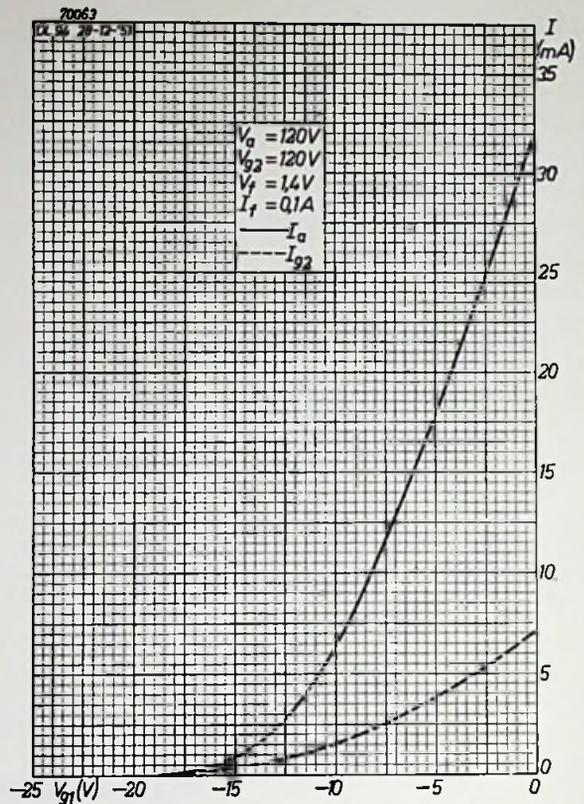

Fig. 61. Anode current and screen-grid current plotted against the control grid voltage for $V_a = V_{g2} = 120$ V and $V_f = 1.4$ V $I_f = 0.1$ A.

Fig. 62. Anode current and screen-grid current plotted against the control grid voltage for $V_a = V_{g2} = 150$ V and $V_f = 1.4$ V, $I_f = 0.1$ A.

Fig. 63. Anode current and screen-grid current plotted against the control grid voltage for $V_a = V_{g2} = 90$ V and $V_f = 2.8$ V, $I_f = 0.05$ A (two filament sections in series).
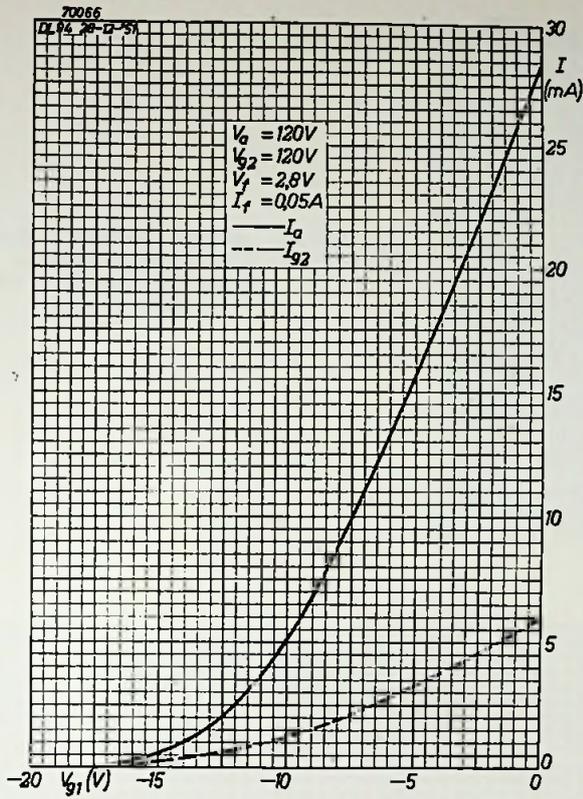
Fig. 64. Anode current and screen-grid current plotted against the control grid voltage for $V_a = V_{a2} = 120$ V and $V_f = 2.8$ V, $I_f = 0.05$ A.
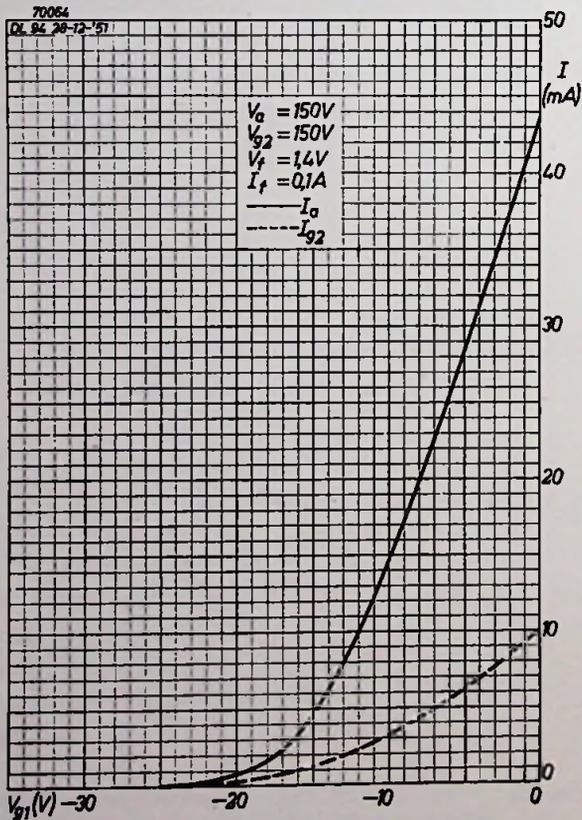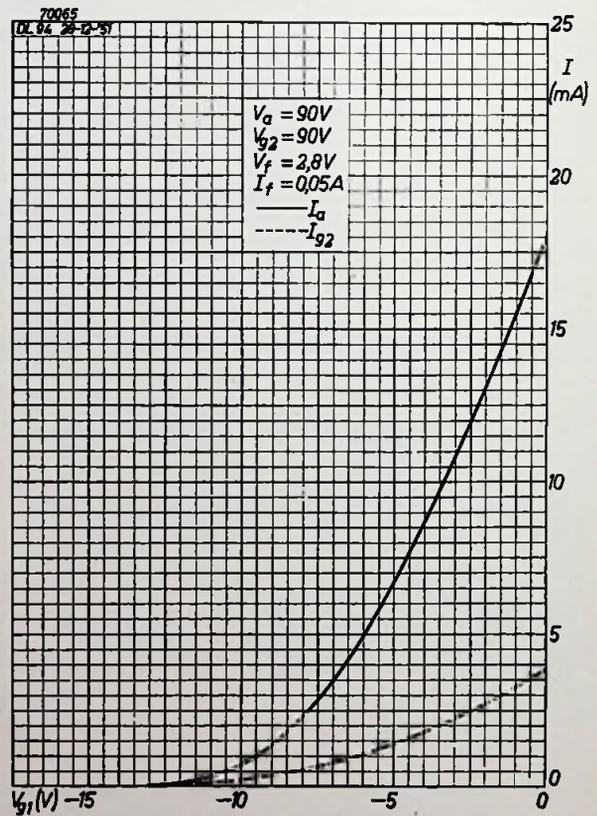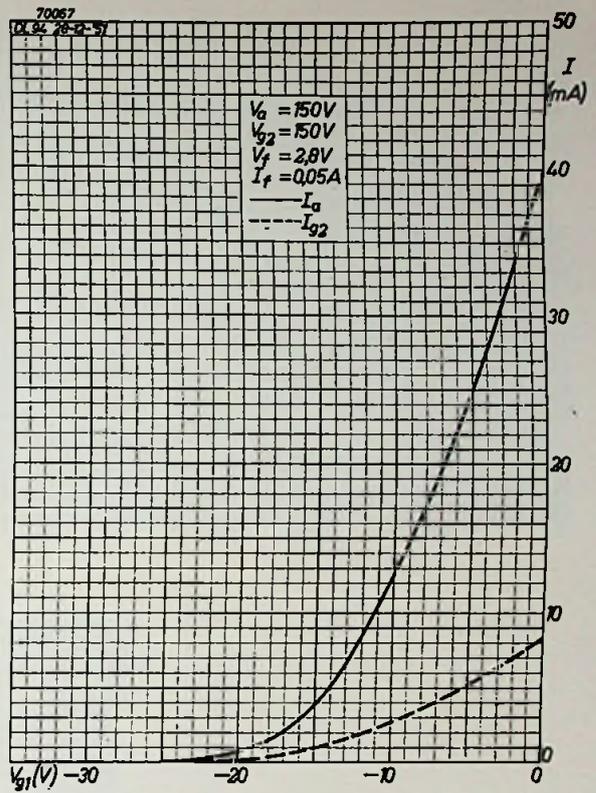

Fig. 65. Anode current and screen-grid current plotted against the control grid voltage for $V_a = V_{a2} = 150$ V and $V_f = 2.8$ V, $I_f = 0.05$ A.

Fig. 66. Anode current plotted against anode voltage for $V_{a2} = 90$ V and $V_f = 1.4$ V. $I_f = 0.05$ A.

39
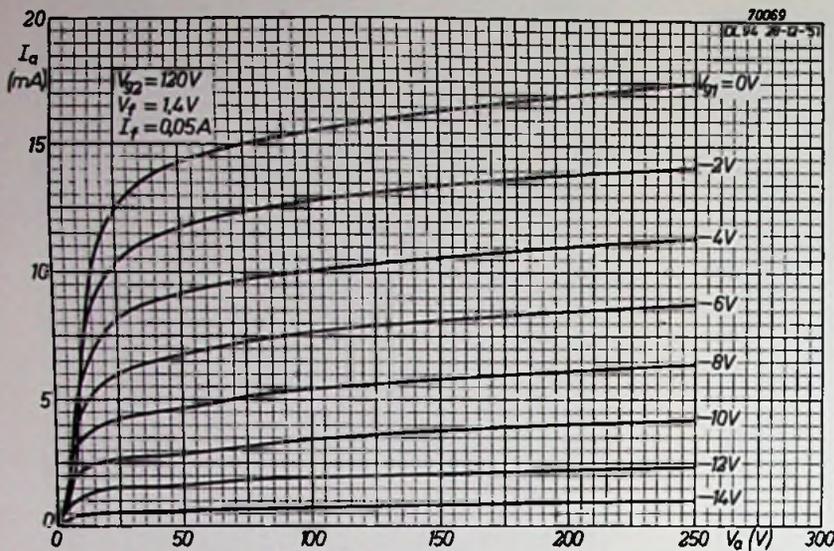
Fig. 67. Anode current plotted against anode voltage for $V_{g2} = 120$ V and $V_f = 1.4$ V, $I_f = 0.05$ A.
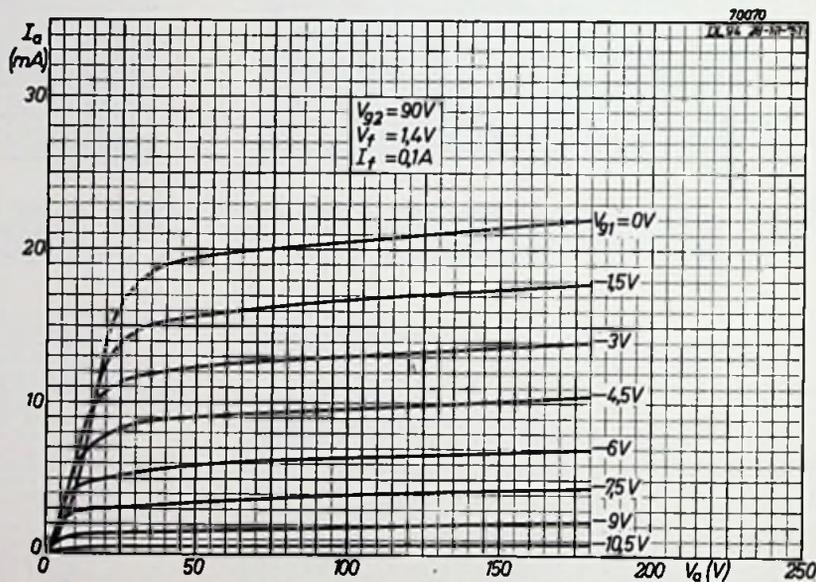
Fig. 68. Anode current plotted against anode voltage for $V_{g2} = 90$ V and $V_f = 1.4$ V, $I_f = 0.1$ A.
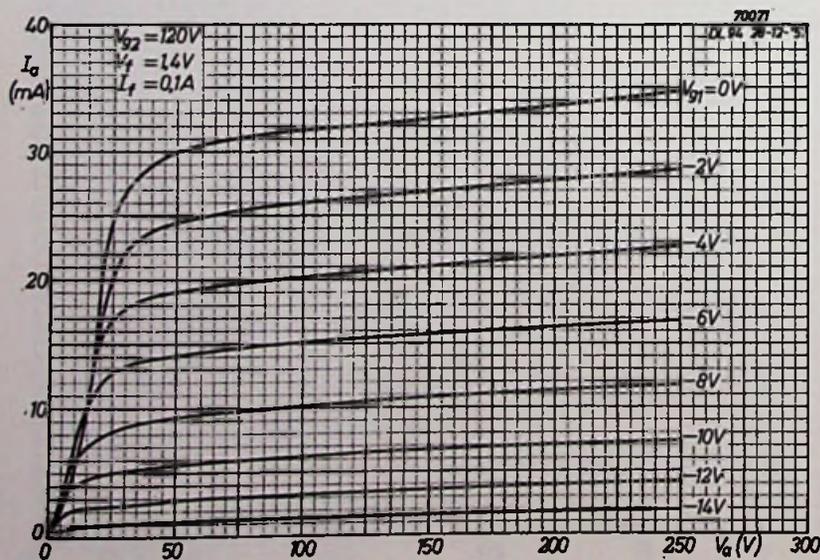
Fig. 69. Anode current plotted against anode voltage for $V_{g2} = 120$ V and $V_f = 1.4$ V, $I_f = 0.1$ A.

Fig. 70. Anode current plotted against anode voltage for $V_{g2} = 150$ V and $V_f = 1.4$ V, $I_f = 0.1$ A.
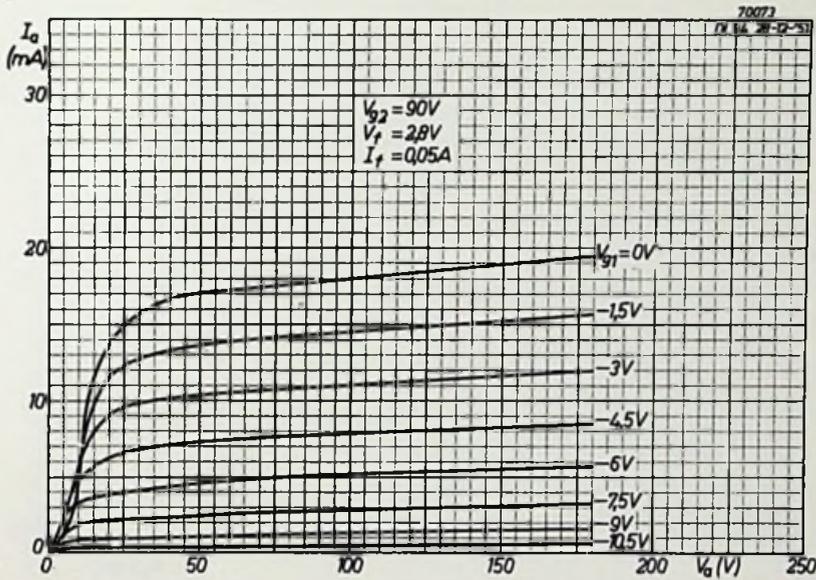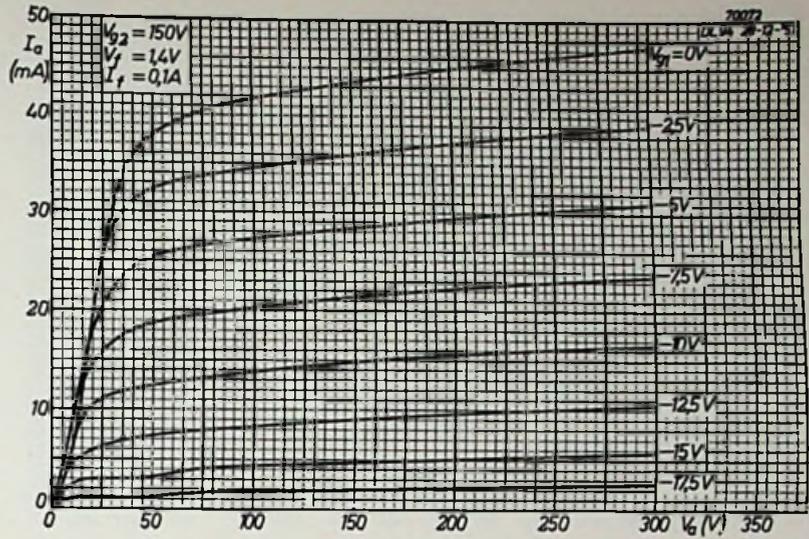
Fig. 71. Anode current plotted against anode voltage for $V_{g2} = 90$ V and $V_f = 2.8$ V, $I_f = 0.05$ A.

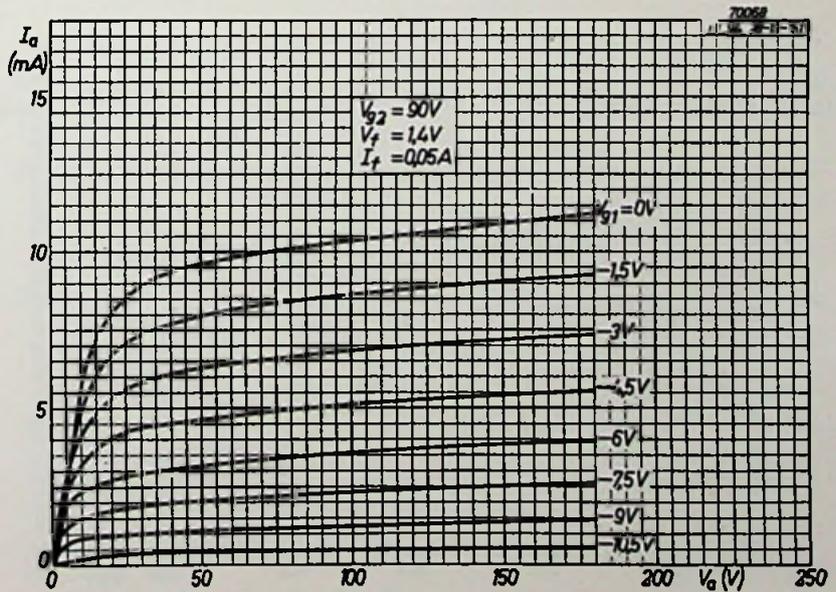**Fig. 72.** Anode current plotted against anode voltage for $V_{g2} = 120$ V and $V_f = 2.8$ V, $I_f = 0.05$ A.
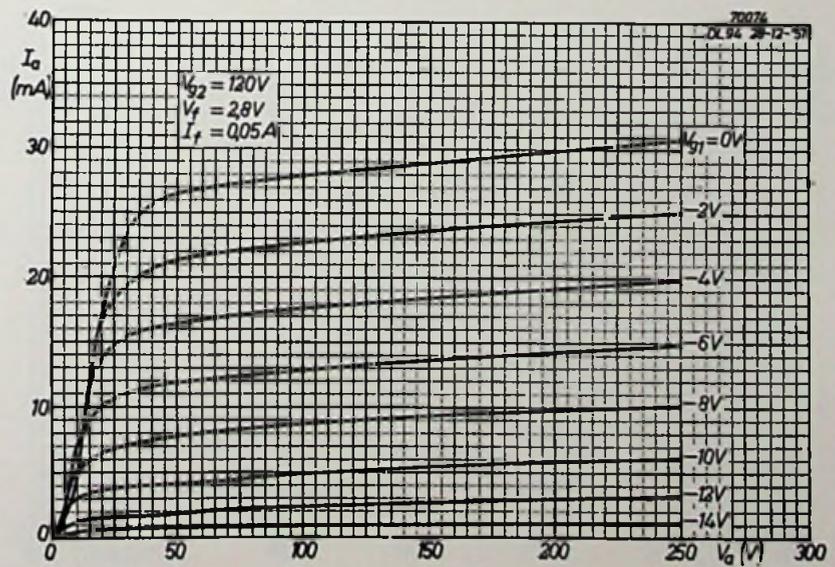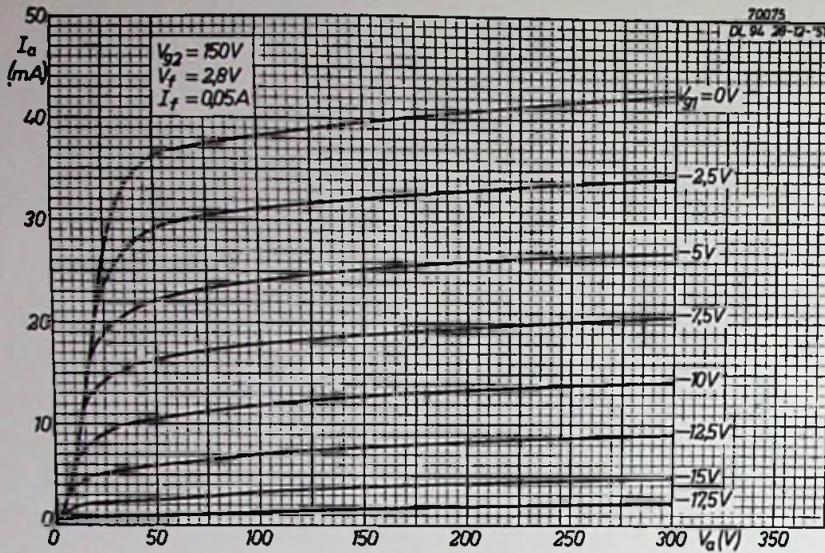
Fig. 73. Anode current plotted against anode voltage for $V_{g2} = 150$ V and $V_f = 2.8$ V, $I_f = 0.05$ A.



Fig. 74. Performance of one DL 94 tube in class A for $V_b = 90$ V and $V_f = 1.4$ V, $I_f = 0.05$ A (using one filament section).
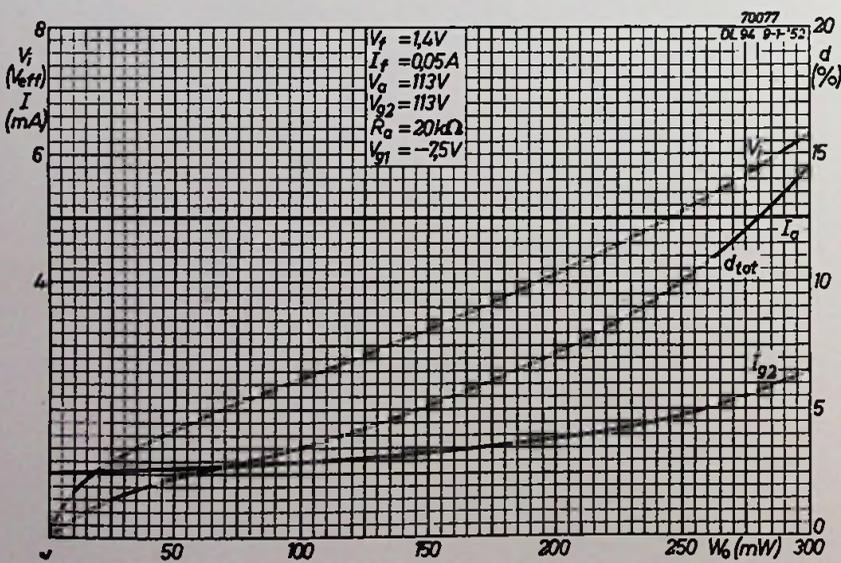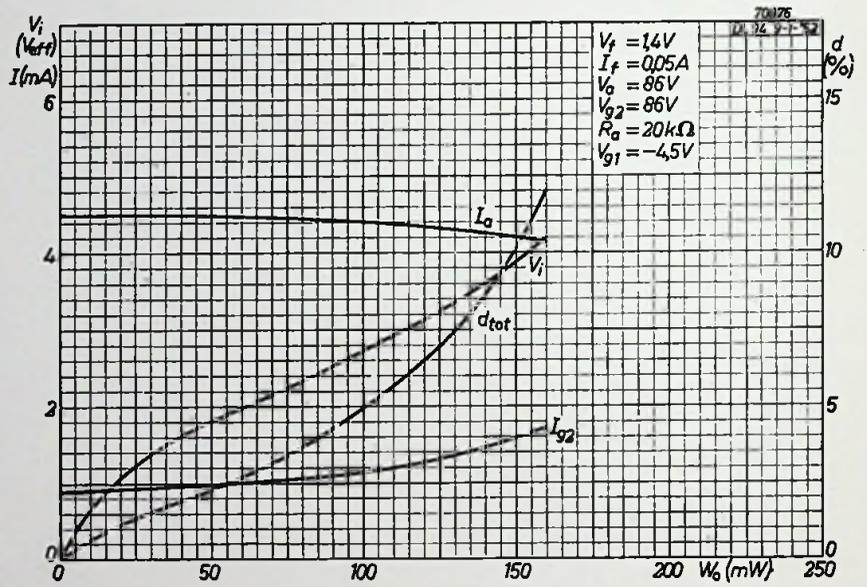
Fig. 75. Performance of one DL 94 tube in class A for $V_b = 120$ V and $V_f = 1.4$ V, $I_f = 0.05$ A.

Fig. 76. Performance of one DL 94 tube in class A for $V_b =$ 90 V and $V_f = 1.4$ V, $I_f = 0.1$ A (two filament sections in parallel).
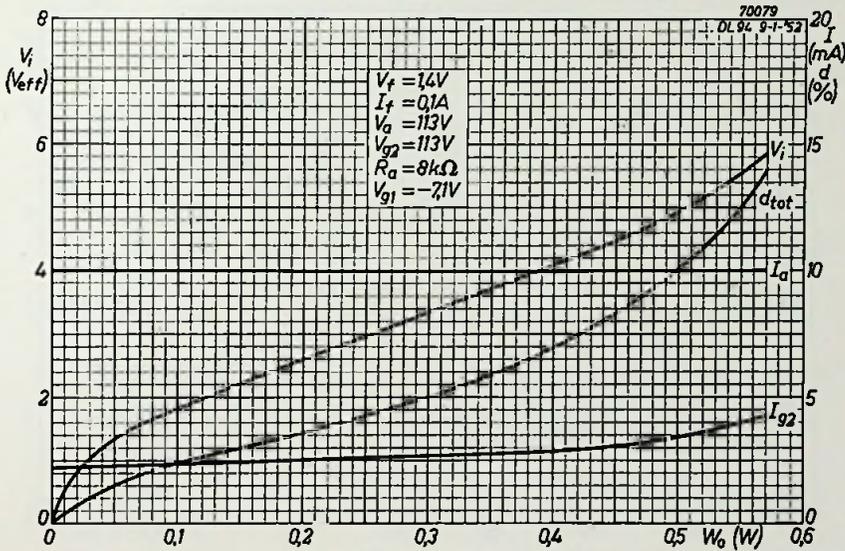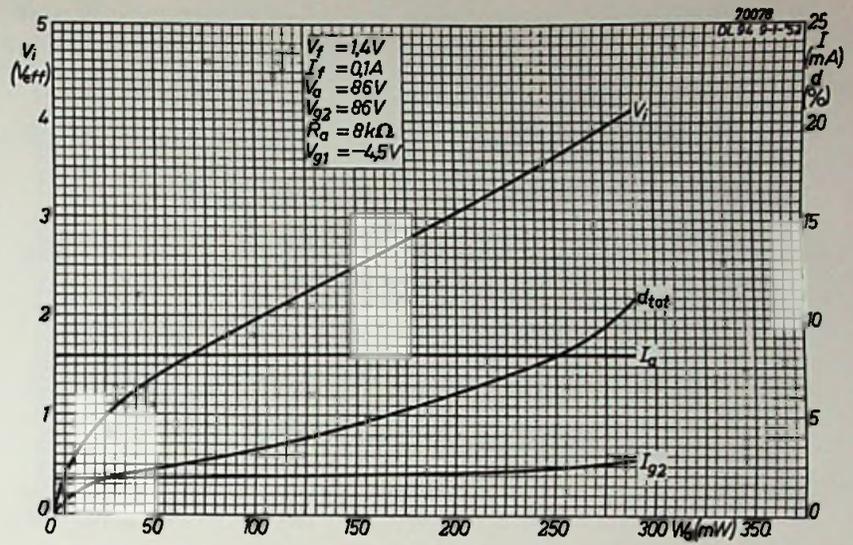
Fig. 77. Performance of one DL 94 tube in class A for $V_b =$ 120 V and $V_f = 1.4$ V, $I_f = 0.1$ A.

Fig. 78. Performance of one DL 94 tube in class A for $V_b =$ 90 V and $V_f = 2.8$ V, $I_f = 0.05$ A (filament sections in series).

43
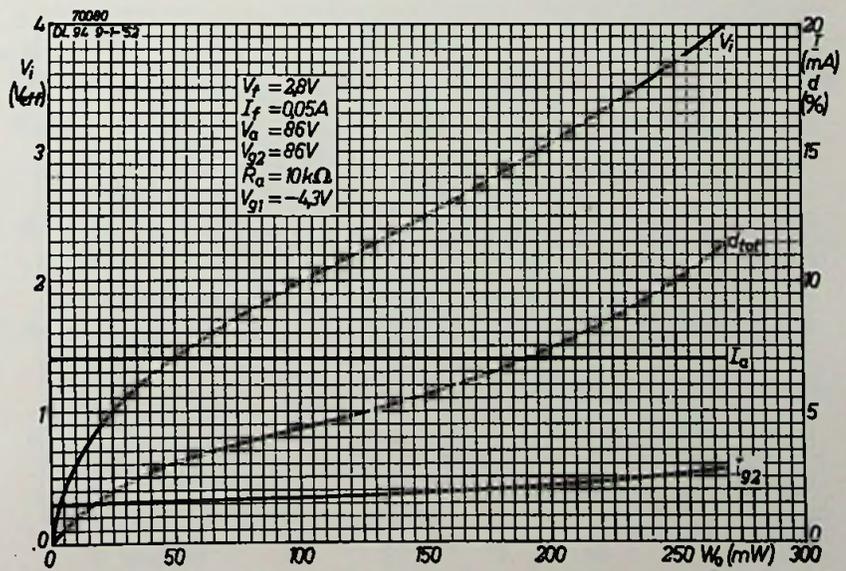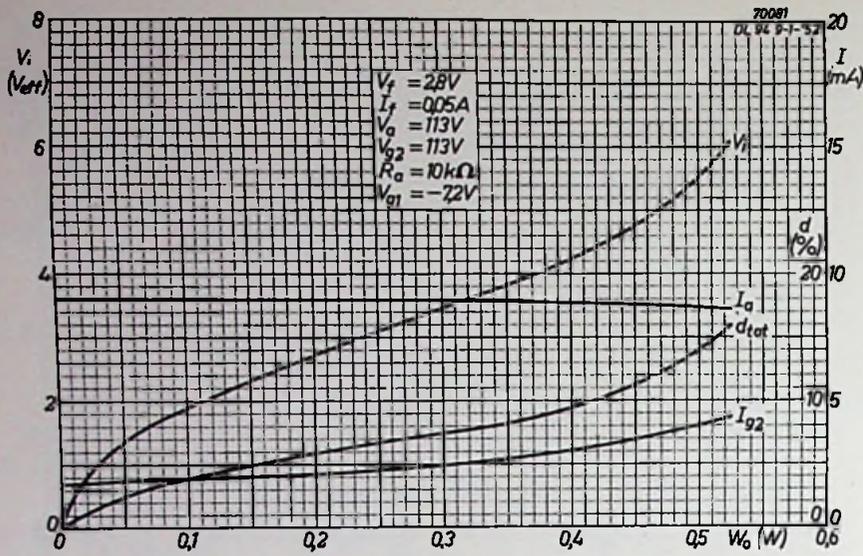
Fig. 79. Performance of one DL 94 tube in class A for $V_b = 120$ V and $V_f = 2.8$ V, $I_f = 0.05$ A.

Fig. 80. Performance of two DL 94 tubes in push-pull class A for $V_b = 90$ V and $V_f = 1.4$ V, $I_f = 2 \times 0.05$ A (parallel arrangement of one filament section of each tube).

Fig. 81. Performance of two DL 94 tubes in push-pull class A for $V_b = 120$ V and $V_f = 1.4$ V, $I_f = 2 \times 0.05$ A (parallel arrangement of one filament section of each tube).

Fig. 82. Performance of two DL 94 tubes in push-pull class A for $V_b = 90$ V and $V_f = 1.4$ V, $I_f = 2 \times 0.1$ A (all filament sections in parallel).

Fig. 83. Performance of two DL 94 tubes in push-pull class A for $V_b = 120$ V and $V_f = 1.4$ V, $I_f = 2 \times 0.1$ A (all filament sections in parallel).

Fig. 84. Performance of two DL 94 tubes in push-pull class A for $V_b = 90$ V and $V_f = 2.8$ V, $I_f = 2 \times 0.05$ A (filament sections of each tube in series, filaments of the two tubes together in parallel).

45

Fig. 85. Performance of two DL 94 tubes in push-pull class A for $V_b = 120$ V and $V_f = 2.8$ V, $I_f = 2 \times 0.05$ A (filament sections of each tube in series, filaments of the two tubes in parallel).

Fig. 86. Performance of two DL 94 tubes in push-pull class B for $V_b = 90$ V and $V_f = 1.4$ V, $I_f = 2 \times 0.05$ A (parallel arrangement of one filament section of each tube).
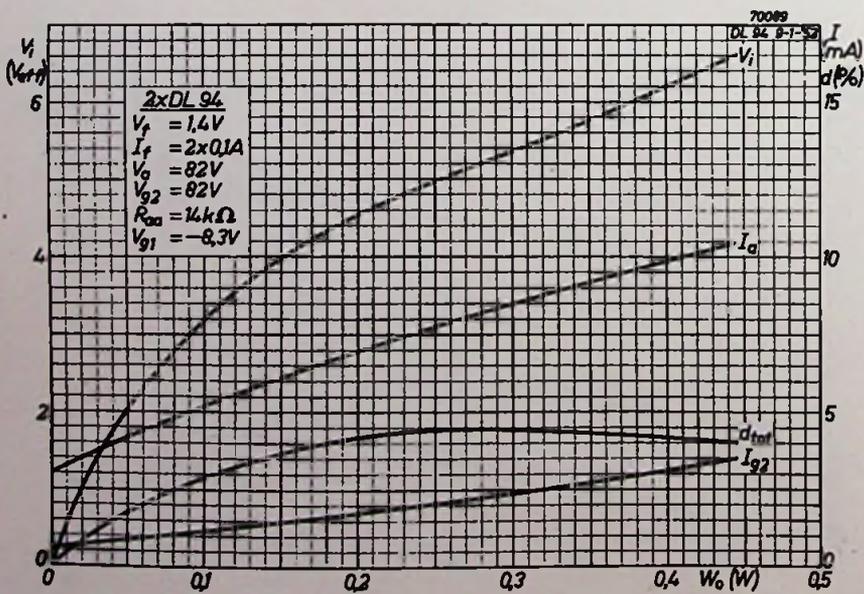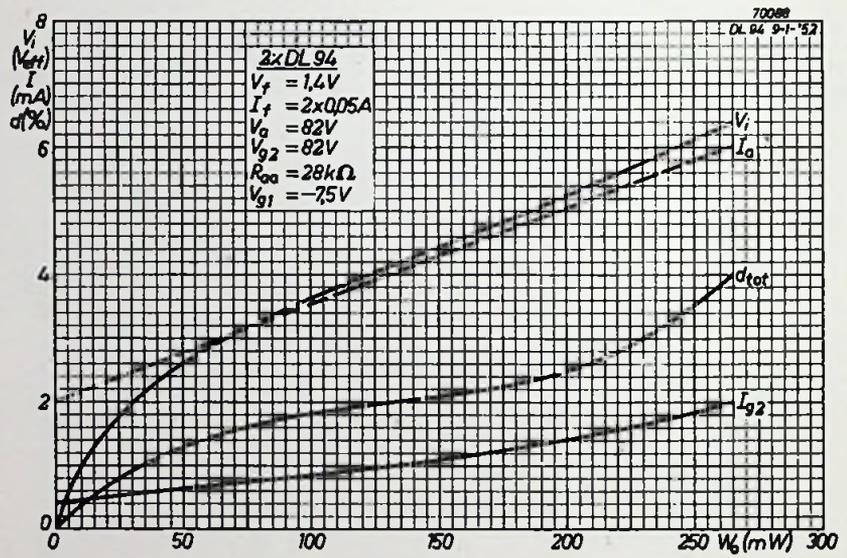
Fig. 87. Performance of two DL 94 tubes in push-pull class B for $V_b = 90$ V and $V_f = 1.4$ V, $I_f = 2 \times 0.1$ A (all filament sections in parallel).

46

Fig. 88. Performance of two DL 94 tubes in push-pull class B for $V_b = 120$ V and $V_f = 1.4$ V, $I_f = 2 \times 0.1$ A (all filament sections in parallel).
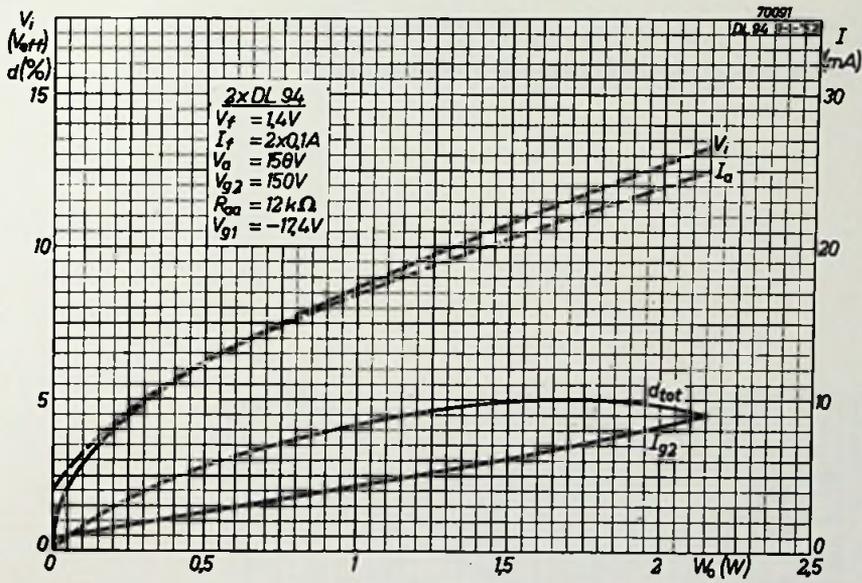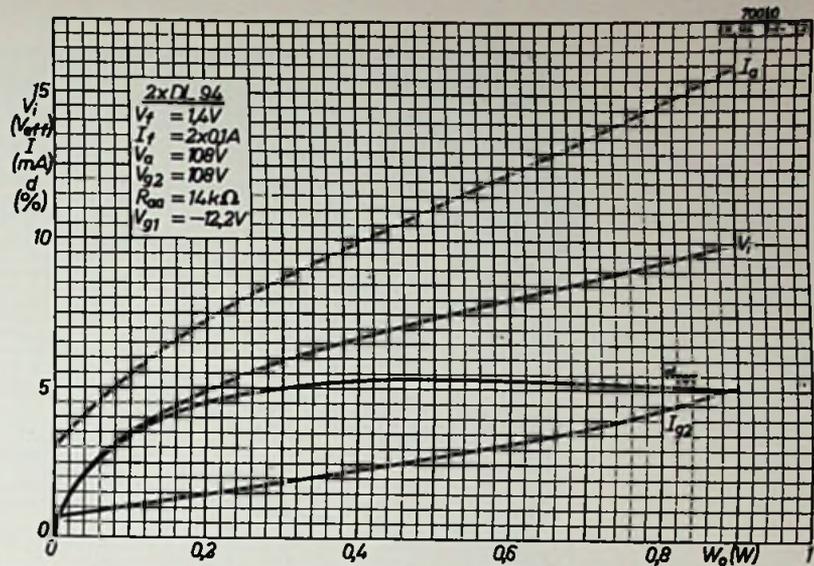
Fig. 89. Performance of two DL 94 tubes in push-pull class B for $V_b = 150$ V and $V_f = 1.4$ V, $I_f = 2 \times 0.1$ A (all filament sections in parallel).

Fig. 90. Performance of two DL 94 tubes in push-pull class B for $V_b = 90$ V and $V_f = 2.8$ V, $I_f = 2 \times 0.05$ A (filament sections of each tube in series, filaments of the two tubes in parallel).
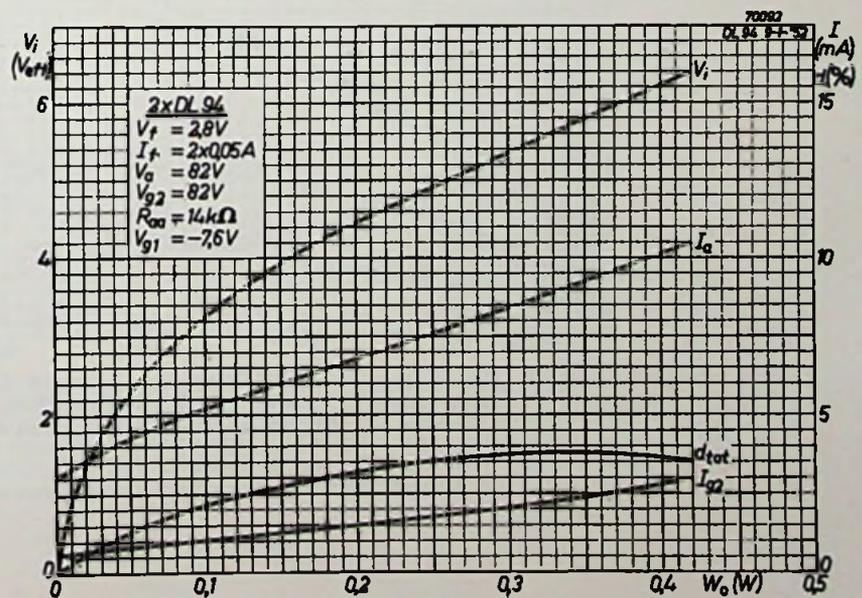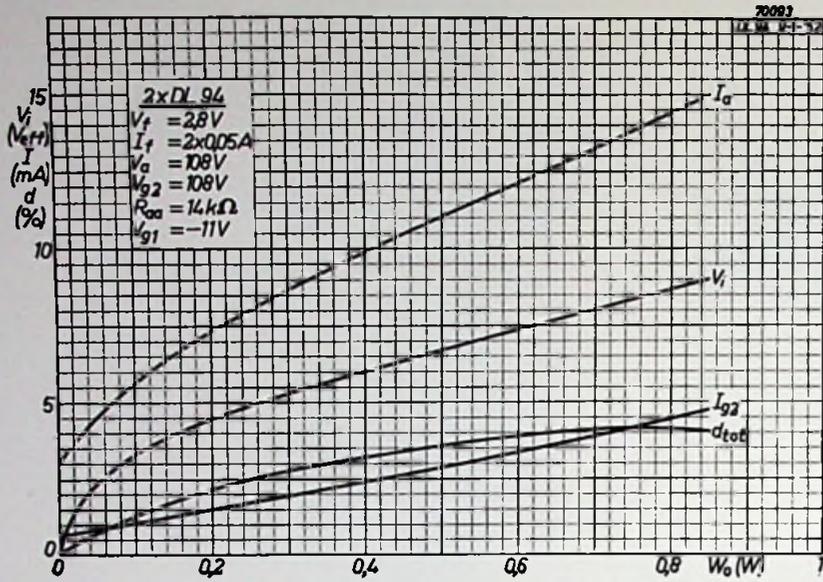
Fig. 91. Performance of two DL 94 tubes in push-pull class B for $V_b =$ 120 V and $V_f = 2.8$ V, $I_f = 2 \times 0.05$ A (filament sections of each tube in series, filaments of the two tubes in parallel).
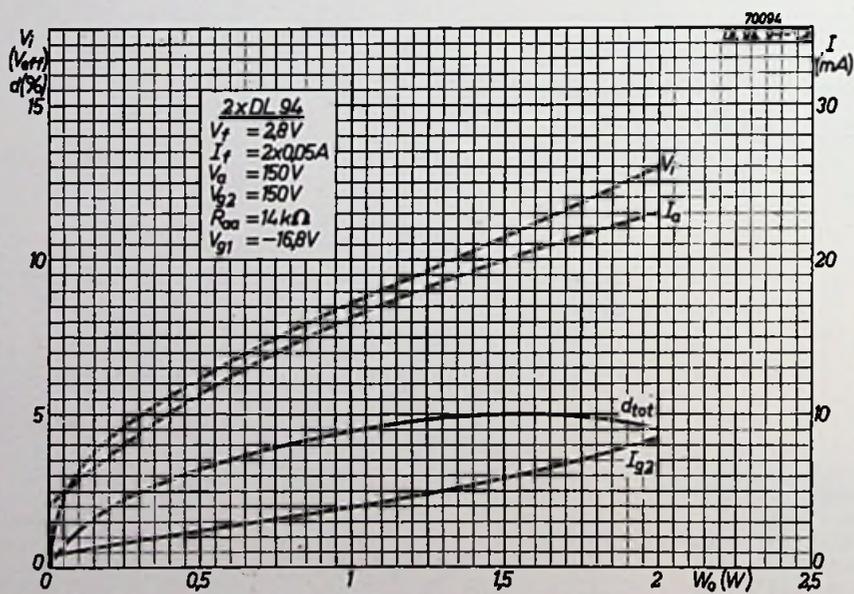
Fig. 92. Performance of two DL 94 tubes in push-pull class B for $V_b =$ 150 V and $V_f = 2.8$ V, $I_f = 2 \times 0.05$ A (filament sections of each tube in series, filaments of the two tubes in parallel).
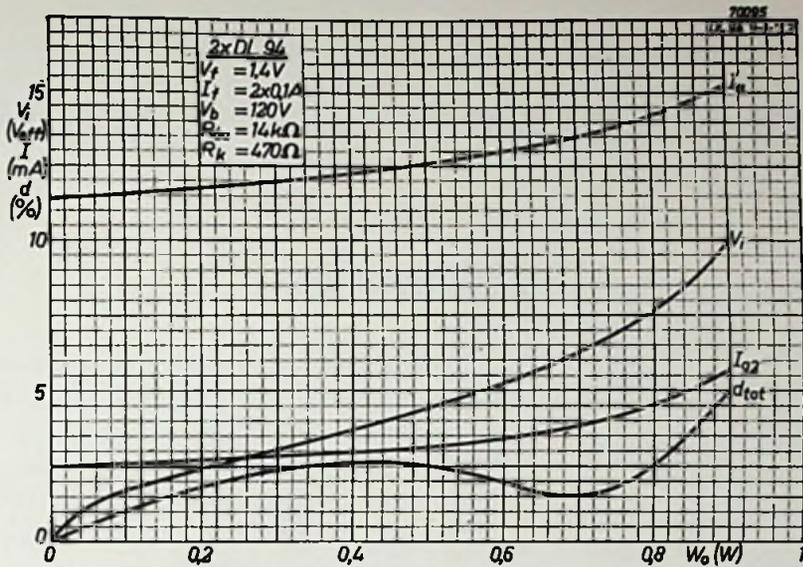
Fig. 93. Performance of two DL 94 tubes in push-pull class AB for $V_b =$ 120 V and $V_f = 1.4$ V, $I_f = 2 \times 0.1$ A (all filament sections in parallel). It is assumed that an additional current of 5 mA from the tubes preceding the push-pull stage also flows through R_k.
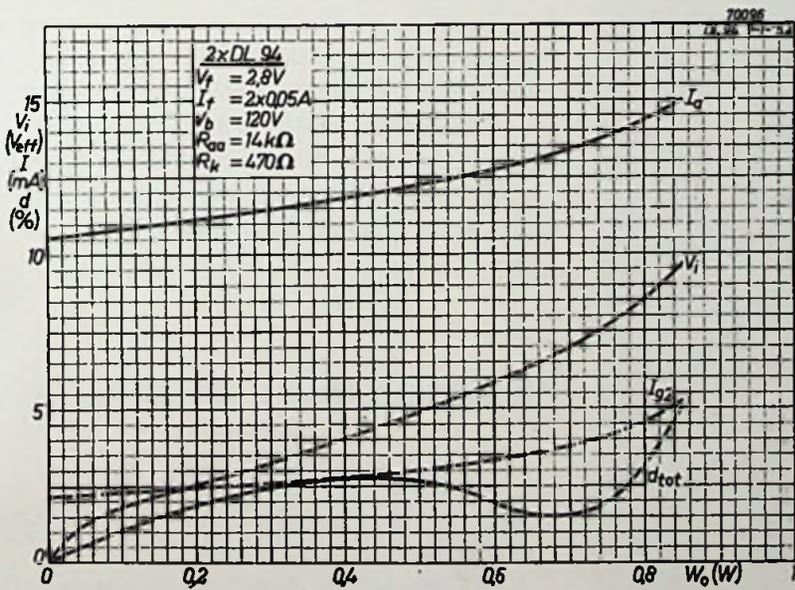
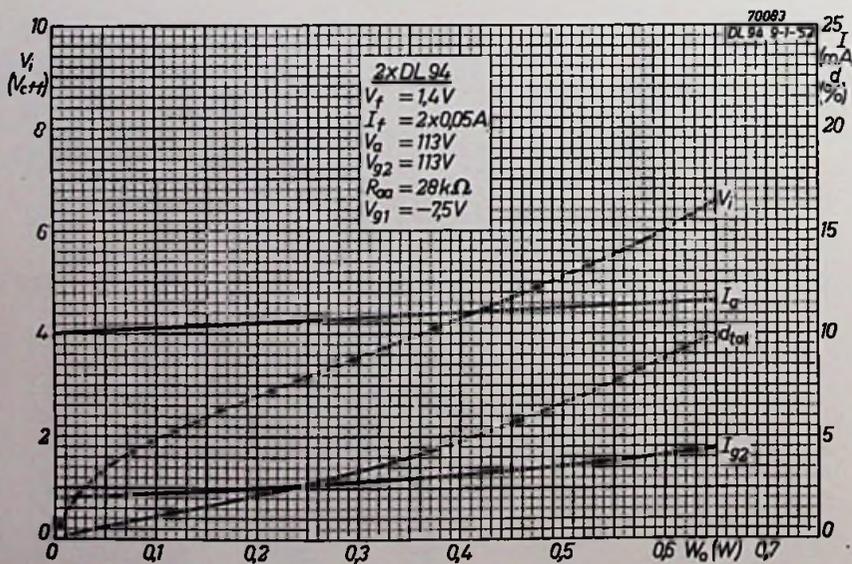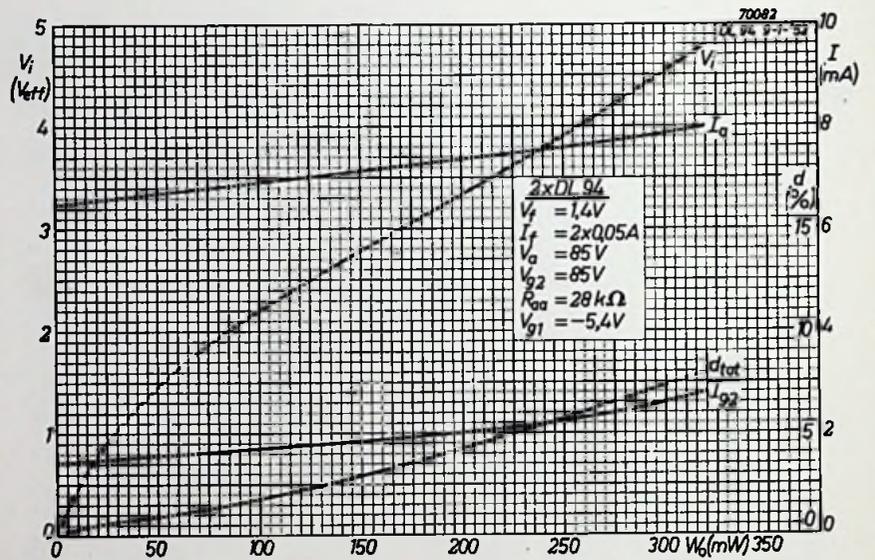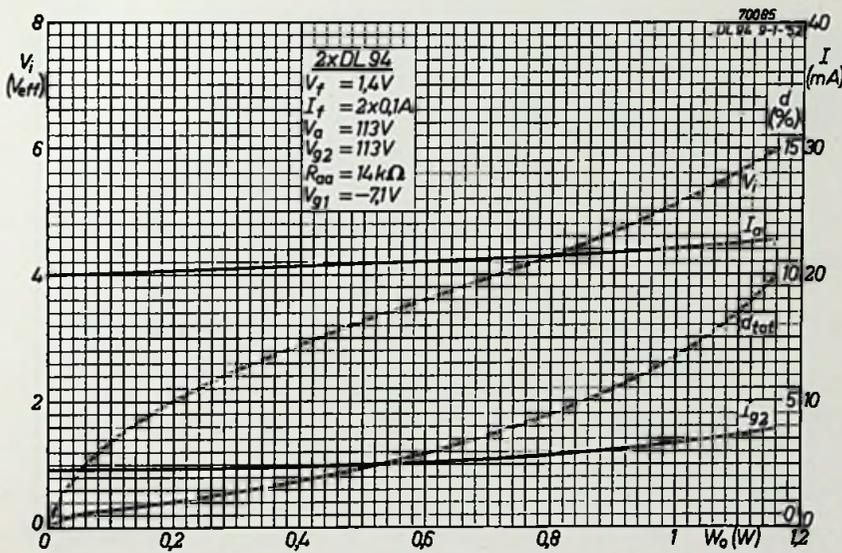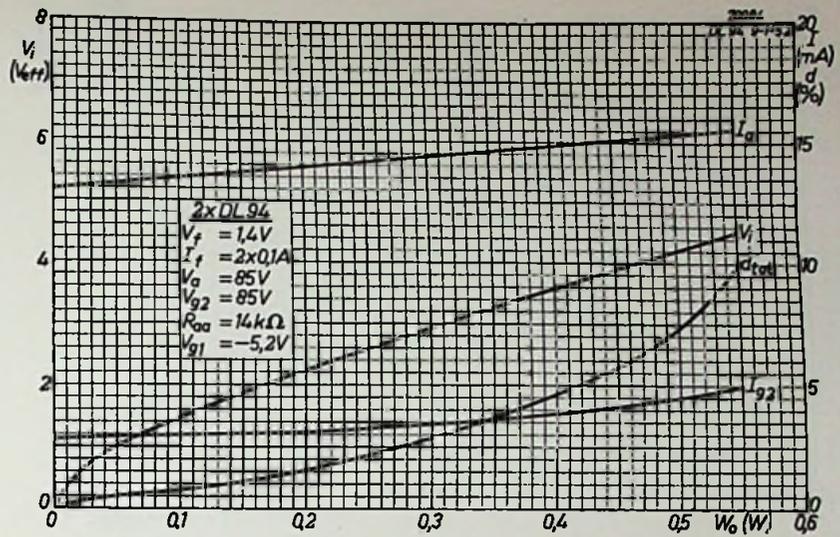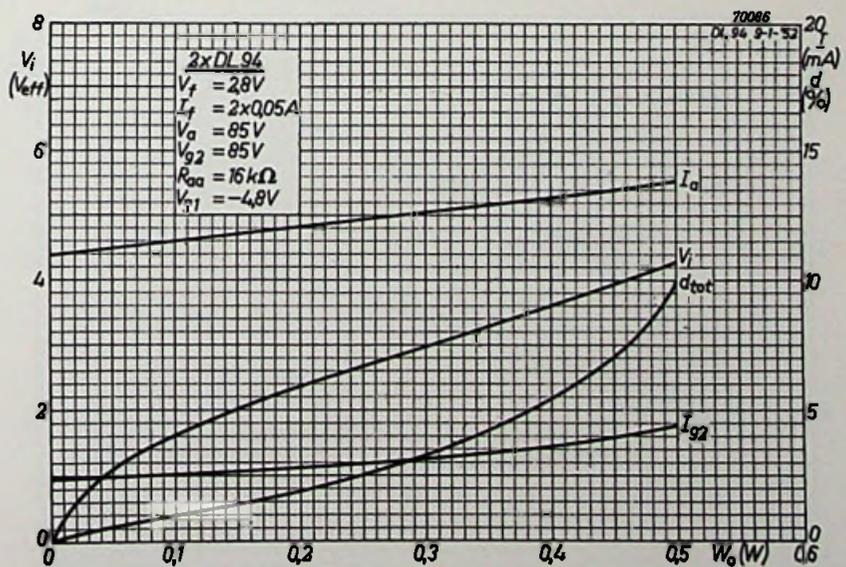Fig. 94. Performance of two DL 94 tubes in push-pull class AB for $V_b =$ 120 V and $V_f = 2.8$ V, $I_f = 2 \times 0.05$ A (filament sections of e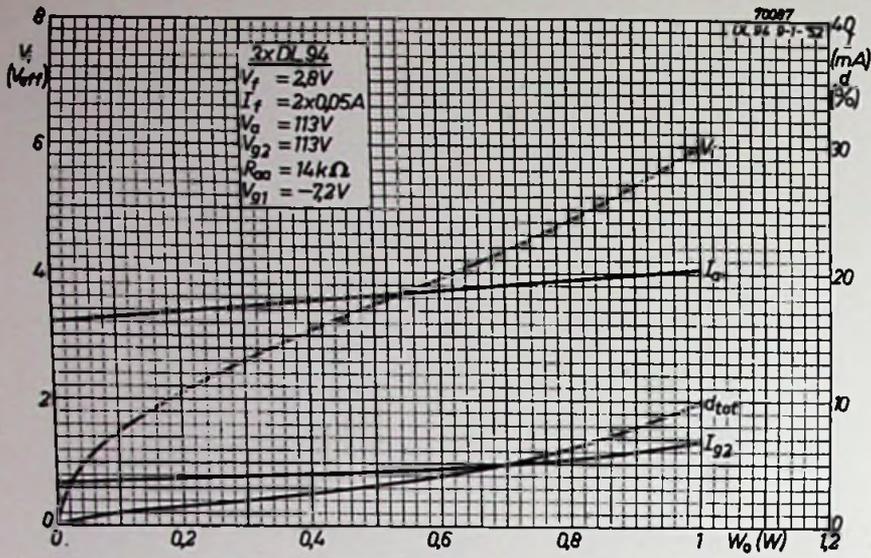ach tube in series, filaments of the two tubes in parallel). It is assumed that an additional current of 5 mA from the tubes preceding the push-pull stage also flows through R_k.

THE DM 70 AND DM 71 TUNING INDICATORS

Fig. 95. The DM 70 tuning indicator (about twice actual size) .

INTRODUCTION

The DM 70 and DM 71 tuning indicators are identical apart from the fact that the DM 70 requires no socket and its leads should be soldered to the circuit wiring, whereas the DM 71 has short connecting leads to be plugged into a socket. For the sake of convenience only type DM 70 will be mentioned henceforth; however, the comments are also applicable in their entirety to the DM 71.

This new type of tuning indicator differs from conventional tuning indicators by the simplicity of its design and its small dimensions. It has a directly-heated filament (1.4 V, 0.025 A) and requires an extremely low anode voltage (minimum rated voltage 60 V), so that it can be used to advantage in battery-fed receivers, where it can also serve as a pilot lamp, indicating whether the set is switched on or off. Its special shape and small size permit this tuning indicator to be so mounted that it moves over the station scale as the receiver is tuned, thus acting as an illuminated pointer.

The use of this rather unconventional, directly-heated tuning indicator in different types of receiver involves certain problems concerning filament and anode voltage supply and the way in which the tube is incorporated in the circuit.

Although the DM 70 has been specially designed for use in battery-fed receivers and its directly-heated filament is necessarily more fragile than the heaters of indirectly-heated tubes, it is quite possible to use this tuning indicator also in mains-fed receivers. [14]

CONSTRUCTION AND OPERATION

The DM 70 tuning indicator (fig. 95) has a subminiature envelope (maximum diameter 10.1 mm; maximum length without connecting leads 38 mm).

Figs 96a and b show cross sections of the triode electrode system. This consists of a filament *f*, a substantially flat control electrode *g* (to be called the "grid") and an anode *a*. The front of the anode is coated with luminescent material.
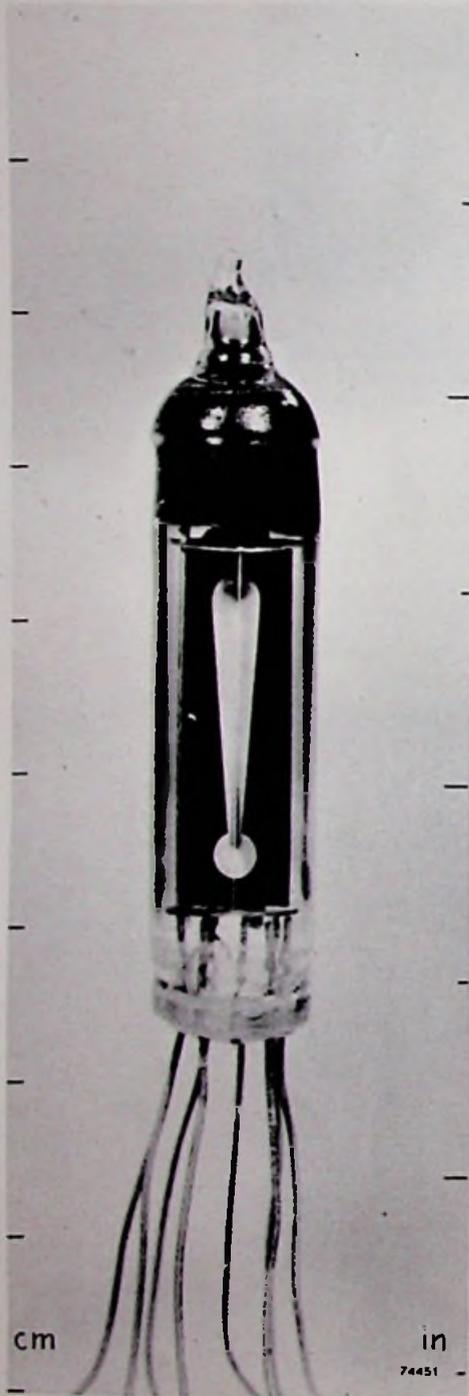
[14] See Electronic Application Bulletin, Vol. 14, No. 1/2, Januari/February 1953.

The grid (fig. 96c) consists of a metal plate having a vertical slot in the form of an exclamation mark, through which part of the luminescent anode is visible. Since the extremely thin, oxide-coated

a   *b*

c   *d*
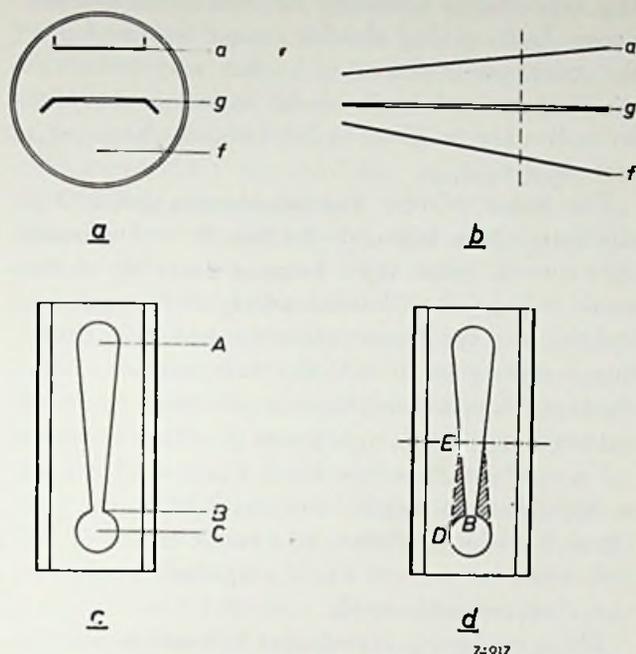
Fig. 96. (a) and (b) Transversal and longitudinal cross sections of the electrode system of the DM 70. f - filament, g - control electrode ("grid"), a - anode.
(c) and (d) Control electrode consisting of a plate with an aperture in the form of an exclamation mark. In (d) the upper half on this aperture has been reflected towards the lower half (broken lines).

filament is a dull emitter, it is hardly perceptible and does not obstruct the fluorescent pattern.

Special measures have been taken to prevent the stream of electrons to the anode from being affected by external fields. The influence of such fields might otherwise be such that the indication is completely upset and trouble might be experienced from hand capacitance effects. For this reason the envelope is provided with a transparent internal conductive coating (connected to the filament), which acts as an electrostatic screen without impeding the observation of the pattern.

The operation of the tube may be briefly described as follows, assuming for the sake of simplicity that the filament can he considered as an equipotential plane. This is, however, by no means the case, since there is a potential difference between the extremities of the filament, and it is therefore essential to ensure that the filament is correctly connected, as will be shown below.

Assume the grid potential to be such that the electrons proceed towards the anode through the entire grid aperture. As a result the anode will fluoresce along the entire length visible through the aperture of the grid, the length L of the light bar then being at a maximum (14 mm).

When the grid voltage is changed in the negative direction, the electron beam is first suppressed in the area where the grid aperture is narrowest (point B, fig. 96c). Further change of the grid potential reduces the length of the light bar as measured from point A. Finally, the stream of electrons flowing towards the anode is almost completely cut off by the grid and even the small fluorescent patches at point A and C. where the pattern is widest, will disappear. As a rule, however, in practice these patches remain visible, and this is particularly useful when the tuning indicator is also used as a pilot lamp or pointer for the station scale.

It should be noted that, in contrast to conventional tuning indicators, the fluorescent area of the DM 70 diminishes as the grid becomes more negative. This is due to the fact that the A.G.C. voltage directly controls the flow of electrons from the filament to the anode.

The design of the electrode system was determined by the following considerations:

(1) The luminous intensity of the fluorescent pattern should be satisfactory even at an anode voltage as low as 60 V.

(2) The characteristic representing the length of the light bar as a function of the grid voltage should have a sufficiently steep slope; the indicator should be cut off at about $V_g = -10$ V, $V_a = 85$ V.

(3) The luminescent patch at the bottom of the exclamation mark should not extinguish at a smaller value of $-V_g$ than required for reducing the length of the light bar to zero. This patch and the light bar should preferably disappear simultaneously.

(4) The penetration factor of the anode at point B should have a well-defined value.

Condition (1) has been satisfied by the use of a special luminescent material and by keeping the spacing between filament and grid fairly small.

In order to satisfy condition (2), i.e. to ensure that the light bar is completely suppressed at a fairly low value of $-V_g$, the penetration factor of the anode at point A is made small. Moreover, in order to satisfy condition (3), the penetration factors at points A and C must be almost equal. If

the anode-to-grid spacing and the grid-to-filament spacing were constant along the entire length of the indicator, the penetration factor would be larger at A than at C. This is shown by fig. 96d, in which a "reflection" of the upper half of the grid aperture is indicated in broken lines below the horizontal centre line. The contribution of the hatched areas EBD of the grid on the field strength at point C is a measure of the difference between the penetration factors at A and C. In order to render these penetration factors about equal, it was therefore necessary to make the anode-to-grid spacing at A larger than at C. Since a maximum is set to this spacing by constructional considerations, it was necessary to make not only the anode-to-grid spacing but also the grid-to-filament spacing at A larger than at C. This explains the oblique positions of the anode and filament with respect to the grid (cf. fig. 96b).

Since the interelectrode spacings at point B are already determined by conditions (1), (2), and (3), the penetration factor a point B — which determines the control starting point to be discussed below — is given the required value by suitable choice of the width of the grid aperture at B.

CONTROL RANGE

The characteristics of this tuning indicator are such that, at a given anode voltage, sensitivity is highest at small control voltages, similar to that of a variable-mu tube. Sensitivity depends to a large extent also on the anode voltage, decreasing with increasing anode voltage.

To investigate the operation of the tube more closely, it is necessary to introduce the concept of control starting point, V_{gr}. This is a tube characteristic, namely the value of the grid potential with respect to that of the earthed filament terminal [15]), at which a small decrease of the grid potential results in a noticable decrease of the maximum length ($= 14$ mm) of the light bar. The rated value of V_{gr} is approximately $+1.2$ V in the basic circuit, that is at an anode voltage of 85 V and D.C. supply to the filament, terminal 4 of which is earthed.

It should furthermore be remembered that the "steady voltage" V_{do} [16]) across the diode detector

[15]) In this description the term "earthed" is used to denote the filament terminal that is connected directly to the lower end of the detector circuit, i.e. as a rule to the chassis.

[16]) See H. H. van Abbe, Calculation of the Efficiency and Damping of Diode Detectors, Electr. Appl. Bull. 13, p. 65, 1952 (No. 5) where this voltage is denoted by V.

in conventional A.M. receivers may range from -0.2 V to -0.6 V. To ensure that even weak signals produce a variation in the length of the light bar of the DM 70, the A.G.C. voltage applied to this tube should obviously be undelayed, and the upper limit of V_{do} should always remain below the minimum value of V_{gr} that may occur in practice, because a threshold region over which no indication is given is introduced when $-V_{gr}$ exceeds $-V_{do}$.

The value of the control starting point V_{gr} obviously varies from tube to tube due to unavoidable spread, apart from being a function of the anode voltage, the filament supply (D.C. or A.C.), and the way the filament is connected. It is therefore necessary to connect the tube in such a way that, on the one hand, there is no risk of the tube not reacting to weak signals due to $-V_{gr}$ exceeding $-V_{do}$, and on the other hand V_{gr} should not be so high that the length L_o of the light bar at zero signal is unduly reduced, as a result of which the indication for a given signal amplitude would become unnecessarily small.

The spread in V_{gr} is such that its value may range from ± 0.1 V to $+2.3$ V at $V_a = 85$ V and D.C. supply to the filament, terminal 4 being earthed. There is thus no risk of the DM 70 being insensitive to weak signals even under the most unfavourable conditions, whilst the value of L_o still remains within reasonable limits.

When an anode voltage other than 85 V is applied, or when the filament is fed with A.C. instead of D.C., the DM 70 may be adapted to the changed conditions, so that V_{gr} again assumes the required value, by connecting the filament in a different manner.

USE OF THE DM 70 IN BATTERY RECEIVERS

In connecting the DM 70, two different types of battery receivers must be considered, namely those having an H.T. battery voltage of $V_b = 90$ V and the receivers designed for $V_b = 67.5$ V.

At $V_b = 90$ V, after deducting the negative grid bias for the output tube, an anode voltage of about $V_a = 85$ V remains available for the DM 70. According to the preceding section, terminal 4 ($-V_f$) of the tuning indicator should then be aerthed. As shown by figs 101 and 102, representing respectively the length L of the light bar as function of the grid voltage V_g with V_a as parameter and the relation between V_a, V_g and L for an average tube

terminal 4 of which is earthed, the control starting point V_{gr} is then $+1.2$ V and L_0 is 11 mm. The grid base of the DM 70 is seen to be 10 V, so that there is no risk of the tube being completely cut off.

Experiments carried out with a conventional 90 V, four-tube battery receiver having a sensitivity of 50 μV for an output of 50 mW, showed that a noticeable variation of the light bar is obtained at an aerial signal of 100 μV.

At $V_b = 67.5$ V the available anode voltage for the DM 70 is approximately $V_a = 60$ V, which — as shown by figs 101 and 102 — would result in V_{gr} assuming the unnecessarily high value of $+1.8$ V, L_0 being reduced to 9 mm.

It is therefore advisable to connect terminal 5 ($-V_f$) instead of terminal 4 to earth in this case, the characteristics shown in figs. 103 and 104 then being applicable to an average tube. It is seen that the control starting point V_{gr} is then reduced to $+1.3$ V, whilst L_0 is now 10 mm for an average tube. The grid base is still 7 V, which is ample for all normal applications.

Figs 99 and 100 show the anode current as a function of the grid voltage with the anode voltage as parameter, fig. 99 applying to a tube with terminal 4 earthed and fig. 100 to a tube with terminal 5 earthed.

USE OF THE DM 70 IN ABC RECEIVERS

In ABC receivers the filament of the DM 70 is connected in series with the filaments of the other D.C. fed receiving tubes, and if necessary shunted by a resistor; in the case of a 50 mA filament circuit this resistor should be $1.4/(0.050-0.025) = 56\ \Omega$. The correct sequence of the tubes in the filament circuit is governed by various requirements, such as hum, A.G.C. and grid bias of the output tube, as a result of which the DM 70 cannot occupy the most suitable place.

This will be illustrated by means of fig. 97, referring to a five-tube ABC receiver; similar considerations apply to four-tube ABC receivers.

It is seen that A.G.C. is applied to the I.F. tubes, to the frequency changer and also to the DM 70 tuning indicator. This is obtained by connecting a voltage divider between the positive side of the
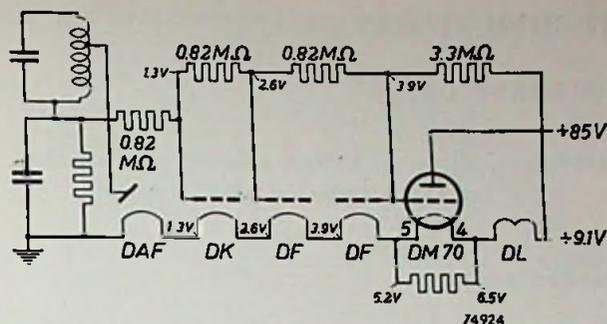
Fig. 97. Connection of the DM 70 in a five-tube ABC receiver. The voltages occurring at zero signal are indicated at various points.

L.T. supply ($+9.1$ V) and the detector diode. This voltage divider should be so designed that under zero signal conditions the bias (with respect to the negative filament terminal) of the controlled amplifying tubes is zero. This necessarily results in a reduction of the available control voltage: the proportion of the total control voltage across the load resistor of the detector that is applied to the frequency changer is 86%, whilst 72% is applied to the first I.F. tube and 57% to the second I.F. tube.

Proceeding in this way and connecting the grid of the DM 70 to a point with the same potential as its negative filament terminal would reduce the proportion of the control voltage applied to the DM 70 to 43%. The control voltage applied to the second I.F. tube is therefore also applied to the DM 70. Connection of the DM 70 in the usual manner for $V_a = 85$ V, i,e, with terminal 4 at a lower potential than terminal 5, would result in L_0 beign considerably reduced, for the effective value of V_{gr} is then $+1.2 + 1.3 = 2.5$ V. This is avoided by connecting the DM 70 so that terminal 5 is negative with respect to terminal 4, as a result of which the effective value of V_{gr} becomes $+0.4 + 1.3 = +1.7$ V for an average tube.

In an experimental ABC receiver with 5 tubes, having a sensitivity of 10 μV for an output of 50 mW, a clear indication was obtained at an aerial signal of 20 μV, while in an ABC receiver with 4 tubes, having a sensitivity of 50 μV for an output of 50 mW, an aerial signal of 50 μV was required.

TECHNICAL DATA [16]

FILAMENT DATA

Heating: direct by battery current, rectified A.C. or D.C.; series or parallel supply.

Parallel supply

Filament voltage	V_f =	1.4 V
Filament current	I_f =	0.025 A

Series supply

Filament voltage	V_f =	1.3 V

Mounting position: any

BASE CONNECTIONS AND DIMENSIONS
(in mm)

Fig. 98. The connecting wires of the DM 70 have the lengths as indicated in this fig. With the DM 71 all wires are cut to a length of 5 mm.

OPERATING CHARACTERISTICS

Filament voltage D.C.	V_f	1.4 [19]	1.4 [20]	V
Anode voltage	V_a	85	60	V
Grid voltage for complete extinction	V_g	—10	—7	V
Length of light bar (at $V_g = 0$v)	L	11	10	mm
Anode current at zero grid voltage	I_a	170	105	μA

LIMITING VALUES

Supply voltage ($I_a = 0$)	V_{bo}	max. 450 V	
Supply voltage	V_b	max. 300 V	
Anode voltage	V_a	max. 90 V	[21]
Anode voltage	V_a	min. 45 V	
Anode dissipation ($V_a \leqslant 90$ V)	W_a	max. 25 mW	[22]
Anode dissipation ($V_a = 200$ V)	W_a	max. 10 mW	[22]
Cathode current	I_k	max. 0.3 mA	
External resistance between grid and minus filament	R_g	max. 10 MΩ	

---

[16] The technical data of the DM 70 given here are provisional.
[17] This part of the leads should not be bent.
[18] This part of the leads should not be soldered.
[19] Pin 4 earthed.

[20] Pin 5 earthed.
[21] In non-controlled condition.
[22] At other values of V_a the maximum anode dissipation can be found by linear interpolation.

Fig. 99. Anode current I_a as a function of the grid voltage V_g with the anode voltage V_a as parameter, the filament being D.C. fed, terminal 4 earthed.

Fig. 100. Anode current I_a as a function of the grid voltage V_g with the anode voltage V_a as parameter, the filament being L.C. fed, terminal 5 earthed.
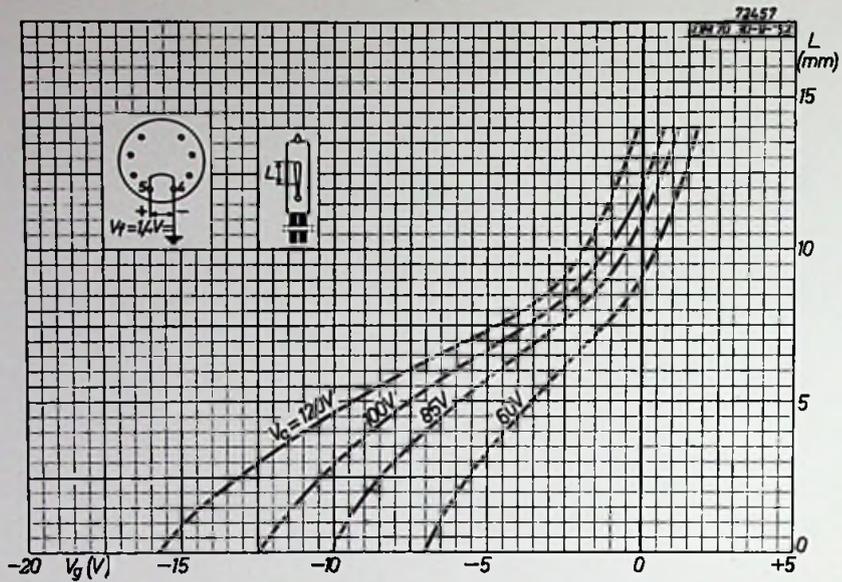
Fig. 101. Length *L* of the light bar as a function of the grid voltage V_g with the anode voltage V_a as parameter, the filament being D.C. fed, terminal 4 earthed.
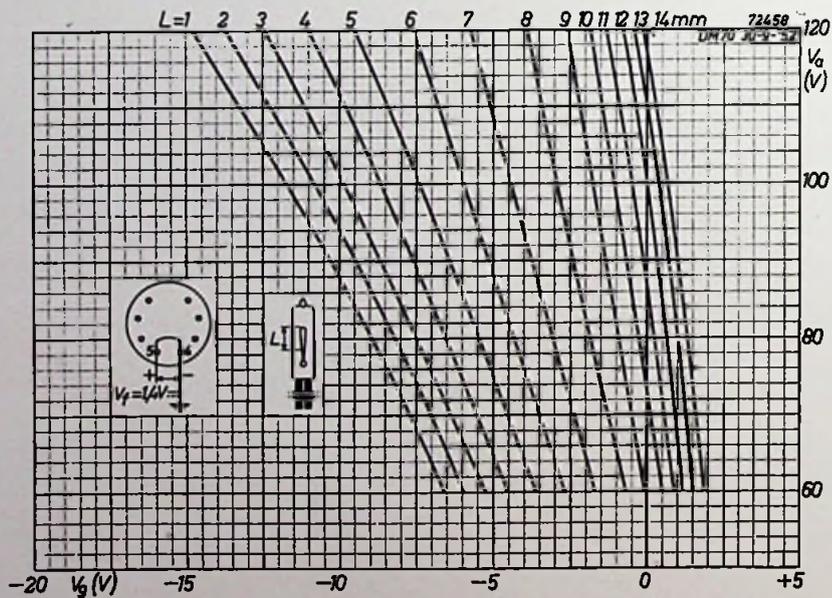
Fig. 102. Relation between V_a, V_g and *L* in the case of the filament being D.C. fed, terminal 4 earthed.
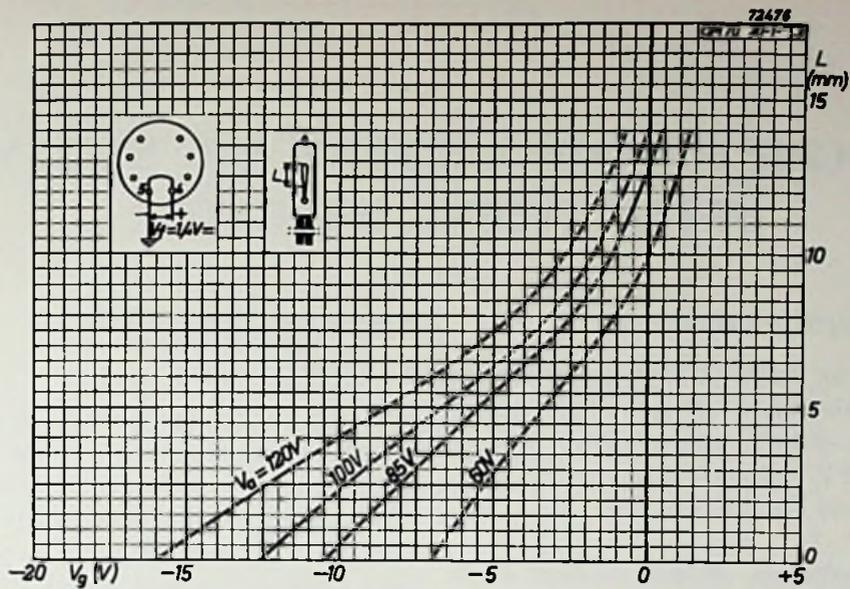
Fig. 103. Length L of the light bar as a function of the grid voltage V_g with the anode voltage V_a as parameter, the filament being D.C. fed, terminal 5 earthed.
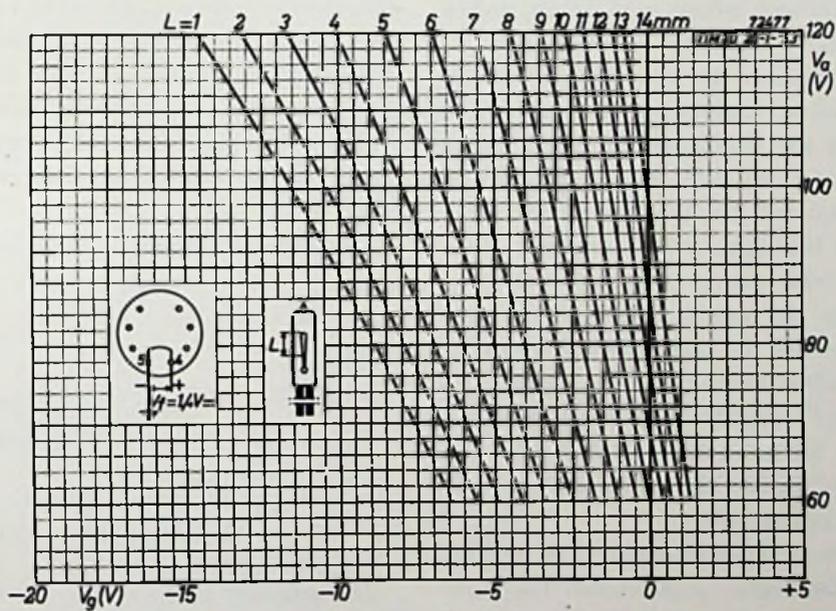
Fig. 104. Relation between V_a, V_g and L in the case of the filament being D.C. fed, terminal 5 earthed.

DESCRIPTION OF A 5-TUBE ABC RECEIVER WITH TUNING INDICATOR

GENERAL DESCRIPTION

The receiver to be described here is suitable for mains supply, either A.C. or D.C. with voltages of 220, 127 or 110 V, and for battery supply with an H.T. battery of 90 V and an L.T. battery of 9.8 V. Series supply is used for the filaments.

The tube complement of this receiver is as follows:

DK 92	frequency changer
DF 91	first I.F. amplifier
DF 91	second I.F. amplifier
DAF 91	detector and A.F. voltage amplifier
DL 94	output tube
DM 70	tuning indicator.

With this tube complement a sensitivity at the signal grid of the frequency changer of about 10 μV has been obtained, which is to be attributed to the use of an extra I.F. stage. The same result could have been obtained by provi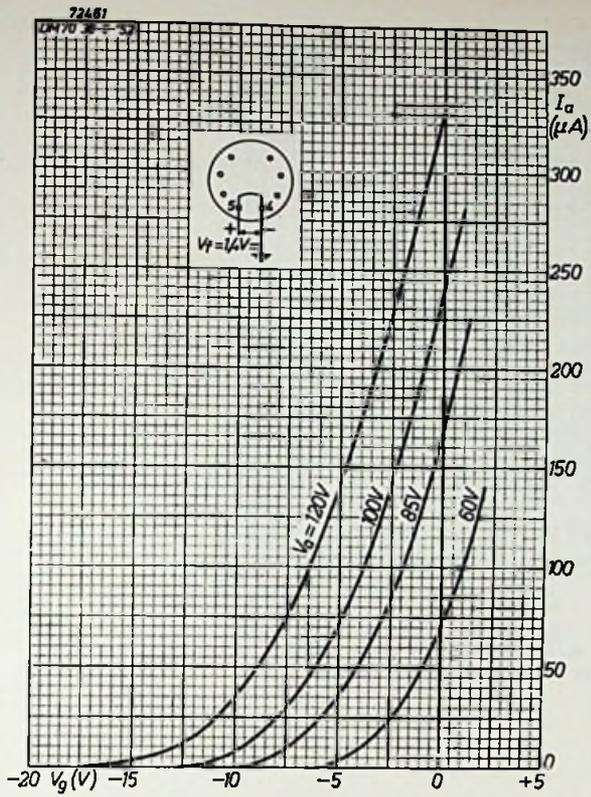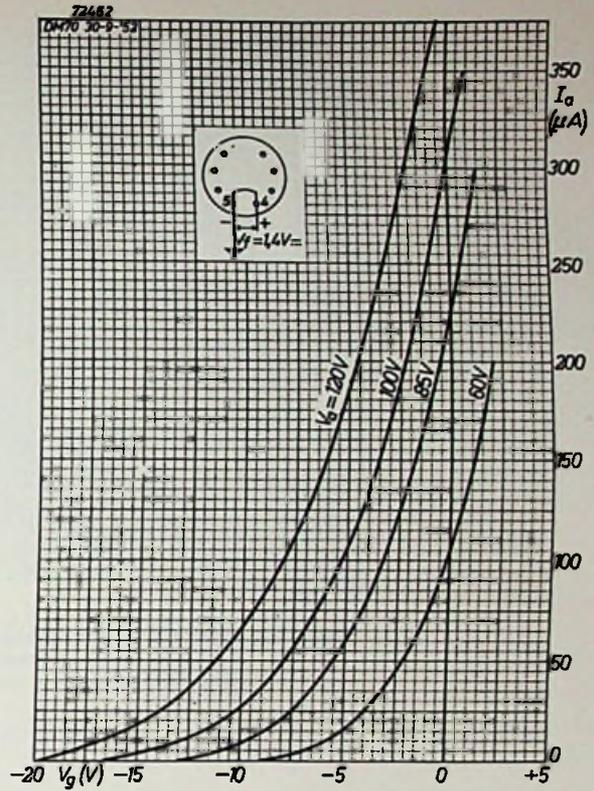ding one stage of H.F. amplification, instead of an extra I.F. stage, but this has the disadvantage that a three-gang tuning capacitor, an extra switch section and more coils are required. On the other hand with H.F. amplification the signal-to-noise ratio is somewhat better than with direct frequency changing. Since, however, in the ranges S.W. 2, M.W. and L.W. the impedance of the aerial circuit normally exceeds the equivalent noise resistance of the frequency changer, H.F. amplification would give better results only in the wave range S.W. 1 This improvement does not justify the expense of a number of additional components.

The complete circuit diagram is given in fig. 105. In this diagram the wave range switch has been drawn in the position for the first short-wave range, the wave ranges being:

S.W. 1	14.3—47	m	(21—6.38	Mc/s)
S.W. 2	48—159	m	(6.25—1.885	Mc/s)
M.W.	172—570	m	(1750—525	kc/s)
L.W.	795—2040	m	(377—147	kc/s)

CIRCUIT DETAILS

1. Frame aerial

In this design use is made of a one-turn frame aerial. Compared with a frame aerial having a large number of turns the type used here has the advantage that the sensitivity for electrostatic interference is small, this being of particular importance when the receiver is used with mains supply. Moreover, the parasitic coupling between different frame aerials, which are required when the multi-turn type is used, is avoided.

In the wave range S.W. 1 the total self-inductance of the aerial circuit is adjusted to the required value by means of an adjustable series coil L_2. In the other wave ranges the frame self-inductance is stepped up via special transformers with a high primary self-inductance, five times the frame self-inductance being sufficient. Other important characteristics of these transformers are: a high coupling factor between primary and secondary, obtained by using pot type cores, and a high quality through the use of litz wire for the windings. In each wave range the self-inductance can be adjusted by the adjustable series coils L_5, L_8 and L_{11} respectively.

The voltage induced in the frame aerial is:

$$V = \mu_0 \, O \, \omega H,$$

in which

$$\mu_0 = 4\pi \cdot 10^{-7} \left(\frac{V \sec}{A \, m} \right)$$

O = cross sectional area in m²,

H = magnetic field strength in A/m.

The relation between the electric and the magnetic field strength may be expressed by:

$$F/H = 120 \, \pi,$$

in which F is in V/m and H in A/m.

The voltage induced in the frame aerial can thus be written:
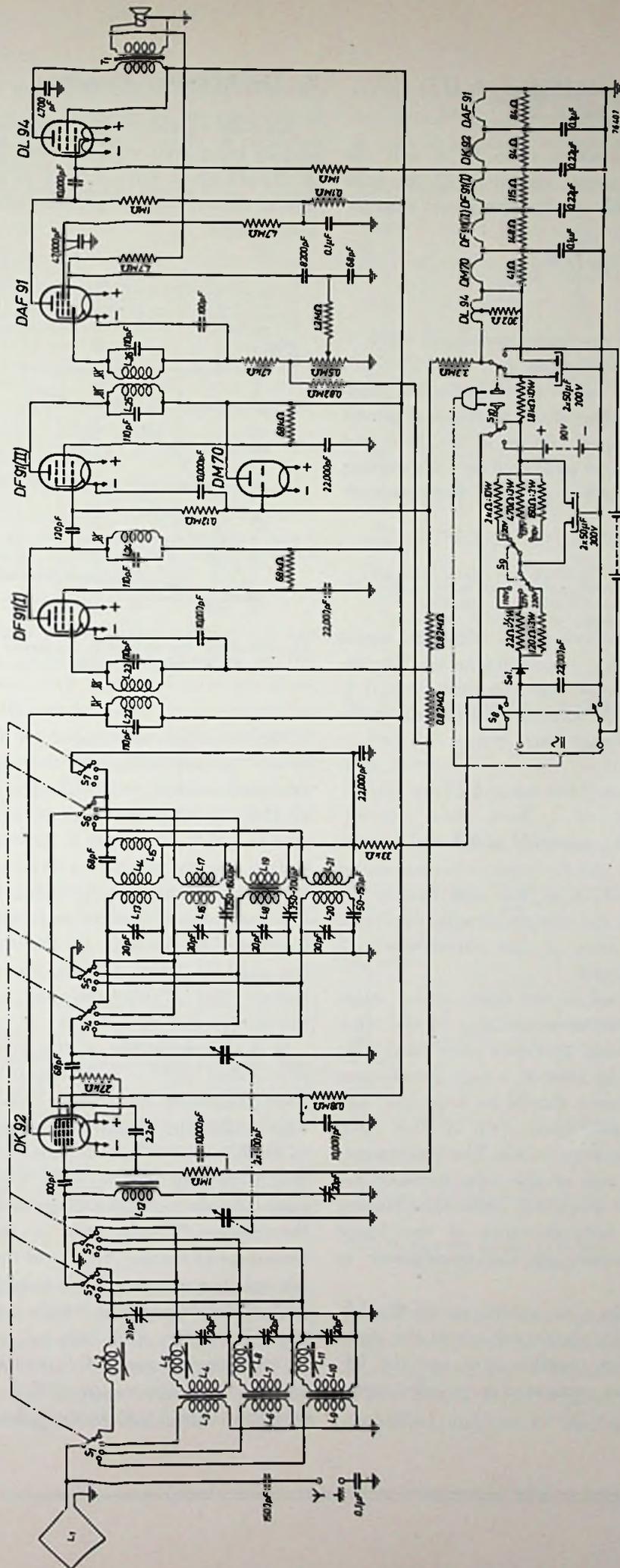
Fig. 105. Circuit diagram of the ABC receiver.

59

$$V = \mu_0 \, O \, \omega \, \frac{F}{120\pi} = \frac{2\pi f \, O \, F}{300 \times 10^6} = \frac{2\pi \, O \, F}{\lambda} \, .$$

Denoting the transformer ratio by n and the quality of the entire aerial circuit by Q, the voltage at the signal grid of the frequency changer becomes:

$$V_g = \frac{2\pi \, O \, F}{\lambda} \, n \, Q.$$

The dimensions of the frame aerial are 0.235×0.320 m and the cross-sectional area $O = 0.075$ m². In the medium-wave range the transformer ratio $n = 18.2$ and the quality of the total aerial circuit Q is about 40. The signal voltage at the third grid of the frequency changer produced by a transmitter on a wavelength of 300 m giving a field strength of 10 μ V/m is:

$$V_g = \frac{2\pi \times 0.075 \times 10}{300} \times 18.2 \times 40 = 11.4 \, \mu\text{V}.$$

This figure can be compared with the signal voltage obtained with a capacitive aerial. The effective height of the average capacitive aerial is about 0.5 m and for the same transmitter the available signal voltage would be:

$$V = F \cdot h = 10 \times 0.5 = 5 \, \mu\text{V}.$$

Assuming with the capacitive aerial a gain of 2, the signal voltage at the frequency changer would have a value of 10 μV. It is thus seen that in the medium wave range the sensitivity with the frame aerial is about the same as that obtained with a normal capacitive aerial.

The voltage induced in the frame aerial is independent of the cross-sectional area of the wire, but the self-inductance decreases with increasing wire diameter. For the sake of a high transformer ratio the self-inductance should be kept low, and for this reason an aluminium strip of 20×2 mm is used for the single-turn frame. The transformer ratio is the square root of the ratio between the total self-inductance required across the tuning capacitor and the self-inductance of the frame aerial with the primary of the transformer in parallel.

In a receiver with a capacitive aerial the I.F. wave trap is normally connected across the input terminals. This is not possible here and the I.F. wave trap is therefore connected in parallel to the tuning capacitor.

2. The frequency changer

Since the operation of the frequency changer has already been dealt with in detail in the description of the DK 92, it suffices here to give a number of curves illustrating its performance on the various wave ranges.
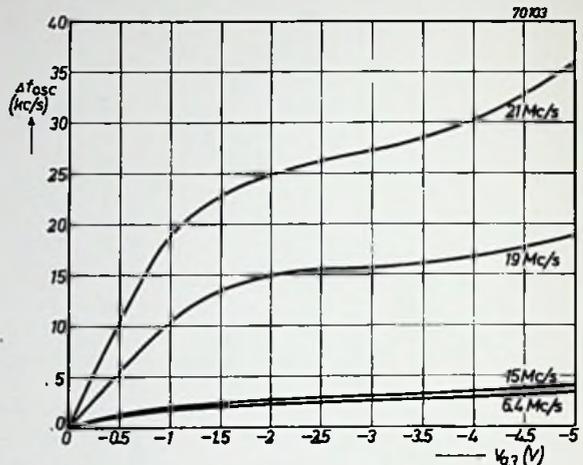
Fig. 106. Shift in oscillator frequency as a result of the A.G.C. with the signal frequency as parameter.

Fig. 106 shows the frequency shift as a function of the control voltage at the signal grid for the automatic volume control. In the wave range S.W. 1 at 21 Mc/s, when the control voltage varies from zero to —5 V, the shift is 36 kc/s. At 19 Mc/s the shift is already reduced to 19 kc/s, whilst at 15 Mc/s (20 m) it is only 4 kc/s, which is an exceedingly low value for a battery heptode. At the highest frequency of 6.4 Mc/s in the wave range S.W. 2 the shift is about 3.5 kc/s for the same control voltage, and at frequencies of 5.5 Mc/s and lower the shift is less than 1 kc/s.

It is thus seen that in the entire wave range of 48 — 159 m (6.25 — 1.885 Mc/s) the shift of oscillator frequency with A.G.C. is sufficiently low. This is also the case in the wave range of 14.3 — 47 m (21 — 6.38 Mc/s) for wavelengths between 20 and 47 m, but below 20 m the frequency shift caused by the control voltage affects the tuning of the receiver. Whether this — compared with the advantage of having A.G.C. on the frequency changer in this wave range — is to be considered an important disadvantage is mainly a matter of personal taste. Frequency shift can, of course, be avoided by switching off the A.G.C. to the frequency changer in the wave range S.W. 1. In the receiver described here A.G.C. is applied on all wave ranges.

In fig. 108 the pulling of the oscillator frequency is plotted against the detuning of the capacitor in the aerial circuit. This curve refers to an oscillator frequency of 20 Mc/s, and it should be realized that on the lower frequencies the ρulling is much smaller.
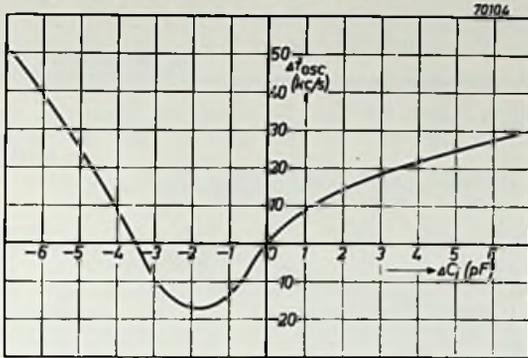
Fig. 108. Pulling of the oscillator frequency plotted against the capacitance variation of the input circuit for an oscillator frequency of 20 Mc/s.

Figs 109—112 give the oscillator current (current in the grid leak of 27 kΩ) as a function of frequency for the four wave ranges. Curves are given for nominal supply voltages and for underrunning of V_b and V_f. In the wave range S.W. 1 a booster coil L_{15} is employed in the oscillator circuit, and from fig. 109 it may be seen that a reasonable constancy of oscillator current is obtained over the whole wave range.
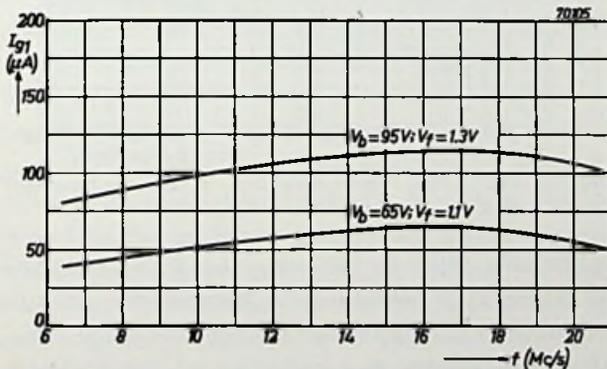
Fig. 109. Current I_{g1} flowing through the grid leak of the oscillator as a function of the frequency for the range S.W. 1 for nominal and reduced supply voltages.

When the oscillator current varies then the sensitivity for 50 mW A.F. output of the receiver measured at the signal grid of the DK 92 will also vary. This is shown in figs 113—116 where the sensitivity is plotted against frequency both for nominal supply voltages and for underrunning. It

should be understood that the reduction in sensitivity caused by underrunning is due to a decrease in gain of all stages in the receiver.
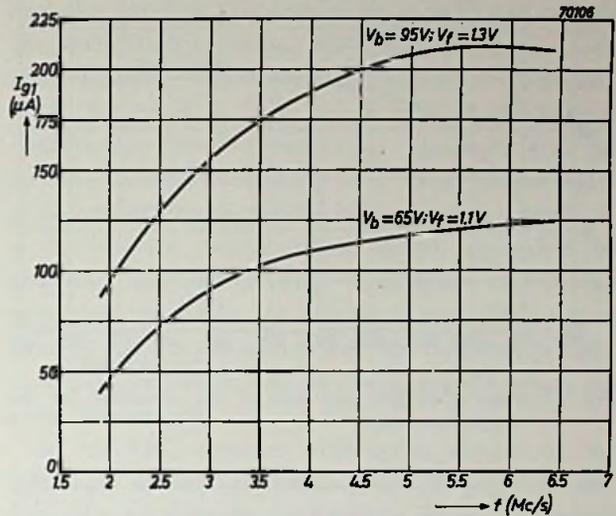
Fig. 110. Current I_{g1} flowing through the grid leak of the oscillator as a function of the frequency for the range S.W. 2 for nominal and reduced supply voltages.

3. I.F. amplification and A.G.C.

Two I.F. stages both with a DF 91 are used in this receiver. In order to reduce the selectivity, which would become too great if three I.F. transformers were used, a single tuned circuit L_{24} damped with 0.12 MΩ is used between the first and
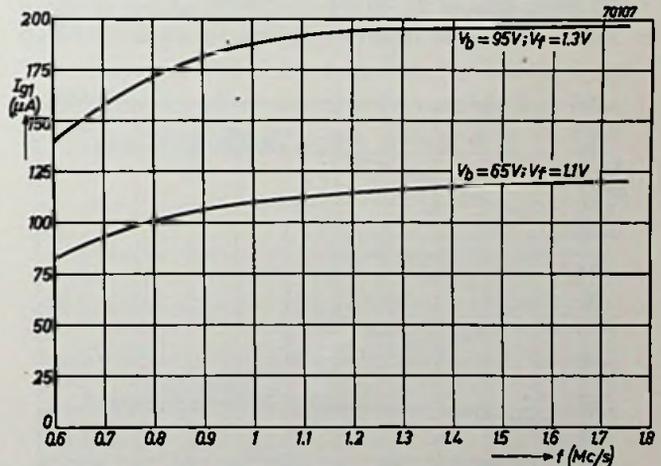
Fig. 111. Current in the grid leak of the oscillator for the medium-wave range.

second I.F. tubes. The bandwidth of the I.F. amplifier for a tenfold reduction of the response is 11.4 kc/s, at an I.F. of 452 kc/s.

The A.G.C. curve is given in fig. 117, whilst a simplified diagram of the A.G.C. network is re-
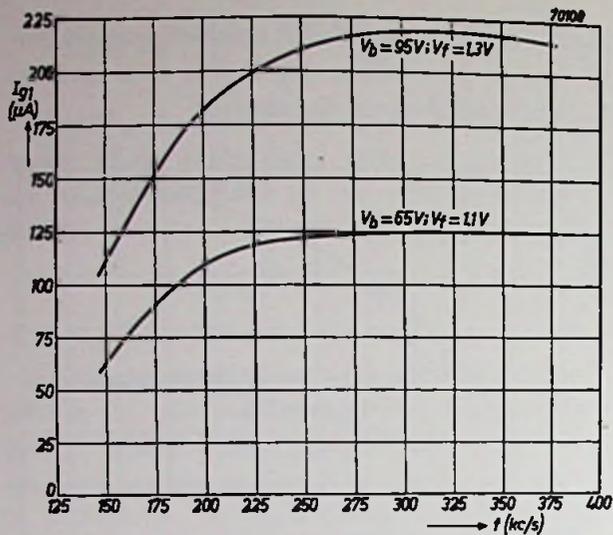
Fig. 112. Current in the grid leak of the oscillator for the long-wave range.
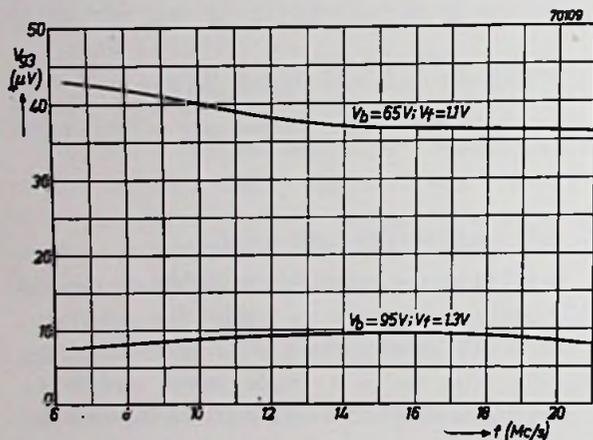
Fig. 113. Sensitivity for 50 mW output measured at the signal grid of the frequency changer for the range S.W. 1.
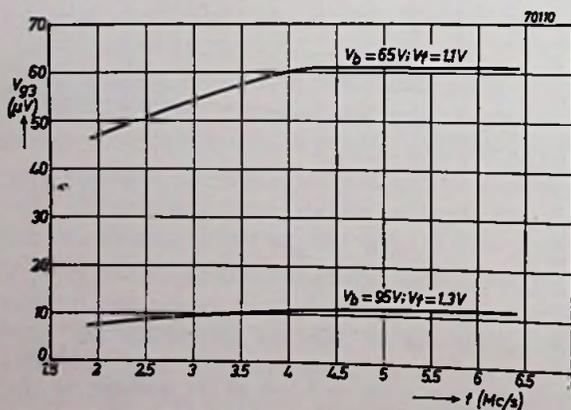
Fig. 114. Sensitivity for the range S.W. 2.

Fig. 115. Sensitivity for the medium-wave range.
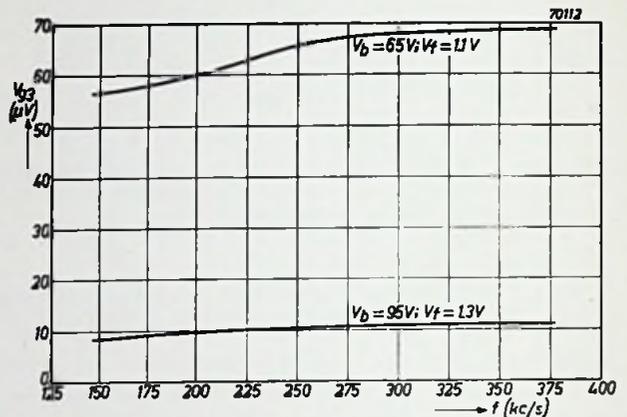
Fig. 116. Sensitivity for the long-wave range.
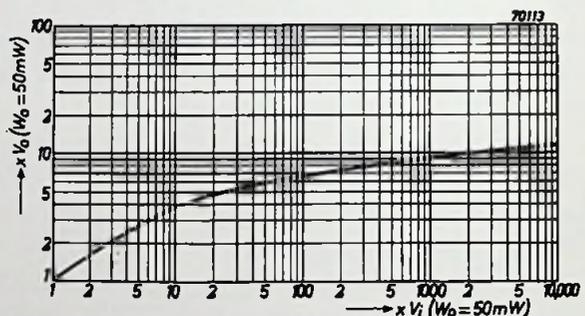
Fig. 117. The A.G.C. curve measured in the medium-wave range.

amplifying tubes is just zero, this being obtained by means of a potentiometer between the positive side of the L.T. supply and the detector diode. This, of course, results in a reduction of the available control voltage. The proportion of the total control voltage at the detector load of 0.5 MΩ applied to the frequency changer is 86%, whilst 72% is applied to the first I.F. tube and 57% to the second I.F. tube. Proceeding in this way in the normal circuit, the proportion of the control voltage applied to the tuning indicator would reduce the proportion of the control voltage applied to the DM 70 to 43% if this tube were connected according to the data given on page 54.

presented in fig. 118. It may be seen that A.G.C. is applied to the I.F. tubes, to the frequency changer and also the tuning indicator DM 70. Under zero signal conditions the bias at the controlled

In the data it is indicated that with an anode voltage of 90 V pin 4 of the tube base should be connected to the negative side of the filament supply, the control of the fluorescent pattern then starting from zero control voltage on the grid. It is, however, possible to delay the control by connecting pin 4 to the positive side of the supply (see fig. 118). Such is done in this receiver, with the advantage that the grid of the DM 70 can be connected to a more negative point on the potentiometer network where 57% of the total control
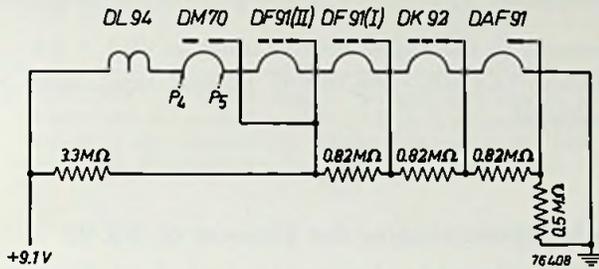
Fig. 118. The A.G.C. circuit.

voltage is available, as has been described on page 53.

4. The A.F. section

With an H.F. signal of 10 μV at the signal grid of the DK 92 the I.F. signal at the diode of the DAF 91 is about 1 V, this signal corresponding to the minimum permissible signal-to-noise ratio. For an I.F. voltage of 1 V at the diode the rectification efficiency is about 70%, so that with a modulation depth of 30% the detected A.F. voltage is 210 mV. Without negative feedback a sensitivity of 22.5 mV for 50 mW output could be reached at the control grid of the DAF 91, but this sensitivity is not permissible on account microphony. Moreover, having regard to the minimum permissible signal-to-noise ratio, there is not much point in making the total sensitivity of the receiver better than 10 μV, so that negative feedback can be applied in the A.F. section. This is done by returning the A.F. voltage at the loudspeaker to the control grid of the DAF 91 via a resistor of 4.7 MΩ. The detected A.F. voltage must then be applied via a resistor of 1.2 MΩ, the A.F. sensitivity measured at the diode then being 210 mV.

5. Power supply

For the H.T. supply with mains operation a selenium rectifier for 220 V A.C. and 90 mA D.C.

is used. It is necessary that with A.C. and D.C. supply the output voltages at the reservoir capacitor are the same. This has been attained by connecting resistors between the reservoir capacitor and the rectifier. To obtain equal D.C. voltages on the smoothing capacitor with different mains voltages, suitable series resistors can be switched in with the aid of S_9. The switch S_8 is of the normal double-pole single-throw type operated by the volume control. Switching over from mains operation to battery operation is done by S_{10}, which is a double-pole double-throw switch operated by inserting the mains plug. A pick-up switch can very well be used for this purpose. This arrangement has the advantage that the receiver is automatically switched over to mains supply when the plug is removed.

In an ABC receiver with series supply of the filaments special attention must be paid to the circuitry to prevent overloading of the filaments of individual tubes. Overloading may occur as a result of the cathode currents of the tubes at the positive end of the chain flowing through the filaments at the negative end. This can be prevented by shunting the individual filaments with suitable resistors. Another form of overloading may be caused by mains voltage fluctuations. For mains operation, therefore, the filament chain must be so arranged that the nominal voltage drop across each filament is 1.3 V.

From fig. 119 which is a typical $I_f V_f$ curve for a single 1.4 V, 50 mA filament, it is seen that the filament current corresponding to 1.3 V is 47.4 mA. The curve in fig. 119, however, is based upon measurements when no cathode current was flowing. In order to maintain the voltage drop of 1.3 V
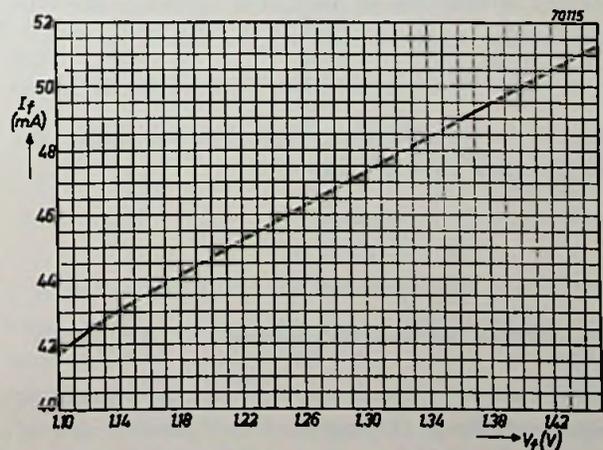
Fig. 119. Filament current plotted against filament voltage for a 50 mA miniature battery tube.

across each filament when cathode current is flowing, the shunt resistor must be so dimensioned that the current flowing into the positive end of the filament is $I_f - \frac{1}{3} I_k$, from which it follows that the current at the negative end becomes $I_f + \frac{2}{3} I_k$.

It is not necessary to shunt the positive limb of the DL 94 (see fig. 105), because this section carries no cathode current of preceding tubes. The filament current flowing into this section must, however, be reduced to compensate for its cathode current.

5.1. Shunt resistor for filament of DL 94

At a filament voltage of 2.6 V the total cathode current of the DL 94 is 9.2 mA, of which 3.7 mA flows to the positive limb and 5.5 mA to the negative limb. The current flowing into the positive end of the positive limb must therefore be $47.4 - \frac{1}{3} \times 3.7 = 46.2$ mA, the 10 W dropping resistor of 1.8 kΩ being based on this value. The current at the negative end of the positive limb is then $47.4 + \frac{2}{3} \times 3.7 = 49.9$ mA.

The current flowing into the positive end of the negative limb should be $47.4 - \frac{1}{3} \times 5.5 = 45.6$ mA.

The current in the shunt resistor should therefore be $49.9 - 45.6 = 4.3$ mA, and the resistor must have a value of $1300/4.2 = 302 \Omega$.

5.2. Shunt resistor for filament of DM 70

The DM 70 has a 25 mA filament, this current being reduced to 24 mA at $V_f = 1.3$ V. The cathode current of this tube is negligible and since the current at the negative end of the DL 94 is $47.4 + \frac{2}{3} \times 5.5 = 51.1$ mA and the current in its shunt resistor is 4.3 mA, the shunt resistor across the DM 70 must have a value of

$$\frac{1300}{51.1 + 4.3 - 24} = 41 \ \Omega.$$

5.3. Shunt resistor for filament of DF 91 (II)

The cathode current of this tube is 2.5 mA, so that the current flowing into the positive end of the filament should be $47.4 - \frac{1}{3} \times 2.5 = 46.6$ mA.

A total current of $24 + 31.4 = 55.4$ mA is available and the shunt resistor must have a value of

$$\frac{1300}{55.4 - 46.6} = 148 \ \Omega.$$

5.4. Shunt resistor for filament of DF 91 (I)

The current in the negative end of the DF 91 (II) filament is $47.4 + \frac{2}{3} \times 2.5 = 49.1$ mA, and the current in its shunt resistor 8.8 mA. The current flowing into the positive end of the DF 91 (1) filament should be $47.4 - \frac{1}{3} \times 2.5 = 46.6$ mA, so that the current in the shunt resistor must be $49.1 + 8.8 - 46.6 = 11.3$ mA. The shunt resistor must have a value of

$$\frac{1300}{11.3} = 115 \ \Omega.$$

5.5. Shunt resistor for filament of DK 92

The current in the negative end of the filament of the preceding tube is 49.1 mA, and the current in its shunt resistor 11.3 mA. The DK 92 has a cathode current of 2.5 mA, so that the current flowing into the positive end of its filament should be 46.6 mA.

A current of $49.1 + 11.3 - 46.6 = 13.8$ mA must flow in the shunt resistor. The DK 92 filament must therefore be shunted with

$$\frac{1300}{13.8} = 94 \ \Omega.$$

5.6. Shunt resistor for filament of DAF 91

The cathode current of the DAF 91 is negligible and the filament current must therefore be 47.4 mA. A current of $49.1 + 13.8 = 62.9$ mA is available and the current in the shunt resistor must therefore be $62.9 - 47.4 = 15.5$ mA. A shunt resistor of $\frac{1300}{15.5} = 84 \ \Omega$ should be employed.

In addition to the D.C. component of the cathode currents also the A.C. components flow through the filament chain. This results in undesirable couplings between stages, so that by-pass capacitors must be used. For the A.F. cathode current of the DL 94 an electrolytic capacitor is required, but for the other tubes capacitors with smaller values are sufficient. (see fig. 105).

As a final note attention should be drawn to the fact that operation of the receiver with a new H.T. battery and a run-down L.T. battery, may lead to overloading of the output tube. It is therefore advisable to replace these batteries simultaneously.

MEASURING RESULTS

Voltages and currents [23])

Tube type	V_a (V)	V_{g4} (V)	V_{g3} (V)	V_{g2} (V)	V_{g1} (V)	I_a (mA)	I_{g4} (mA)	I_{g2} (mA)
DK 92	95	70	0	37		0.68	0.14	1.76
DF 91 (I)	95			42	—0.1	1.8		0.78
DF 91 (II)	95			48	—0.3	1.8		0.69
DAF 91	24.3			22.1	0	0.062		0.014
DL 94	89			95	—3.9	7.5		1.7
DM 70	95				—1.3			

[23]) With 220 V A.C. mains supply. Voltages with respect to chassis with the exception of V_{g1}, which is measured with respect to the negative side of the filament of the tube concerned. Measuremen s are taken with zero signal.

Sensitivities with mains supply (220 V AC) and with battery supply ($V_b = 90$ V; $V_f = 1.3$ V per filament) for 50 mW output

A.F. voltage at diode	210 mV
I.F. voltage at diode	1050 mV (m = 30%)
I.F. input DF 91 (II)	17 mV
I.F. input DF 91 (I)	355 μV
H.F. input DK 92	9.5 μV (1 Mc/s)

Sensitivities with battery supply and underrunning of V_b and V_f ($V_b = 65$ V; $V_f = 1.1$ V per filament) for 50 mW output

A.F. voltage at diode	229 mV
I.F. voltage at diode	1185 mV (m = 30%)
I.F. input DF 91 (II)	27 mV
I.F. input DF 91 (I)	800 μV
H.F. input DK 92	63 μV (1 Mc/s)

Calculated field strength in frame aerial [24])

L.W.			M.W.		
0.16	0.2	0.3	0.55	0.8	1.6 Mc/s
57	50.5	29	14.9	11.6	10.5 μV/m

S.W. 2			S.W. 1		
2	3.5	6	7	10	19 Mc/s
10.4	9.0	10.6	19.1	17.3	10.9 μV/mi

Calculated field strength in frame aerial

L.W.			M.W.		
0.16	0.2	0.3	0.55	0.8	1.6 Mc/s
388	305	179	97.5	79	62.5 μV/m

S.W. 2			S.W. 1		
2	3.5	6	7	10	19 Mc/s
65	49.5	57	103	73	42.5 μV/m

[24]) The field strength is calculated from the measured e.m.f. required in the frame aerial for 50 mW output of the receiver. The measurement is taken by connecting a resistor of 0.01 Ω in series with the frame aerial and applying a known voltage from a standard signal generator via a resistor of 10 Ω. Corrections must be made for the influence of the resistor of 0.01 Ω upon the quality of the total aerial circuit, and for the self-inductance of this resistor, which gives rise to an increase of the impedance at high frequencies.

With underrunning the low-frequency end of the wave range 14.3 — 47 m (21 — 6.38 Mc/s) is the most difficult point of all wave ranges for maintaining oscillation. When the total filament voltage $V_f = 7.7$ V (1.1 V per filament), oscillation stops at $V_b = 34$ V, and when $V_f = 6.25$ V (0.9 V per filament) at $V_b = 65$ V.

Image rejection ratio, quality factor of total input circuit and radiation voltage at frame aerial as functions of frequency

	L.W.			M.W.			S.W. 2			S.W. 1		
Frequency	0.16	0.2	0.3	0.55	0.8	1.6	2	3.5	6	7	10	19 Mc/s
Image rejection	67	84	27	74	46	24	60	17	12	10	8.2	7.5
Quality factor Q	11	12	15.5	41.5	43	28.5	77	52	35	46.5	41.5	31.5
Radiation	0.06	0.35	1.5	0.1	2	15	0.45	12	150	200	180	150 mV

Total I.F. bandwidth at 452 kc/s

Reduction in response	Bandwidth
$1 : \sqrt{2}$	3 kc/s
$1 : 10$	11.4 kc/s
$1 : 100$	21 kc/s
$1 : 1000$	33 kc/s

COMPONENT VALUES

The values of resistors and capacitors are indicated in the circuit diagram of fig. 105. Unless otherwise indicated resistors with a power rating of 0.25 W can be used throughout.

L_1 — Frame aerial: 1 turn of aluminium strip 20 × 2 mm, bent into a rectangle of 32 × 23.5 cm. Self-inductance $L = 0.68\ \mu$H.

L_2 — Correction coil for S.W. 1 Coil former with iron dust core of 6 mm length, type 7977. Number of turns 5, of 1 mm enamelled copper wire, pitch 2 mm. Self-inductance $L_1 + L_2 = 1.17\ \mu$H.

L_3L_4 — H.F. transformer for S.W. 2 with turns ratio 4.5. An iron-dust pot core [25]) is used; L_3 having 4 turns of litz wire 4 × 60 × 0.03 mm and L_4 18 turns of litz wire 90 × 0.03 mm. The self-inductance of L_4 is about 47 μH.

L_5 — Correction coil for S.W. 2. Coil former with iron dust core of 6 mm length, type 7977. Number of turns 15, of litz wire 90 × 0.03 mm, pitch 0.7 mm. The total self-inductance of L_5, L_4, L_3 and L_1 measured across the tuning capacitor is 13.2 μH.

L_6L_7 — H.F. transformer for M.W. with turns ratio 18.25. The same type of core as in the case of L_3L_4 is used, L_6 having 4 turns of litz wire 4 × 60 × 0.03 mm and L_7 73 turns of litz wire 30 × 0.03 mm. The self-inductance of L_7 is about 765 μH.

L_8 — Correction coil for M.W. Coil former with iron-dust core of 6 mm length, type 7977. Number of turns 36, of litz wire 30 × 0.03 mm, wave wound width 6 mm. The total self-inductance of L_8, L_7, L_6 and L_1 measured across the tuning capacitor is 185.2 μH.

L_9L_{10} — H.F. transformer for L.W. with turns ratio 65. The same type of core as in the case of L_3L_4 is used, L_9 having 4 turns of litz wire 4 × 60 × 0.03 mm and L_{10} 260 turns of litz wire 7 × 0.03 mm. The self-inductance of L_{10} is about 9.7 mH.

L_{11} — Correction coil for L.W. Coil former with iron-dust core of 6 mm length, type 7977. Number of turns 104, of litz wire 7 × 0.03 mm, wave wound, width 4 mm. The total self-inductance of L_{11}, L_{10}, L_9 and L_1 measured across the tuning capacitor is 2.365 mH.

L_{12} — I.F. ware trap tuned to 452 kc/s; self-inductance 5 mH and quality $Q = 135$.

$L_{13}L_{14}L_{15}$ — Oscillator coils for S.W. 1 and S.W. 2. These coils are wound on one former having a diameter of 14 mm and a length of 60 mm (see fig. 120). A screening can is used of 30 mm diameter and 60 mm length.
$L_{16}L_{17}$

L_{13} has 11 turns of 1 mm enamelled copper; pitch 1.325 mm. Self-inductance 1.15 μH.

L_{14} is wound between the turns of L_{13} starting at the earthed end. The number of turns is 7¾ of 0.1 mm enamelled and double silk covered copper.

L_{15} is the booster coil and has 29 turns of 0.1 mm enamelled and double silk covered copper. The coil is wave wound with a width of 2 mm.

---

[25]) For the H.F. transformers L_3L_4, L_6L_7 and L_9L_{10} Ferroxcube pot cores can also be used, this having the advantage of smaller dimensions and a closer coupling.

L_{16} has $39\frac{7}{8}$ turns of 0.25 mm enamelled copper; pitch 0.38 mm. Self-inductance 12.15 μH.

L_{17} is wound between the turns of L_{16}
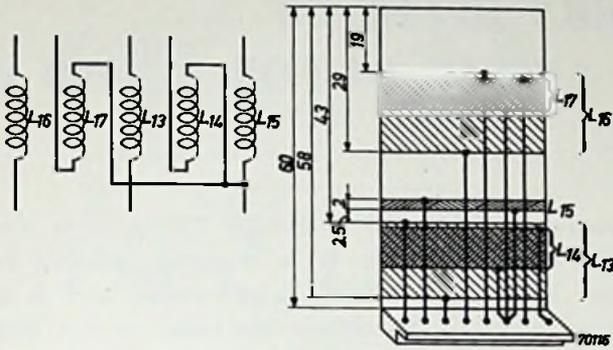
Fig. 120. Development of the oscillator coil combination for the ranges S.W. 1 and S.W. 2.

starting at the end connected to the padding capacitor. The number of turns is $27\frac{7}{8}$ of 0.1 mm enamelled and double silk covered copper.

$L_{18}L_{19}$ $L_{20}L_{21}$ Oscillator coils for M.W. and L.W. These coils are wave wound (width 2 mm) on one former having a diameter of 10 mm and a length of 48 mm (see fig. 121). The former is threaded on the inside to receive an iron dust core of 6 mm diameter and 6 mm length. The core is used for the medium wave coils $L_{18}L_{19}$. A screening can is used of 30 mm diameter and 60 mm length.

L_{18} has 80 turns of 0.1 mm enamelled copper. Self-inductance 108.8 μH.

L_{19} has 24 turns of 0.1 mm enamelled

copper. A layer of 0.1 mm insulating tissue is interposed between L_{18} and L_{19}

L_{20} has 207 turns of 0.1 mm enamelled copper. Self-inductance 612 μH.

L_{21} has 45 turns of 0.1 mm enamelled
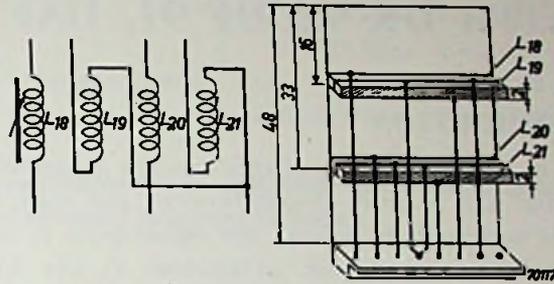
Fig. 121. Development of the oscillator coil combination for the ranges M.W. and L.W.

copper. A layer of 0.1 mm insulating tissue is interposed between L_{20} and L_{21}.

$L_{22}L_{23}$ I.F. transformer type 5731/52.
Quality $Q = 120$ (without extra damping and capacitance).
Coupling $KQ = 0.9$.

L_{24} I.F. circuit.
Quality $Q = 120$; self-inductance 1 mH.

$L_{25}L_{26}$ I.F. transformer type 5731/52.
Quality $Q = 120$ (without extra damping and capacitance).
Coupling $KQ = 0.9$.

T_1 Output transformer for primary matching resistance of 10 kΩ.

$Sel.$ Selenium rectifier for 220 V, 90 mA.

67

A 4-TUBE BATTERY RECEIVER
WITH DK 92, DF 91, DAF 91 AND DL 94 FOR $V_b = 90$ V

DESCRIPTION

The circuit diagram of this receiver represented in fig. 122 is quite straightforward and calls for little comment. Following the signal path it may first be remarked that, in contrast to the ABC receiver previously described, inductively coupled input circuits for a capacitive aerial are used. The input is shunted by an I.F. wave trap L_1, whilst two aerial terminals are provided, one of which is connected directly to the coupling coils and the other via a resistor of 220 Ω. The latter terminal can be used when receiving large signals, which would otherwise overload the I.F. stage. It is, of course, possible to use the same input circuit with frame aerial as in the case of the ABC receiver.

The A.G.C., voltage is applied to the bottom end of the signal-grid resistor when the receiver is switched for the reception of medium or long waves. In the short-wave range A.G.C. is not applied to the frequency changer.

In this receiver the oscillator circuit is parallel fed. Although the DK 92 gives better H.F. performance with series feed, in certain countries regulations exist which do not permit the use of this circuit. For this reason the circuit with parallel feed is given here by way of illustration.

In the short-wave range a booster coil L_{10} has been used. Owing to the favourable oscillator performance of the DK 92, it is not strictly necessary to use this arrangement for maintaining oscillation over the entire wave range, but is has the advantage that a better constancy of the oscillator voltage can be obtained (see description of ABC receiver).

The receiver comprises three wave ranges. viz.:

short wave	50 — 16.7 m	(6 — 18 Mc/s)
medium wave	600 — 200 m	(0.5 — 1.5 Mc/s)
long wave	2000 — 750 m	(150 — 400 kc/s)

The intermediate frequency is 452 kc/s.

Another noteworthy feature of this receiver is that the L.T. and the H.T. current drain is considerably reduced. This is obtained by using only one filament section of the DL 94. The cathode current of this tube is thereby halved, as is also the available output. It is, of course, possible to use both filament sections in parallel, and it is then necessary to change the value of the bias resistor from 470 Ω to 390 Ω, indicated between parentheses in the circuit diagram. Since the sensitivity of the output stage is increased when two filament sections are used, on account of microphony of the pre-amplifying stage the A.F. gain of the DAF 91 should be slightly reduced. This can be done by altering the grid resistor of the DL 94 to 0.33 MΩ. It will be clear that it also makes a difference in the optimum load resistance of the output stage whether one or two filament sections of the DL 94 are used.

An explanation of the 1 MΩ resistor connected across the H.T. contacts of the on-off switch will be given on page 71.

MEASURING RESULTS
Voltages and currents [26])

Tube type	V_a (V)	V_{g1} (V)	V_{g2} (V)	V_{g1} (V)	I_a (mA)	I_{g4} (mA)	I_{g2} (mA)
DK 92	85	58	32		0.6	0.14	1.6
DF 91	85		52		2.0		0.6
DAF 91	20		21		0.065		0.014
DL 94	82		85	—4.8	3.9		0.82

Variation of oscillator current, with nominal supply

Range	I_{g1} DK 92
6 — 18 Mc/s	8 — 90 μA
0.5 — 1.5 Mc/s	200 — 350 μA
150 — 400 kc/s	190 —360 μA

[26]) The figures given refer to the case where one filament section of the DL 94 is used and to zero signal conditions. Voltages are with respect to chassis. When two filament sections of the DL 94 are used in parallel the control-grid voltage becomes —5.1 V, the anode current 6.8 mA and the screen-grid current 1.5 mA. The resistor in the negative H.T. lead must then be changed to 390 Ω.

Fig. 122. Circuit diagram of the 4-tube battery receiver for $V_b = 90$ V.

Sensitivities for 50 mW output, with nominal supply voltages

A.F. voltage at control grid of DAF 91	40 mV
I.F. input DF 91 (452 kc/s, m = 30%	5.8 mV

H.F. input DK 92		
6— 18 Mc/s	130—130 μV
0.5— 1.5 Mc/s	160—200 μV
150—400 kc/s	175—200 μV

H.F. signal at aerial		
6— 18 Mc/s	100—100 μV
0.5— 1.5 Mc/s	68— 68 μV
150—400 kc/s	68—110 μV

Sensitivities for 50 mW with underrunning of V_b and nominal filament voltage

V_b	80	70	60	V
A.F. voltage at control grid of DAF 91	43	54	130	mV
I.F. input DF 91 (452 kc/s, m = 30%)	6.5	9.5	25	mV
H.F. signal at aerial:				
6—18 Mc/s	115—130	170—215	470—580	μV
0.5—1.5 Mc/s	95—105	155—170	525—525	μV
150—400 kc/s	105—130	170—340	470—950	μV

Sensitivities for 50 mW with underrunning of V_f and nominal V_b

V_f	1.3	1.2	1.1	V
A.F. voltage at control grid of DAF 91	43	46	49	mV
I.F. input DF 91 (452 kc/s, m = 30%)	6.5	7.4	8.6	mV
H.F. signal at aerial:				
6—18 Mc/s	125—135	145—180	190—215	μV
0.5—1.5 Mc/s	95—95	140—140	165—190	μV
150—400 kc/s	125—135	260—290	215—250	μV

Sensitivities for 50 mW with underrunning of V_b and V_f

($V_b = 65$ V; $V_f = 1.1$ V).

A.F. voltage at control grid of DAF 91	75 mV
I.F. input DF 91 (452 kc/s, m = 30%)	12 mV

H.F. signal at aerial		
6— 18 Mc/s	360—420 μV
0.5— 1.5 Mc/s	300—360 μV
150—400 kc/s	300—420 μV

COMPONENT VALUES

The values of resistors and capacitors are indicated in the circuit diagram of fig. 122. Resistors with a power rating of 0.25 W can be used throughout.

L_1 I.F. wave trap tuned to 452 kc/s; self-inductance 5 mH and quality $Q = 135$.

L_2L_3 Aerial coils for short-wave range.

Diameter of coil former	14 mm
Diameter of screening can	30 mm

L_2 22 turns of 0.1 mm enamelled copper; wound without spacing. Inductance 10 μH.

L_3 12 turns of 0.6 mm enamelled copper; wound without spacing. Inductance 1.25 μH.

Distance between ends of L_2 and L_3 1 mm.

L_4L_5 Aerial coils for medium-ware range.

Diameter of coil former	14 mm
Diameter of screening can	30 mm

L_4 468 turns of 0.07 mm enamelled copper wire; wave wound, width 2 mm. Inductance 4 mH.

L_5 112 turns of litz wire 12×0.04 mm: wave wound, width 2.5 mm. Inductance 207 μH.

Distance between ends of L_4 and L_5 2.6 mm.

L_6L_7 Aerial coils for long-wave range.

Diameter of coil former	8 mm
Diameter of screening can	25 mm

L_6 1072 turns of 0.07 mm enamelled copper wire; wave wound, width 3 mm. Inductance 10 mH.

L_7 504 turns of 0.1 mm enamelled copper wire; wave wound, width 3 mm. Inductance 2.56 mH.

Distance between ends of L_6 and L_7 1.2 mm.

$L_8L_9L_{10}$ Oscillator coils for short-wave range and booster coil.

Diameter of coil former	8 mm
Diameter of screening can	25 mm

L_8 15 turns of 0.4 mm enamelled copper wire; wound in one layer, pitch 0.5 mm. Inductance 1.17 mH.

L_9 $9\frac{3}{8}$ turns of 0.1 mm copper wire enamelled and silk covered; wound in one layer between turns of L_8.
Voltage ratio L_9L_8 is 0.48.

L_{10} $39\frac{7}{8}$ turns of 0.1 mm enamelled copper wire; wave wound, width 2 mm. Inductance 15 μH.
Distance between ends of L_8 and L_{10} 2.5 mm.

$L_{11}L_{12}$ Oscillator coils for medium-wave range.

Diameter of coil former	10 mm
Diameter of screening can	25 mm

L_{11} $92\frac{2}{8}$ turns of 0.1 mm enamelled copper wire; wave wound, width 2 mm. Inductance 114 μH.

L_{12} $46\frac{6}{8}$ turns of 0.1 mm enamelled copper wire; wave wound, width 2 mm.
L_{12} is wound over L_{11} with two layers of 0.1 mm insulating tissue interposed.
Voltage ratio $L_{12}L_{11}$ is 0.4.

$L_{13}L_{14}$ Oscillator coils for long-wave range.

Diameter of coil former	10 mm
Diameter of screening can	25 mm

L_{13} 225 turns of 0.1 mm enamelled copper wire; wave wound, width 2 mm. Inductance 641 μH.

L_{14} $89\frac{7}{8}$ turns of 0.1 mm enamelled copper wire; wave wound, width 2 mm.
L_{14} is wound over L_{13} with two layers of 0.1 mm insulating tissue interposed.
Voltage ratio $L_{14}L_{13}$ is 0.30.

$L_{15}L_{16}$ I.F. transformer for 452 kc/s, type 5730/52.
Quality factor $Q = 140$ (without extra damping).
Coupling $KQ = 1.05$.

$L_{17}L_{18}$ As $L_{15}L_{16}$, but with the diode of the DAF 91 connected to a tap at 0.7 on the secondary.

T_1 Matching transformer.
When one filament section of the DL 94 is used the optimum load resistance is 20 kΩ, and with two filament sections in parallel 8 kΩ.

A 4-TUBE BATTERY RECEIVER
WITH DK 92, DF 91, DAF 91 AND DL 92 FOR $V_b = 67.5$ V

DESCRIPTION

The only difference beween the battery receiver described here and that previously dealt with lies in the fact that in the output stage a DL 92 output tube is used instead of a DL 94. The H.T. battery voltage could thus be reduced to 67.5 V, making the design specially suitable for receivers of very small dimensions. A circuit diagram is given in fig. 123.

At the low H.T. voltage the dropper resistor in series with the oscillator anode (second grid) of the DK 92 must have a comparatively low value. For this reason series feed of the oscillator is employed instead of parallel feed. This does not mean, of course, that parallel feed is impossible at a battery voltage of 67.5 V. On medium and long waves parallel feed can be used without any alteration in the oscillator coils, but on short waves it would be advisable to employ one or two more turns on the feedback coil.

In all other respects the circuit of fig. 123 corresponds to that of fig. 122. Resistance values are different, but the same coils are used throughout. The output transformer T_1 should have a matching resistance of 7 kΩ.

In this circuit, and that of fig. 122, the contacts of the H.T. on-off switch are bridged by a resistor of 1 MΩ. This resistor has been inserted to protect the output tube against heavy overload immediately after switching the receiver on.

When this resistor is not used, the coupling capacitor of 10 000 pF, between the anode of the DAF 91 and the grid of the output tube, will be completely discharged after switching off. When the set is now switched on, this capacitor will be charged again via the anode resistor of the DAF 91 and the grid leak of the output tube, which have approximately equal values. Hence, at the moment of switching on, the surge voltage of the H.T. battery is about equally divided over the resistors with the result that the grid of the output tube is at a high positive potential. Because of the low temperature inertia of the output tube filament, its emission increases rapidly with the result that with the positive grid potential a heavy grid current flows, be it for a very short time. However, this grid current has proved to be of unfavourable influence on the life of output tubes for battery supply.

When the 1 MΩ resistor is connected across the switch contacts the coupling capacitor retains a charge, sufficiently high, to prevent damage to the output tube.

MEASURING RESULTS

Voltage and currents [27)]

Tube type	V_a (V)	V_{g4} (V)	V_{g2} (V)	V_{g1} (V)	I_a (mA)	I_{g4} (mA)	I_{g2} (mA)
DK 92	61	61	29		0.54	0.13	1.52
DF 91	61		45		1.7		0.72
DAF 91	29		21		0.032		0.012
DL 92	56		61	—6.2	6.4		1.3

Variation of oscillator current, with nominal supply voltages

Range	I_{g1} DK 92
6 — 18 Mc/s	55 — 50 μA
0.5 — 1.5 Mc/s	170 — 350 μA
150 — 400 kc/s	185 — 350 μA

Sensitivities for 50 mW output, with nominal supply voltages

A.F. voltage at control grid of DAF 91	40 mV
I.F. input DF 91 (452 kc/s, m = 30%)	5.9 mV

H.F. input DK 92	6— 18 Mc/s	215—280 μV
	0.5— 1.5 Mc/s	165—280 μV
	150—400 kc/s	190—255 μV

[27)] The figures given here refer to zero signal conditions. Voltages are measured with respect to chassis.

Fig. 123. Circuit diagram of the 4-tube battery receiver for $V_b = 67.5$ V.

H.F. signal at aerial		
6— 18 Mc/s	190—240 μV
0.5— 1.5 Mc/s	48—120 μV
150—400 kc/s	135—160 μV

Sensitivities for 50 mW output and oscillator current, with underrunning of V_b

$V_b = 45$ V; $V_f = 1.4$ V.

A.F. voltage at control grid of DAF 91	72 mV
I.F. input DF 91 (452 kc/s, m = 30%)	25 mV
H.F. input DK 92 (1 Mc/s)	1.6 mV
Oscillator current I_{g1}	200 μA

Sensitivities for 50 mW output and oscillator current, with underrunning of V_f

$V_b = 67.5$ V; $V_f = 1.1$ V.

A.F. voltage at control grid of DAF 91	40 mV
I.F. input DF 91 (452 kc/s, m = 30%)	7 mV
H.F. input DK 92 (1 Mc/s)	240 μV
Oscillator current I_{g1}	280 μA

Sensitivities for 50 mW output and oscillator current, with underrunning of V_b and V_f

$V_b = 45$ V; $V_f = 1.1$ V.

A.F. voltage at control grid of DAF 91	75 mV
I.F. input DF 91 (452 kc/s; m = 30%)	30 mV
H.F. input DK 92 (1 Mc/s)	2.8 mV
Oscillator current I_{g1}	175 μA

COMPONENT VALUES

The values of resistors and capacitors are indicated in the circuit diagram of fig. 123. Resistors with a power rating of 0.25 W can be used. The data of the coils are identical to those given in the description of the 4-tube battery receiver with DL 94 output tube. The output transformer must have a matching resistance of 7 kΩ.